Epigenetic and Central Nervous System function.

Insights from the study of the

Rett syndrome mouse model.

Inauguraldissertation

zur
Erlangung der Würde eines Doktors der Philosophie
vorgelegt der
Philosophisch-Naturwissenschaftlichen Fakultät
der Universität Basel
von

Emanuela Giacometti

Treviso, Italien, 10. April 2008

Genehmigt von der Philosophisch-Naturwissen-
schaftlichen Fakultät auf Antrag der Herren
Professoren M.A. Rüegg, R. Jaensch und A. Lüthi

Basel, den 11. Dezember 2007

Prof. Dr. Hans-Peter Hauri

ACKNOWLEDGMENTS

First and foremost I would like to thank my parents for their understanding and patience. In particular my mother De Sabbata D. for moral guidance and for devoting her prayers too the happiness and health of myself and all members of the lab. I would like to thank my thesis supervisor, Rudolf Jaenisch for financial support and for giving me the opportunity to conduct truly independent and exciting work. I am very grateful to all past and present members of the Jaenisch lab for providing a constant source of scientific knowledge and great entertainment. In particular I would like to thank Caroline Beard and Sandra Luikenhuis for useful scientific discussions and for teaching me how good molecular biology should be done, Ruth Flannery and Jessie Dausmann for making my work with a big mouse colony both possible and fun. A special thought and thanks also go to Mathias Pawlak, Tobias Brambrink, Konrad Hochkedlinger and James White for patiently taking my bad and good moods and supplying constant encouragement. Last but not least I would like to thank Stefano Marchetti, Margaret Heck and Kerry Tucker to whom I owe my dedication to science.

TABLE OF CONTENTS. PAGES

Abbreviations: RS (Rett syndrome), m^5C (5methyl-cytosine), KO (knock out), CNS (central nervous system) , MR (mental retardation), MECP2 (human protein), *MECP2* (human gene), *Mecp2* (mouse gene), Mecp2 (mouse transgene), MeCP2 (mouse protein).

Introduction.

The central nervous system and epigenetic regulation.

Adaptation to the environment is one of the fundamental regulatory processes in biology. In a changing environment, simple organisms enhance their chances of survival by high rates of spontaneous mutations and by natural selection the mutations that better fit the changes will be retained [1]. Natural selection also affects complex multi cellular organisms. However in these organisms the rates of maturation and reproduction are much slower so that changes in the environment outpace genetic evolution. A solution to this problem is the development of complex physiological and behavioral systems coordinated by the central nervous system (CNS).

The nervous system permits rapid adaptation by coordinating impulses from internal and external cues and executes a physiological response that will

maintain homeostasis [2]. To cope with environmental complexity and ambiguity, an organism requires mechanisms that allow experience to affect relatively long-lasting changes in behavior. This mechanism is called learning [3]. So how does the nervous system generate the diversity in cell types and connections to respond to environmental changes or experience?

Although somatic mutation has been proposed to generate diversity in neuronal precursors through retrotransposon hopping as it does in the immune system it is more likely that permanent changes in gene expression not involving changes in DNA sequence itself are achieved by modifications of the chromatin structure. Self-perpetuating changes in the chromatin structure of a locus that induce long lasting changes in gene expression are referred to as epigenetic modifications. Epigenetic changes allow genotypically identical cells to be phenotypically different. Thus the concept of chromatin remodeling potentially addresses one of the key challenges in neurobiology of how stable changes in gene expression are induced in neurons and glia in response to environmental clues. In this view chromatin is a dynamic structure that potentially can integrate hundreds of signals from the cell surface and effect a coordinated and appropriate transcriptional response.

Epigenetic modifications.

Chromatin is composed of a complex of DNA, histones and non-histone proteins in the cell nucleus. The fundamental unit of chromatin is the nucleosome: 147 base pairs of DNA wrapped around a core histone octamer.

Each octamer contains two copies of each of the histones H2A,H2B,H3 and H4. This nucleosome structure allows DNA to be tightly packaged into the nucleus. Chromatin remodeling affects the DNA-protein interactions to ensure that appropriate loci remain accessible to the transcriptional machinery with high spatial and temporal resolution.

One of the best characterized chromatin remodeling mechanisms is the post-translational modification of histones at distinct amino acid residues in their N-terminal tails. Such modifications include acetylation, ubiquitylation or methylation (on lysine and arginine residues), phosphorylation (serine or threonine) and ADP ribosylation (glutamate residues). DNA methylation is another important mechanism of epigenetic gene regulation. It occurs by transfer of a methyl group from S-adenosyl methionine (SAM) to the cytosine in a CpG dinucleotide. Patterns of DNA methylation are intricately linked to patterns of histone modification [4].

Epigenetic tagging of DNA: CpG methylation.

One class of epigenetic regulation involves direct chemical modification to the DNA molecule by addition of a methyl group (from S-adenosyl methionine) to the C5 position of the cytosine in a CpG dinucleotide (m^5C). This modification is found in all eukaryotic phyla [5-7] and the fact that the genes involved in DNA methylation seem to be conserved suggests that proficiency for cytosine methylation is ancestral. However there are numerous species which show no or little methylation, like *Saccharomyces sp.* and *Caenorhabditis*

elegans. *Drosophila melanogaster* is reported to have a trace amount of methylation only in early embryos [8]. Nevertheless the existence of trace of methylation in *Drosophila m.* and *S. Pombe* and the fully functional methylation system in other insects and fungi suggests that some evolutionary lineages have lost methylation as opposed to never having had it.

DNA methylation was first noticed by Hotchkiss in 1948 in calf thymus DNA [9]. It was then discovered that the sequences of satellite DNA and parasitic elements (such as long interspersed transposable elements (LINES), short interspersed transposable elements (SINES) and endogenous retroviruses) contained CpG dinucleotides where the cytosine were methylated [10, 11]. Subsequently a role for this nucleotide signature was suggested by the observation that gene expression levels inversely correlated with the density of methylated CpG dinucleotides. These observations were made both in the developmentally regulated genes [12, 13] [14, 15], and in viral elements [16]. Cytosine 5 methylation of eukaryotic genomes was then causally associated with repression of transcription. Consistent with this view, pharmacological agents that reduce the level of cytosine methylation were found to increase gene expression [17]. Importantly, it was also noticed that these treatments lead to dramatic changes in culture phenotypes reminiscent of differentiation [18] which suggested that methylation of genes could be regulating development. The palindromic CpG dinucleotide provides a semi conservative mechanism for the maintenance of methylation, and thus regulatory information, through replication [19]. Sites are symmetrically methylated prior to DNA synthesis [20], replication then renders them hemimethylated by incorporation of unmethylated cytosines into the daughter strands, and the sites are subsequently restored to

full methylation by the maintenance DNA methyl transferases. Subsequent transfection experiments have demonstrated that arbitrary methylation patterns are maintained through cell division, confirming the clonal heritability of methylation patterns [21].

Maintenance and establishment of DNA methylation is accomplished by at least three independent catalytically active DNA methyltransferases: Dnmt 1, Dnmt3a and Dnmt3b [22, 23]. There are two isoforms of Dnmt1, an oocyte specific isoform (Dnmt1o) and a somatic isoform. Somatic Dnmt1 is believed to be responsible for copying methylation patterns during DNA replication, while the Dnmt3 enzymes (Dnmt3a, 3b, 3l and a number of isoforms) are required for the de- novo methylation that occurs after implantation and methylation that is found on newly integrated retroviral sequences in mouse ES (embryonic stem) cells [22, 24], and for establishment of imprints (Dnmt3l) [25]. DNA methyltransferase 3a (Dnmt3a) and its regulatory factor, DNA methyltransferase 3-like protein (Dnmt3L), are both required for the de novo DNA methylation of imprinted genes in mammalian germ cells. Dnmt3L interacts specifically with unmethylated lysine 4 of histone H3 and induces de novo DNA methylation by recruitment or activation of DNMT3a2 [26, 27]. The essential role of DNA methylation in mammalian development is highlighted by the fact that mutant mice lacking each of the enzymes die either during early embryonic development (Dnmt1 and Dnmt3b) or shortly after birth (Dnmt3a) [24, 28]. The knock out of Dnmt3l leads to male infertility and failure to establish imprinting in female eggs [29]. DNA methyltransferase 2 (Dnmt2) has a dual-specificity, a weak DNA methyltransferase and novel tRNA methyltransferase activity. However, its biological function is still unknown.

In human somatic cells, m^5C accounts for ~1% of total DNA bases and therefore affects 70-80% of all CpG dinucleotides in the genome [30]. In mouse somatic dells, during a discrete phase of early development, methylation levels decline sharply to 30% of the typical somatic level [31] [32]. De novo methylation restores normal levels by the time of implantation.

The most striking feature of vertebrate DNA methylation patterns is the presence of CpG islands, which are unmethylated GC-rich regions that possess high relative densities of CpG and are positioned at the 5' end of many human genes. Computational analysis of the human genome sequence predicts 29000 CpG islands [33] [34]. Earlier studies estimated that 60% of all human genes are associated with a CpG island, the great majority of which are unmethylated at all stages of development and in all tissue types [35]. Because many CpG islands are located at genes that have a tissue restricted expression pattern, it follows that CpG islands can remain methylation free even when their associated genes are silent. For example the tissue specific human a-globin [36] gene and a-2(1) collagen gene [37] have CpG islands that remain unmethylated in all tested tissues regardless of expression. A small but significant proportion of CpG islands become methylated during development, and when this happens the associated promoter is stably silent. In fact, this developmentally programmed methylation of CpG islands is involved in genomic imprinting and X-chromosome inactivation. These de-novo methylation events occur in germ cells or in the early embryo [38], suggesting that de novo methylation is particularly active at these stages. There is evidence, however, that de novo methylation can also occur in adult somatic cells. A significant fraction of all human CpG islands

are prone to progressive methylation in certain tissues during aging or in abnormal cells such as cancers [39] and permanent cell lines [40] [41].

Methyl CpG binding Proteins.

There are several potential mechanisms that might lead to transcriptional repression at methylated loci. For example certain transcription factors are unable to bind to their recognition sites when 5-methyl cytosine occurs within a critical base (e.g. myc, E2F, NF-kB). Or DNA methylation might conceivably result in structural effects on local chromatin architecture (e.g. CTCF insulator at the Igf2/H19 locus) by influencing nucleosome position or stability, or by affecting higher order chromatin structure. While these are likely to be biologically significant regulatory mechanisms in some cases, it is believed that the repressive effects of DNA methylation result mostly from selective recognition of the 5-methyl CpG dinucleotide by a conserved family of proteins, the methyl CpG-binding domain (MBD) family (figure 1).

The first evidence of the existence of CpG binding proteins was reported in the late 1980s' when it was shown that the majority of m^5C but not adjacent sequences were specifically protected from nucleases [42]. Then an electrophoretic mobility shift assay was used to demonstrate a m^5C specific binding activity in mouse tissue: only symmetrically methylated probes were shifted, and the binding could be competed only by artificially methylated DNA or mouse genomic DNA [43]. This activity, called MeCP1 (Methyl CpG-binding Protein 1) remained enigmatic for several years. Subsequently a second methyl

CpG binding (MeCP2) protein was identified and cloned [44]. This protein was found to bind with high affinity and specificity to a single symmetrically methylated CpG and to co localize with heterochromatin rich areas in the nucleus of mouse cells [45, 46]. Further characterization showed that this was not responsible for the (still uncloned) MeCP1 activity. Domain mapping of MeCP2 identified an 85 amino acid domain which could by itself bind specifically to sequences containing a single methylated CpG with nanomolar affinity [47]. The sequence of the methyl CpG binding domain (MBD) of MeCP2 was used to identify a number of related domains in the mammalian genome which were named MBD1-4 [48]. MBD2 was found to be responsible for the methyl-CpG-binding activity of the MeCP1 complex [49]. Apart from MBD3, these proteins have been shown to have specific methyl CpG binding activities. Recently a novel protein, Kaiso, was identified as a methyl CpG binding protein even though this protein lacks a classical MBD but appears to bind specifically to methylated DNA via a zinc finger domain [50]. Several MBD proteins have been reported to interact with histone deacetylases (HDACs) as well as histone methyltransferases. MeCP2 has been shown to interact with the Sin3/HDAC co repressor complex and Brahma, as well as with the histone H3 lysine-9 methyltransferase, Suvar 3-9, although these interactions may not be stable [51]. MBD2 and MBD3 have been identified as core subunits of the Mi-2/NuRD complex, whereas Kaiso is part of the HDAC-containing N-CoR complex that plays an important role in transcriptional regulation by nuclear hormone receptors. These findings show a functional link between DNA methylation, histone deacetylation, and histone methylation and indicate that these

epigenetic events functionally cooperate to regulate transcription and cellular memory.

Functions of DNA methylation.

Tissue specific regulation by DNA methylation has been hypothesized by Riggs [52] and Holliday and Pugh [19]. According to their prediction, tissue specific genes would be methylated or demethylated according to the developmental program. This hypothesis is particularly attractive because it provides a mechanism for controlling gene expression in a tissue specific manner. Because convincing examples of tissue specific genes that undergo demethylation during development were absent for many years, this hypothesis was met with skepticism. However since then many studies have correlated DNA methylation with the control of cell type specific gene. For example glial fibrillary acid protein (Gfap) is implicated in the so-called neurogenic to gliogenic switch. Gfap is expressed in astroglia but not in neurons, and is regulated by the transcription factor STAT3, which binds directly to elements in the Gfap promoter to activate transcription. STAT3 expression alone though is not sufficient to activate Gfap expression. There are CpG sites in the Gfap promote that are methylated early in development (E11.5) and then become de-methylated at E14.5 in cells differentiating to become astroglia [53]. One differentially methylated CpG lies within the STAT-binding element. Takizawa et

al. (2001) found that methylation at that site prevents binding by the STAT3 and is present in neurons but not in glia. As the central nervous system develops, this CpG site becomes de-methylated in cells differentiating along the glial lineage [54]. Moreover, cultured neuron precursor cells lacking Dnmt1 become hypomethylated and differentiate prematurely in astrocites [55]. Consistent with these observations, cervical spinal cord from Dnmt1 mutant early embryos (E15 and E18) exhibit enhanced staining of glial markers such as Gfap and S100b.

Another example of epigenetic regulation in neural differentiation is provided by the Re1-silencing transcription factor (REST/NSRF). This factor binds to neuron-restrictive silencer element (RE1), usually found in promoters of genes that are expressed specifically in neurons [56]. REST mediated silencing of neuronal-specific genes occurs in conjunction with CoREST [57], which recruits additional silencing machinery including the methyl DNA binding protein MeCP2 and the histone H3 K9 methyltransferases G9a and SuVar39H [58]. Targets of REST are important neuronal house keeping genes such as sodium channels *(Nach typeII/Nav1.2)*, synaptic vesicle proteins, and neurotransmitter receptors. The mechanism of action of the REST complex differs in different cell types and developmental stages. In embryonic stem cells REST utilizes a repression mechanism independent of histone H3 methylation and DNA methylation. When ES cells differentiate into neuron progenitors REST protein is then down-regulated and further differentiation of progenitors to mature neurons occurs via the loss of REST complex from the RE1 site of neuronal genes [59, 60]. Some neuronal genes, such as Calbindin and brain-derived neurotrophic factor (BDNF), remain expressed at low levels in neurons due to the continued presence of CoREST and MeCP2 on an adjacent site of

methylated DNA. Interestingly membrane depolarization increases the level of expression of the BDNF gene through selective release of MeCP2 but not CoREST from its methylated site. The persistence of CoREST after REST departure may provide a mechanism for dynamic recruitment and dismissal of repressor complexes required for plasticity in mature neurons [59].

Genome defense.

Transposable elements comprise as much as 35% of the human genome. Because they are capable of insertional mutagenesis, generating aberrant transcripts and improperly activating nearby genes [61, 62], they threaten the integrity of the host genome. The host's genome primary mechanism of defense is CpG methylation of these elements. This modification attracts chromatin remodeling factors that induce a silent state [5]. Most of methylated CpG, in the mammalian genome are found at these repetitive elements, and complete de-methylation of the genome in mice leads to increased transposon activation [63]. Retroviruses are also transcriptionally silenced in mammalian embryonic and hematopoietic stem cells [64] by a mechanism that involves *de novo* methylation of cytosine residues in CpG dinucleotides of the integrated provirus[65].

Genomic imprinting.

A function of cytosine methylation that is specific to mammals and flowering plants is the regulation of imprinted genes. Imprinted genes are

differentially expressed depending on the parental origin of the allele. The maternal or the paternal alleles have differentially methylated regions (DMRs). The best characterized imprinted genes are involved in fetal growth, though not all have known function. Perhaps the most widely accepted explanation for the occurrence of genomic imprinting is the "parental conflict hypothesis "[66]. According to this theory imprinting is the evolutionary result of a conflict between the paternal and maternal genes, whose expression is either promoting or limiting embryonic growth, respectively. The father is in theory most interested in the growth of his offspring, at the expense of the mother, while the mother is more interested in conserving resources for her own survival while providing sufficient nourishment for current and future litters. Consistent with this hypothesis the paternally expressed genes *Igf2* and *Ins2* enhance growth, while the maternally expressed genes *H19, Igf2r*, and $p57^{KIP2}$ restrict growth. H19 encodes an untranslated RNA that represses transcription of the *Igf2* gene, which is located about 100 Kb from the H19 locus [67]. A differentially methylated domain upstream of *H19* is methylated during spermatogenesis, resulting in suppression of paternal expression of *H19* [68, 69]. *Igf2* is a paternally expressed fetal growth factor that is also antagonized by the *Igf2r*. *Igf2r* opposes Igf2 function by acting as a scavenger receptor for Igf2 [70]. The Igf2r gene acquires methylation marks in intron 2 on the maternal allele during oogenesis [71]. These marks ensure maternal expression by inhibiting transcription of Air, the antisense non-coding RNA that is expressed from a promoter located in intron 2 of the *Igf2r* gene [72]. Another hypothesis behind the origin of imprinting is that this phenomenon evolved to silence foreign DNA

elements. Retrotransposons seem to be over represented around imprinted genes sequences.

Some genetic diseases that map to 15q11 (band 11 of the long arm of chromosome 15) in humans have abnormal imprinting. This region is differentially imprinted on the maternal and paternal chromosomes, and both imprints are needed for normal development. It is possible for an individual to fail to inherit a properly imprinted 15q11 region due to a deletion of the imprinted region or less frequently due to uniparental disomy. If neither chromosome of 15q11 has a paternal imprint, the result is Prader-Willi syndrome (PWS), while if neither chromosome has the maternal imprint, the result is Angelman syndrome (AS)[73]. AS is caused by loss of expression of the E6-associated protein ubiquitin-protein ligase gene (*UB3A*), which is maternally imprinted only in the brain. AS is characterized by epilepsy, tremors and perpetually distorted facial expression. The main cause of PWS is attributed to the paternally imprinted *SNRPN* gene, which encodes the expressed SNURF and SmN spliceosomal proteins (SNRPN-small nuclear ribonucloprotein associated proteins polypeptide N). PWS is characterized by hypotonia, obesity and hypogonadism.

X-chromosome inactivation.

DNA methylation is also involved in the silencing of an entire chromosome in mammals. In each cell in female mammals, one of the two X-chromosomes undergoes inactivation in order to match the gene dosage of the single X chromosome in males. This process also relies on DNA methylation.

Xist, which encodes an untranslated RNA that is involved in X-inactivation, is unmethylated on the inactive X and is methylated on the active X-chromosome. Xist RNA coats the chromosome from which it is transcribed and through a still unclear mechanism contributes to silencing the genes on that chromosome [74]. The maintenance of the silent state on the inactive X chromosome requires methylation [75] [76]. The existence of genes along the inactive X that escape silencing accounts for the defects seen in humans who have an abnormal numbers of the X chromosomes, such as Turner syndrome (X0) or Klinefelter syndrome (XXY). Theoretically, X-inactivation should eliminate the differences in gene dosage between affected individuals and individuals with a normal chromosome complement, but in affected individuals the dosage of these non-silenced genes will differ as they escape X-inactivation.

Cancer.

The signal encoded by methylation of CpG dinucleotides is rather important, so it is at first surprising to note that this dinucleotide is actually underrepresented in 80% of the mammalian genome. This phenomenon is due to the mutagenic nature of CpG methylation: whereas spontaneous deamination of cytosine leads to uracil, deamination of 5-methyl cytosine yields thymine. Since the repair mechanism for G-U base pairs are more efficient than for G-T base pairs, non essential methylated CpGs are frequently mutated, resulting in their under-representation in the genome [77, 78]. (an exception to this are CpG islands as discussed earlier).

Most human cancers display genome wide hypomethylation and concomitant promoter specific hypomethylation of tumor suppressor genes [79-81]. One problem with the idea that alterations in DNA methylation underlie cancer is that no mutations in the recognition machinery have been identified in human cancer. On the other hand there is convincing evidence that constitutive epigenetic alterations are linked to increased cancer risk. An example of this is Beckwith-Wiedemann syndrome, which leads to a 800 fold increased risk of embryonic tumor. Loss of imprinting (LOI) of Igf2 is specifically associated with increased cancer risks in children with Beckwith-Wiedemann syndrome. LOI of Igf2 is also found in adults at a frequency of 5-10%, and it is associated with a 5-fold increase in frequency of malignant or benign colorectal neoplasms.

Generation of mice carrying a hypomorphic allele for Dnmt1 demonstrated that global hypomethylation resulted in aggressive T cell lymphomas that displayed a high frequency of chromosome 15 trisomy. These results indicated that DNA hypomethylation plays a causal role in tumor formation, possibly by promoting chromosomal instability.

Using conditional inactivation of Dnmt3b in Apc $^{min/+}$ mice, our lab has demonstrated that loss of Dnmt3b has no impact on microadenoma formation, which is considered the earliest stage of intestinal tumor formation. However we observed a significant decrease in formation of macroscopic colonic adenomas. Many large adenomas showed regions with Dnmt3b inactivation, indicating that Dnmt3b is required for initiation of macroscopic adenomas but is not required for their maintenance [82]. Consistent with the notion that both promoter hypomethylation and genome wide hypomethylation are functionally important in tumorigenesis, genetic or pharmacologic reduction of DNA methylation levels

results in suppression or promotion of tumor incidence, respectively, depending on the tumor cell type. For instance, DNA hypomethylation promotes tumors that rely predominantly on loss of heterozygosity (LOH) or chromosomal instability mechanisms, whereas loss of DNA methylation suppresses tumors that rely on epigenetic silencing. Apc $^{min/+}$ mice were used to investigate the effect of hypomethylation on intestinal and liver tumor formation. Intestinal carcinogenesis in Apc $^{min/+}$ mice occurs in two stages, with the formation of microadenomas leading to the development of macroscopic polyps. Using a Dnmt1 hypomorphic allele to reduce genome methylation Yamada et al. [83] showed an elevated incidence of microadenomas associated with LOH at the Apc locus. In contrast the incidence and growth of macroscopic intestinal tumors in the same animals was strongly suppressed. These findings suggest a dual role for DNA hypomethylation in suppressing later stages of intestinal tumorigenesis by promoting early lesions in the colon and liver through an LOH mechanism.

Evidence for a function of DNA methylation in the adult CNS.

DNA methylation provides a mode of gene regulation that is maintained through mitosis, providing a mechanism for heritable transcriptional control through development. Are these epigenetic mechanisms also operable in non-dividing, terminally differentiated cells in the adults CNS?

There is a considerable body of evidence, although indirect, implicating the disruption of epigenetic mechanisms as a causal basis for human cognitive disorders. For example, two well characterized disorders caused directly by

improper setting or reading of DNA methylation signals are Rett syndrome and Fragile X syndrome.

Rett syndrome involves a mutation of the methyl CpG-binding protein 2 (*MECP2*)gene, which encodes a protein that binds to methylated DNA sequences. In Rett syndrome, DNA methylation patterns are laid out normally but epigenetic silencing is impaired because of failure of the mutated MECp2 protein to properly recognize this mark. Rett syndrome is an X-linked, pervasive mental retardation disorder, with a prevalence of 1 in 10000 live female births, which is associated with microcephaly and severe cognitive decline.

Fragile X syndrome, also X-linked mental retardation disorder, is brought about by an abnormal expansion of repeated trinucleotide sequences within one of two Fragile genes FMR1 and FMR2 [84, 85]. The genes each contain a polymorphic trinucleotide repeat (CGG or CCG) in their 5' untranslated region. Normally there are 6-50 of these repeats while in Fragile X patients there are up to 230 repeats. The expansion of these repeats results in hypermethylation and transcriptional silencing of the FMR and surrounding genes.

Schizophrenia is a serious disorder of cognition and behavior. A large amount of data indicates that deficiencies in the extra cellular matrix protein reelin are responsible for the etiology of schizophrenia [86]. The promoter of reelin contains several sites for DNA methylation, and inhibitors of histone deacetylase and DNA methyltransferase activities increase expression of reelin, indicating that an epigenetic mechanism governs the expression of this protein [87].

When considering these cases, it is important to distinguish between the developmental need for epigenetic mechanisms that allow formation of a normal

nervous system versus an ongoing need for these epigenetic modifications involved in the cognitive process and the normal functioning of the adult brain. Most of the attention so far has focused on the role of epigenetics in development; however more and more experimental evidence implicates an ongoing and active role for epigenetic mechanism in adult brain function.

MeCP2 and Rett Syndrome.

Rett syndrome (OMIM 312750) provided one of the first strong evidences that epigenetic mechanisms operate in the adult nervous system. The disease was named after the Austrian physician Andreas Rett who first described it. Two young girls with a similar and rather peculiar compulsory hand movement had caught his attention among a group of patients sitting in his waiting room. He followed the two girls' physical and behavioral development and published (in German) a short report on the Viennese Medical Journal [88]. The paper and the condition it described were virtually overlooked until Hagberg and colleagues reported in "Annuals of Neurology" of 35 European girls with Rett Syndrome (RS) and described them as follows: "After normal general and psychomotor development up to the age of 7 to 18 months, developmental stagnation occurred, followed by rapid deterioration of higher brain functions. Within one-and-a-half years this deterioration led to severe dementia, autism, loss of purposeful use of the hands, jerky truncal ataxia, and acquired microcephaly. The destructive stage was followed by apparent stability lasting through decades. Additional insidious neurological abnormalities supervened, mainly spastic parapareses, vasomotor disturbances of the lower limbs, and epilepsy.

Prior extensive laboratory investigations have not revealed the cause. The condition is similar to a virtually overlooked syndrome described by Rett in the German literature. The exclusive involvement of females, correlated with findings in family data analyses, suggests a dominant mutation on one X chromosome that results in affected girls and nonviable male hemizygous conceptuses." [89]. Ten years later the mutation causing RS was located to Xq28 by exclusion mapping studies [90]. Finally in 1999 Amir et al. pinpointed the mutation to the methyl-CpG-binding protein 2 (*MECP2*) locus as the cause of some cases of RTT [91] leading to this unexpected conclusion: "Our study [...] points to abnormal epigenetic regulation as the mechanism underlying the pathogenesis of RTT. By 2001 mutations in the *MECP2* gene were identified in 72% of patients with classical RTT and one third of atypical cases [92]. Over the past few years, more that 2,000 mutations have been reported in females with Rett syndrome [93-96]. There are eight common mutations that arise at CpG hotspots in *MECP2* and result in loss of function due to truncated, unstable or abnormally folded proteins. Genotype-phenotype correlations have given conflicting results but in general truncating mutations tend to be more severe than missense mutations [97]. In addition, skewing of X-chromosome inactivation might modulate the severity of the disorder. More recently, large rearrangements that involve *MECP2*, including deletions, were reported in a significant proportion of patients with Rett syndrome [98]. Altogether, mutations in the *MECP2* gene might account for more than 95% of the sporadic cases of classical Rett syndrome in females. In almost all cases the mutations are de-novo, and there is evidence that they might arise on the paternal X chromosome [99, 100].

As mentioned above there is a proportion of individuals with clinical diagnosis of RS that do not appear to have mutation in the *MECP2* gene. Mutations in two other genes CDKL-5 and *Netrin-G [101]* have been shown to be associated with a phenotype that strongly overlaps with that of RS. In all the cases reported CDKL5 mutations have been associated with an early-onset-seizures variant of RS, the so-called Hanefiled variant. There is some evidence for a direct interaction between CDKL-5 and MECP2, suggesting the possibility of a common pathway in the regulation of neuronal cell function, but it remains to be confirmed how this interaction contributes to the pathogenesis of RS [102, 103]. Conversely *MECP2* mutations have also been found in other clinical phenotypes, including individuals with Angelman-like, non-syndromic X-linked mental retardation [104] and autism [105].

The symptoms and disease progression.

Classic RS diagnosis is based on a number of criteria first defined by Hagberg. The necessary criteria for diagnosis are the following: 1) Normal pre and perinatal history, 2) normal psychomotor development for the first 6 months, 3) normal head circumference at birth followed by 4) postnatal deceleration of head growth. 5) Subsequent loss of purposeful hand skills between 6 month and 2 years, 6) evolving social withdraw 7) loss of acquired speech 8) deterioration of locomotion and cognitive functions. Supportive diagnostic criteria are also: 1) breathing disturbances during waking hours, 2)

abnormal muscle tone (dystonia, muscle wasting), 3) disturbed sleep patterns, 4) progressive kyphosis or scoliosis.

Although it was initially believed that the recognizable features of RS appear after an apparently normal prenatal, perinatal and early infancy period, more recent studies have clearly shown that even in the first 6 months of life the female infants display subtle behavioral abnormalities [106, 107]. A general stagnation of development is followed by the loss of fine and gross motor skills and intellectual functioning. A more definitive clinical presentation evolves in stages over a number of years, culminating in motor deterioration and death in early adulthood. It is clear now that females with RS have a much broader phenotype than first thought, with a number of variants which can be more (patients who never go through a period of normal development) or less (patients with speech preservation and normal head growth) severe symptoms than these seen in classical RS. Moreover it now known that there exists, although rarely, males with *MECP2* mutation who present a severe neonatal onset encephalopathy associated with prominent breathing abnormalities [108].

Human pathology.

A characteristic neuroanatomical finding in RS patients is an overall decrease in brain size that manifest only after 12 months of age. MRI and autopsy examinations reveal that the brain of Rett syndrome patients is smaller than age matched controls, and that, unlike the brain in a degenerative disease, it does not become progressively smaller over time. Moreover, only the brain, and no other organ, is small, emphasizing the susceptibility of the nervous

system in the Rett disorder. Volumetric studies in patients (MRI) show preferential decrease in prefrontal, posterior and anterior temporal regions. The neuron's soma is smaller and there is an accompanying increase in cell density per unit of volume [109] but the total number of neurons appears normal. No neurodegeneration has ever been observed [110] and there seem to be no problems with neuronal migration [111].

According to some early reports, there is a selective decrease in dendritic branching and spine number with a concomitant reduction in cortical thickness in the same areas where the reduced volume was observed [112-114]. Immunocytochemical studies defined alterations in synaptic sites, early-response genes and MAP-2 immunoreactivity was altered in selected neuronal populations. Studies of neurotransmitters expression using various techniques in diverse brain regions or cerebrospinal fluid have given contrasting results, with only, the studies on cholinergic neurotransmission showing a consistent decrease. The hypothesis that neurotransmitters levels are decreased in Rett syndrome remains attractive, because it explains many of the functional deficits in Rett syndrome, and suggests a mechanism for defective brain maturation. However, the measurement of neurotransmitters and the interpretation of the results is problematic because the studies have included girls and women at different stages of the Rett disorder using different techniques on different tissues.

Other genes have been found to have altered expression in post-mortem tissue from Rett patients, for example mRNA levels for the N-methyl D-Aspartate (NMDA) type glutamate receptors NR1 subunit and metabotropic mGluR1 receptor were increased 1.5 folds while synapse related proteins such

as synapsin II, synaptogirin 3, synaptogamins 1,5 and syntaxin 1a were decreased [112].

It has to be taken in consideration that all of the data regarding the dendritic morphology and the synaptic markers come from autopsies of small cohorts of patients at different ages and stages of the disease published by two research groups. In contrast to the finding in humans, morphological studies on fully symptomatic MeCP2 mutant mice [115] [116] did not reveal any dendritic abnormality or misexpression of synaptic markers. Conversely Fukuda et al. [117] noticed a reduction in cortical thickness and reduced spine counts in the MeCP2 null mice [118]. So, in our opinion it remains an open question of whether the morphological abnormalities observed in post-mortem human tissues are the cause or the consequence of the functional defects in RS.

Cause of death in patients.

Rett patients (females) might be able to survive into middle and old age but their life expectancy is reduced by a higher incidence (26%) of sudden death (SD) compared to that seen in the normal population (1/100K). Possible causes of SD in RS are autonomic failures, apnoea and cardiac arrhythmias. In 1997 histological examination of 6 postmortem samples from Rett patients who died of SD revealed some anatomic abnormalities. In contrasts a more recent study involving 32 Rett syndrome girls evaluated by echocardiography did not show any cardiomyopathy [119]. Around 20% of the patients show a significant prolongation of QT corrected intervals (QT interval is a measure of the time between the start of the Q wave and the end of the T wave in the heart's

electrical cycle). The cause of this abnormality is still not clear. There does not seem to be a sympathetic hyperactivity but low NGF (Nerve Growth Factor) plasma levels were observed suggesting a possible role for neurotrophic factors in the pathology. Another 26% of the deaths in RS girls is attributed to sudden respiratory arrhythmias [120]. Breathing seems normal during sleep but can switch from highly irregular to regular breathing during wakefulness [121], which would suggest a disturbed cortical rather than a brainstem problem. This symptom might also be caused by an improper expression of neuromodulators in the medulla [122]. The bioaminergic alterations observed in *Mecp2*-deficient mice could be responsible for their respiratory disorders and compensating for these bioaminergic deficits could alleviate their respiratory disorders.

Structure of the mouse *Mecp2* gene.

The *Mecp2* gene which is located on the X-chromosome (Xq28) spans over ~ 50 Kb. It is composed of 4 exons which are alternatively spliced, creating two transcripts that produce two different protein (MeCP2e1 and MeCP2e2) that have different ATGs and differ by only 17 amino acids at the N-terminus. Although both forms are highly expressed in the brain, they differ in translational efficiency and are expressed at different amounts in various tissues, with MeCP2e1 being more prevalent in the brain, thymus and lung [123]. Additional *Mecp2* transcripts with 3' UTRs of different length are also

produced by the use of alternative poly-adenylation sites. Their expression also varies between tissues and developmental stages (figure 2).

Structure of the protein and expression pattern.

The *Mecp2* gene encodes a ~500 amino acid protein that has three recognizable domains. A methyl binding domain (MBD) that mediates the DNA-protein interaction, a transcription repression domain (TRD) that mediates protein-protein interaction and a third domain in the carboxy terminus that has homology to the members of the forkhead family of transcription factors but has no known function in MeCP2 [124]. MeCP2 has an important role in interpreting the methylation mark on DNA, but how does this translate into functional consequences? Several different mechanisms have been proposed. First, MeCP2 binding might influence local nucleosome position; alternatively MeCP2 could serve to recruit a enzymatic machinery which is responsible for the stable transcriptional repression. The transcriptional repressor domain (TRD) has been shown to interact with various co-repressor complexes such as Sin3a, ci-Ski, and N-Cor [125-127]. These silencing complexes include histone methyltransferases [128] and histone deacetylases (HDAC1 and 2) [126]. MECP2 transcriptional repressor activity is in fact sensitive to HDAC inhibitors, but there is also a MeCP2-dependent repression that is refractory to HDAC inhibitors, suggesting that some other mechanism might be involved. Harikrishnan et al. reported an interaction between MeCP2 and the SWI/SNF chromatin-remodeling complex [129] although this finding has been recently disputed [130].The SWI/SNF complex uses energy from ATP hydrolysis to alter local chromatin

structure [131]. Interestingly MBD2 and MBD3 also, have been found in a stable complex with a chromatin-remodeling ATPase similar to SWI/SNF [131].Another interesting mechanism of action for MeCP2 mediated silencing was proposed in 2005 by Horike et al. The group has found that MeCP2 binds to a cluster of imprinted genes comprising Dlx5 and DLX6 on chromosome 6 and induces the formation of a 11kb long silent chromatin loop [132]. Moreover Dlx5 and Dlx6 were found upregulated (having biallelic instead of monoallelic expression) in MeCP2 KO mice and in lymphoblastoid cells of Rett syndrome patients. Dlx5 regulates production of enzymes that synthesize gamma-aminobutyric acid (GABA); therefore loss of imprinting of Dlx5 may alter GABAergic neuron activity an in individuals with Rett syndrome. (An increased density of GABA receptors in Rett syndrome patients was reported years before [133]) . The conclusion from these observations was that formation of a silent-chromatin loop is the mechanism underlying gene regulation by MeCP2. However, once again, these results turned out difficult to reproduce, to the point that it is even debatable whether in human cells Dlx5 and Dlx6 are subject to imprinting at all [134].

There is little correlation between the levels of *Mecp2* mRNA and protein suggesting that regulation of this gene is at the translational level [135, 136]. The protein is expressed in several tissues in adult mice; in particular it is high in brain, lung and spleen, lower in heart and kidney and barely detectable in liver, stomach and small intestine [135, 136] (figure 3).

In the mouse brain MeCP2 is expressed strongly in neurons (a weak expression has been reported in astroglia) and its expression starts at around E18.5 and correlates with the maturation of the nervous system. Ontogenically older structures such as brain stem and spinal cord express MeCP2 before

newer structures such as hippocampus and cerebral cortex. In the cortex MeCP2 first appears in the Cajal-Retzius cells, then in the deeper and more mature cortical layers and progressively comes on in the neurons of the more superficial layers. Eventually all neurons become positive although differences in the intensity of the staining persist among different neuronal populations. This suggests that MeCP2 becomes abundant only when a neuron has reached a certain stage of maturity. [135, 136] (figure 4).

Interestingly, in the human brain, the number of MeCP2 positive neurons increases dramatically through gestation and continues to increase in the cortex from birth until 10 years of age. This difference between the mouse and human expression in the brain could represent the extended period of developmental plasticity in humans, in which neurons have not achieved their fully differentiated state [136] Examples of experience-dependent plasticity are abundant for several areas of the brain like visual, auditory and somatosensory cortex [137]. The cellular basis of this plasticity is thought to involve several aspects of neuronal physiology like synaptogenesis, myelination, and neuronal transmitter expression. Also in humans the time course of glucose utilization and synaptogenesis increases between birth and 4 years, followed by a plateau until age 10, after which it slowly declines during adolescence to adult levels [138]. The correlation between MeCP2 expression, glucose utilization, synaptogenesis and experience-dependent plasticity in humans is again very suggestive of a role for MeCP2 in very mature neurons. Indeed several studies conducted in the olfactory bulb [139], hippocampus, and cerebellum [140] in mice have shown that MeCP2 expression is exactly timed with synapse formation. Indeed lower levels of several dendritic specific and synaptic proteins

have been found in brain tissue from patients with Rett syndrome [141] [112, 142, 143]. Yet it is not clear what it is the functional relevance of these observations.

Mouse models for Rett syndrome.

The interest in creating a transgenic mouse with a deletion of the *Mecp2* gene arose well before the discovery that mutations in this locus were responsible for Rett syndrome. In 1999 Tate et al., using homologous recombination created male ES cells with a complete deletion of the *Mecp2* coding sequence and showed that these cells were unable to support embryonic development beyond E8.5-12 (E: embryonic day) [144]. The conclusion was that MeCP2 and DNA methylation were essential for embryonic development. To overcome the problems connected with studying an early lethality phenotype two groups subsequently generated conditional *Mecp2* alleles in which exon3 [145] or exon 3 and 4 [118] were flanked by loxP sites. In this set of experiments the *Mecp2* conditional allele was deleted using a Cre recombinase driven by a promoter (Nestin) that becomes active in neuronal precursors at around E10.5 (it is also weakly active in kidney, heart, lungs and germ cells). Both germline and CNS recombined hemizygous null males were derived from the experiment and surprisingly both sets of mice displayed an almost identical phenotype. *Mecp2* germline and CNS recombined null males (hemizygous) were born seemingly normal, but developed symptoms between 3 and 8 weeks and died within 15 weeks. They exhibited severe motor deficits, stereotypic back limb clasping, abnormalities in gait and grip strength, reduced motor

coordination, reduced dark cycle locomotor activity, severely impaired swim performance and they were not fertile. In addition to motor and cognitive deficits, the nulls exhibited changes such as piloerection, breathing irregularities, and body tremors that may reflect impaired autonomic functioning. These motor deficits are consistent with the human pathology of Rett syndrome; moreover, these behavioral changes are associated with a significant volumetric reduction in the striatum (29%), the amygdala and the hippocampus. Surprisingly, in the mice the reduced volumes in two other motor regions frequently noted in the human pathology, the frontal cortex and cerebellum, were not observed [141]. However one group has reported decreased cortical thickness in the motor and somatosensory cortex of the hemizygous mice with reduced spine density in layer II and III [117]. Female mice that are heterozygous for MeCP2 were also viable, fertile and seemed normal until adulthood. However at about 6 months of age these mice began to show the same neurological symptoms that were seen in the null males.

In another set of experiments the conditional *Mecp2* allele was ablated using a cre recombinase driven by the Cam kinase promoter that is active postnatally (P0-P15) in the forebrain, hippocampus and brainstem. The development of these mice (male hemizygous) was normal until 3 months when some mild symptoms appeared such as ataxia, hypoactivity, and reduced brain weight [146]. This was the first evidence that MeCP2 is required not only during neuronal development but also in the mature CNS. The analysis of the conditional knock out mice was remarkably informative because it demonstrated that MeCP2 is dispensable for early embryonic development and that a restricted deletion of MeCP2 in the CNS is sufficient to induce symptoms.

Because Rett syndrome patients do not carry deletions of the *Mecp2* coding sequence but rather have point mutations that cause missense or premature stop codons, a third mouse model that would better mimic the human disease was generated in 2001 by Shahbazian et al.[147]. In this model the MeCP2 protein is truncated after codon 308 ($MeCP2^{308}$), retaining all the known functional domains such as the methyl binding domain, the transcriptional repression domain and the nuclear localization signal.

$MeCP2^{308}$ mutants are viable and fertile (both males and females) but at around 6 months of age exhibit some motor coordination and social interaction defects. Early experiments performed in $Mecp2^{308}/Y$ mice with mixed genetic background did not reveal learning abnormalities using the Morris water maze and fear conditioning tests [147]. Later experiments by Moretti et al. on a pure inbred strain (129/SvEv) and using a less intense training schedule did instead show a deficit in learning and memory [115]. (A summary of the mouse models and their respective features is presented in figure 5).

A poorly understood aspect of RS is the disease progression. Early development seems relatively normal and, although recent studies have shown that even in the first 6 months of age RS girls display subtle behavioral abnormalities, the diagnosis of the disease occurs usually at 1year of age or later. A long standing question, therefore, has been whether the appearance of symptoms is the manifestation of irreparable damage to the brain that occurred during pre and peri natal development or if it is due to the specific requirement for MeCP2 in mature CNS function. The question is particularly relevant as the answer will impact the development of a therapy. Would post-natal treatment be efficacious, at least in principle, or is there need for pre-natal screening?

Using the mouse models it has been possible to demonstrate that MeCP2 is indeed required in the adult CNS, as shown by the fact that post-natal deletion (P0-P15) induced the appearance of RS like symptoms. This study, however, did not rule out the possibility that MeCP2 was also required for proper neurogenesis and early brain development. In Chapter 1 evidence that MeCP2 is in fact dispensable for neurogenesis is presented.

Further characterization of the disease progression.

A further question that arises from these experiments is how late in development or adulthood can reactivation of MeCP2 function lead to rescue of the symptoms? The presence of largely normal brain architecture and the absence of neurodegeneration in RS would suggest that no irreparable damage to the structure has occurred because of MeCP2 deficiency and that once this function is restored there is the potential for reversal of the symptoms, partial or complete. Alternatively, MeCP2 might be essential for neuronal function during a specific time window, after which physiological damage caused by its absence is irreversible. Evidence that specific reactivation of MeCP2 in the brain during postnatal development does indeed lead to partial rescue of the RS phenotype is described in Chapter 2.

Rett syndrome a disease of synapse formation?

Physiological characterization of the MeCP2 null mutant mouse.

Some of the cognitive and behavioral abnormalities observed in RS patients have interesting similarities with non-syndromic mental retardation in males and females [148], mild learning disabilities [149] and autism [105]. So understanding the role of MeCP2 in normal and pathological brain function might be informative not only for RS but for other disorders. The development of mouse models has made possible a more detailed characterization of the molecular anatomical and behavioral aspects of the disease yet a clear understanding of the functional aspects of neurotransmission and synaptic plasticity affected by the loss of MeCP2 remains elusive.

In recent years there has been an effort to shed light in this direction and to test the hypothesis that RS is a disease of improper synaptic development/plasticity. Dani et al. in 2005 first characterized cortical activity in male KO mice [150] using whole cell patch clamp recordings in acute cortical slices and observed a reduced spontaneous firing rate. This decrease was apparently not caused by a change in the intrinsic excitability of these cells but rather by an increase in total inhibitory input over excitatory inputs. Moreover a small reduction in miniature EPSCs (excitatory postsynaptic currents) was observed. Interestingly Dani et al. were able to measure a reduction in firing rate also in samples from 2 weeks old mice, suggesting that what they were observing was causative of the symptoms and not consequential. Unfortunately given the complexity of cortical circuitry it was not possible to identify exactly the signaling pathways that link the lack of MeCP2 to a shift in balance between excitation and inhibition. Chao et al. using autaptic hippocampal cultures (from neonatal brain) carried out an in depth electrophysiological analysis of the reduced excitatory activity and put forward an explanation for the decrease. The

group reported a reduced number of glutamatergic synapses both in vitro and in vivo, in the hippocampal CA1 neurons, as demonstrated by a 40% decrease in VGLUT1 (Vescicular Glutamate Transporter 1) and PSD95 (Post-synaptic density 95) staining [151]. This difference in synapse number was present only in 2 weeks old autaptic MeCP2 KO cultures or in mice younger than 4 weeks of age. It is difficult to explain why the observed anatomic abnormalities disappear after two weeks while the symptoms (both electrophysiological and behavioral) worsen. It is conceivable that MeCP2 plays a role in synapse development, which is at the basis of what Chao et al. observed, and also has a role in synapse maintenance, which becomes more important later in age. MeCP2 deficiency could affect different brain regions in different ways, so conclusion from experiments conducted in the cortex might not be generalized to the whole system.

Another effort to understand the functional aspects of neurotransmission that are lost in the absence of MeCP2 was made by Asaka et al. and Moretti et al.. Both groups looked at long-term potentiation (LTP) and depression (LTD) in the CA1 of the hippocampus either in MeCP2 KO mice or in MeCP2^{308} mouse mice. LTP and LTD are a measure of activity dependent synaptic plasticity, which according to some studies provides the basic mechanism for learning and memory. Although memory per se has not be investigated in RS girls, cognitive abnormalities are definitively present and the study of LTP and LTD might shed some light on the fundamental synaptic mechanisms affected by RS. A common finding in the study of Asaka et al. and Moretti et al. is a general reduction of both LTP and LTD response (this phenotype was observable in fully symptomatic animals only). In order to look for the origin of the reduction in LTP response,

both groups examined general basal neurotransmission (in the Shaffer collateral synapses), and found that while MeCP2^{308} mice showed an enhancement in synaptic transmission, the MeCP2 KO mice did not show any change in basal transmission. Moreover both MeCP2 KO and MeCP2^{308} mice showed a reduction in PPF (paired pulse facilitation), which would suggest the presence of a defect in pre-synaptic function as well. Given that the precise molecular mechanism underling the LTP and LTD responses are not well understood it is difficult to draw conclusions about the role of MeCP2 in synaptic plasticity from these experiments. It remains an open question in fact whether these experiments are measuring direct effects of the loss of MeCP2 or the result of the compensatory responses. In support of the former hypothesis is the fact that a similar reduction in LTP responses has been noticed also in cortical slices from Huntington's mouse models [152] l. Interestingly in both in the Huntington's mouse ad in the Rett mouse the authors noticed that despite the finding that LTP, on average, was significantly impaired in mutant compared with wild-type animals, a small number of mutant slices had an LTP that was comparable to wild type levels suggesting that the mutation does not disable the LTP mechanism all together, but rather raised the threshold for inducing it. Reduced LTP responses are consistent with the overall reduced excitatory cortical activity seen by Dani et al. but are somewhat in discordance with some of the clinical observation in patients which often display abnormal electro-encephalograms, seizures, and prolonged episoded of screaming or crying. In patients motor cortex stimulation evoked motor action potentials at low threshold and with abnormally short latencies and prolonged durations, suggesting an enhanced excitatory activity in the motor cortex in RS subjects under investigation

[153].Previous studies have speculated that the RS brain may be stalled in an immature stage of development but if this was the case one would expect increased synaptic plasticity and LTP and LTD responses.

Neurotrophic factors.

One very important piece of information that would help to correctly interpret the behavioral and physiological data gathered so far is the systematic knowledge of all direct targets of MeCP2 regulation. Gene expression profiling in the mouse knock out model of *Mecp2* have been unable to point at any disregulation of potential target genes in the MeCP2 KO brain [154]. The heterogeneity of brain tissue might have increased noise levels in these experiments and masked some potential targets. It is also possible that MeCP2 controls a different sets of genes in different neuronal populations. For this reason attempts to repeat gene profiling experiments using genetic markers to isolate specific neuronal subpopulations is underway in several laboratories. At the same time the advent of a new technology that combines chromatin immunprecipitations and genome wide hybridization (Chip-CHIP) could potentially reveal genes that are specifically bound by MeCP2.

So far though only a handful of targets of MeCP2 are known. One of the first to be isolated is Brain Derived Neurotrophic Factor (BDNF) [155]. BDNF is a trophic factor that plays an important role in neuronal survival, development [156, 157] and plasticity [158, 159]. BDNF is highly expressed in neurons and its transcription is upregulated by membrane depolarization in vitro and by neuronal activity during kindeling or induction of long term potentiation.

In primary cortical neuron cultures MeCP2 binds specifically to *BDNF* promoter III and functions as a negative regulator of expression. In response to neuronal activity-dependent calcium influx, MeCP2 becomes phosphorylated and is released from the *BDNF* promoter thereby facilitating transcritption [160]. Chen et al. concluded that MeCP2 plays a key role in the control of neuronal activity-dependent gene regulation and that the deregulation of this process is a key cause to the pathology. Contrary to expectations though, MeCP2 KO mice have lower BDNF levels than normal (70% of wt). Qiang et al. postulated that, given that BDNF transcription is activity dependent, the observed low excitatory cortical activity in the KO mice might explain why levels of BDNF are lower instead of higher. In this circular argument low BDNF levels are both causative and consequential to the symptoms. In support of the causative hypothesis Qiang et al. also points at the similarities between the phenotypes of MECP2 KO mice and BDNF conditional KO mice, namely a decreased brain and neuronal cell size in the hippocampus which are consistent with an generic atrophic response. In their study Qiang et al. were able to show that over expression of BDNF in the frontal cortex can delay the onset of Rett like symptoms and rescue some of the behavioral and electrophysiological phenotypes described for the MeCP2 KO mice in Dani et al. Ectopic overexpression of BDNF also rescued the cells size phenotype (no data are presented on the brain weight phenotype) [161]. So although the study does not reveal whether BDNF and MeCP2 act through the same pathway it suggests that some of the symptoms might be an atrophic response driven by the low levels of BDNF expression, and although BDNF is only one of the targets of MeCP2 it is the first one shown to be able to modulate the disease progression. Over expression of such a pleiotrophic factor in the

brain has been shown to ameliorate symptoms also in a mouse model of Huntington's disease [162, 163]. This suggests a possible therapeutic opportunity by the manipulation of the expression of BDNF or other neurotrophic factors in cognitive disorders such as RS, schizophrenia, depression and other autistic spectrum disorders. Some data in support of this hypothesis are presented in Chapter 3.

Figure 1. The methyl-CpG-binding proteins (MBPs) family. Six mammalian MBPs have been characterized so far. Kaiso is an atypical MBP, because it depends on a zinc-finger domain (ZF) to recognize methylated DNA and a POZ/BTB domain to repress transcription. MBD1 uses its methyl-binding domain (MBD) to bind methylated DNA sequences. In addition, MBD1 contains three zinc-binding domains (CxxC), one of which binds specifically to non-methylated CpG dinucleotides, and a C-terminal transcriptional repression domain (TRD). MBD2 possesses an MBD that overlaps with its TRD domain, and a GR repeat at its N terminus. MBD3 contains a well-conserved MBD domain that does not recognize methylated DNA owing to crucial amino acid changes. MBD4 binds methylated DNA through an MBD domain and has a C-terminal glycosylase domain that is important for is function in DNA repair. MeCP2 is the founding member of the MBD protein family and contains a conserved MBD domain and an adjacent TRD domain.
Klose R.J. et al. Trends in Biochemical Sciences 2006 31: 89-97

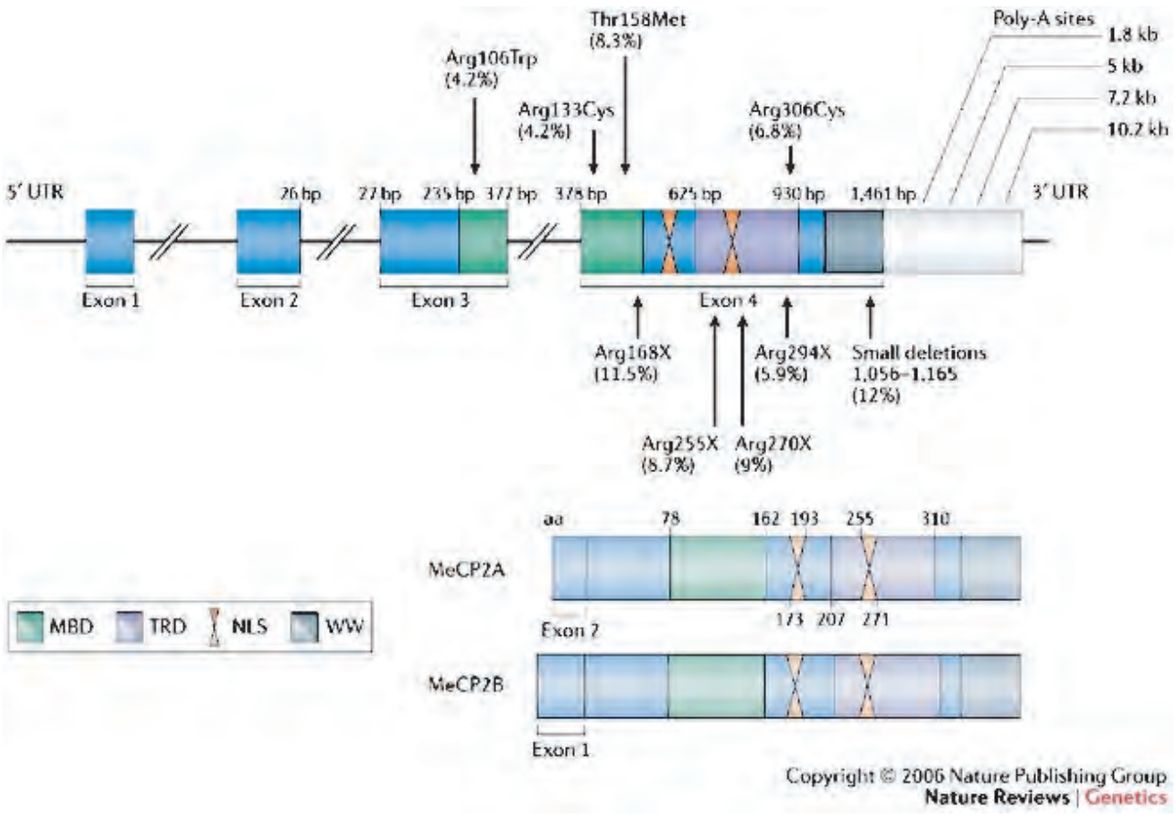

Figure 2. MECP2 (methyl-CpG-binding protein 2) gene structure. The positions and frequencies of the most common mutations that are associated with Rett syndrome in females are indicated. b | The two main protein isoforms, MeCP2A (486 amino acids) and MeCP2B (498 amino acids), are produced by alternative splicing of the MECP2 transcript and differ in their N-terminal regions, which are encoded by exon 2 of the gene in the case of MeCP2A and exon 1 in MeCP2B. MBD, methyl-CpG binding domain; NLS, nuclear localization signal; poly(A), polyadenylation; TRD, transcriptional repression domain; X, stop codon.
Bienvenu et al. Nature Reviews Genetics (2006) 7, 415-426

Figure 3

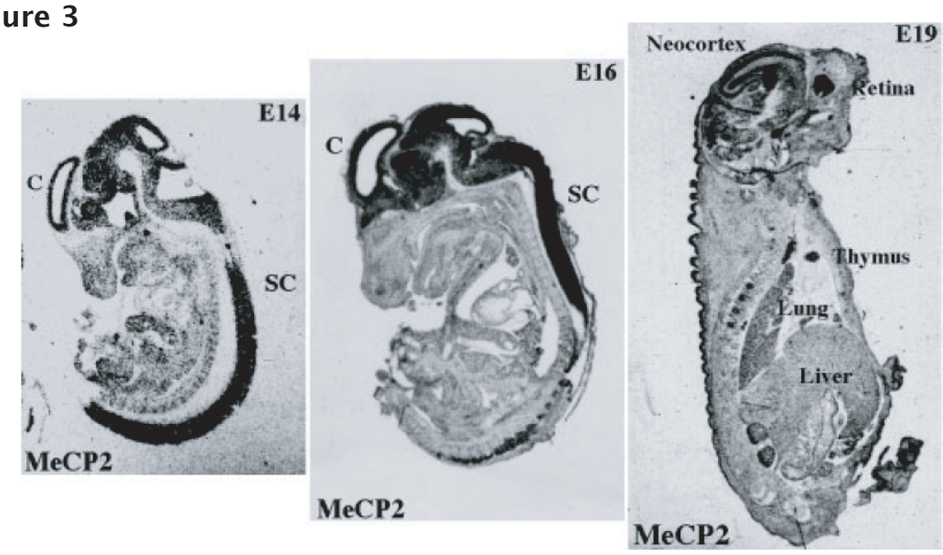

A. MeCP2 mRNA is strongly expressed in the embryonic brain. Antisense in situ hybridization conducted on sagittal sections obtained from days E14, E16, and E19 embryos illustrating the mRNA expression pattern of MeCP2. Peripheral tissues are as indicated. SC, spinal cord;

Embryonic Peripheral Tissues										
	Heart	Liv	Int	Lung	Thy	Kid	Spleen	Skin	Musc	Adp
E14	+	+	+	−	NT	NT	NT	NT	+	NT
E16	+	++	+	++	+	+	NT	+	−	−
E19	+	++	++	++	++	+++	+	+++	++	++

Central Nervous System											
	Cor	Pir	Hippo	Stri	OB	Thal	Amy	Pons	Cer	SC	Ret
E14	++	ND	ND	+	NT	+	NT	ND	ND	+++	NT
E16	+++	ND	+	+	++	+	NT	+	+	+++	+++
E19	+++	ND	+	++	++	+	NT	+	+	+++	+++
P0	+++	+	+	++	++	+	NT	++	+	++	NT
P2	+++	++	++	++	+++	++	+	++	++	++	NT
P8	+++	++	+++	++	+++	++	+	+	++	++	NT
P16	+++	+++	+++	++	+++	++	+	+	+++	++	NT
Adult	+++	+++	+++	++	+++	++	+	+	+++	++	NT

B.The relative expression levels of MeCP2 mRNA are presented for peripheral tissues during late embryonic development, and for different regions of the brain throughout development. Strong (+++), moderate (++), faint but above background (-), and background ( ) reflect the relative intensity of equal exposure time images. ND indicates the structure was not developed at the time of examination, and NT indicates the region was not tested. The abbreviations are as follows: Liv=liver, Int=small intestine, Thy=thymus, Kid=kidney, Musc=muscle, Adp=adipose tissue, Cor=neocortex, Pir=piriform cortex, Hippo=hippocampus, Stri=striatum, OB=olfactory bulb, Thal=thalamus,Amy=amygdala,Pons=pontinenucleus,Cer=cerebellum, SC=cervical spinal cord, Ret=retina.
Jung, B. P. J Neurobiol (2003) 55:86-96

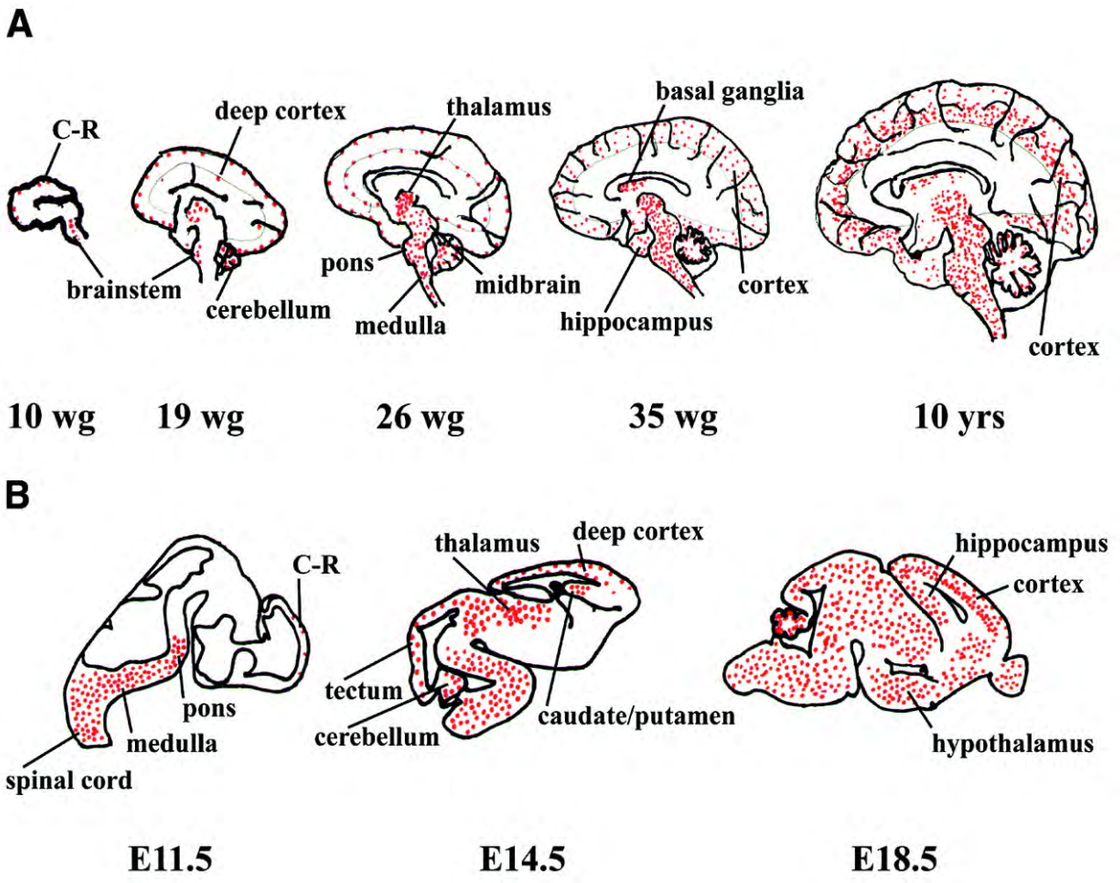

Figure 4. Schematic representation of the spatial and temporal distribution of MeCP2 during human and mouse development. The distribution of MeCP2 at selected ages during (A) human and (B) mouse CNS development is illustrated. The presence of MeCP2 is indicated with red dots. MeCP2 initially appears in the spinal cord, specific brainstem nuclei and in the Cajal–Retzius neurons (C–R) of the cerebral cortex. Expression is then seen in the midbrain, thalamus, cerebellum and deep cortical layers. MeCP2 appears later in the basal ganglia, hypothalamus, hippocampus and latest in the superficial cortical layers.
Shahbazian M. D. et al. Hum. Mol. Genet. 2002 11:115–124;

Figure 5
Comparison between mouse models and human RTT

Characteristic	Chen et al. (2001) (current study)	Guy et al. (2001)	Shahbazian et al. (2002)	Pelka et al. (2006)	Rett syndrome (Hagberg et al. 1985)
Mutation	Deletion of exon 3	Deletion of exon 3 and part of exon 4	Truncated after amino acid 308	Deletion of exon 3 and part of exon 4	Mutations in the MECP2 in about 80% of cases
Onset of symptoms	M: 3 wk F: ~3 mo	M: 4 wk	M: 6 wk	M: 4 wk F: 13 wk	F: 6–10 mo
Lifespan	M: ~75 d F: >1 y	M: ~10 wk	M: Most >1 y, but some die by 10 mo	M: ~5 wk	Shorter than normal
Motor deficits/gait ataxia	M: Hypoactive,[a] swimming difficulties,[a] hind limb clasping[a] F: Hypoactive,[a] normal swimming[a] at 6–8 wk	M: Stiff, uncoordinated gait at 3–8 wk F: Stiff, uncoordinated gait; hypoactive at 3–8 wk	M: Difficulties with wire suspension; rotorod deficits at ~8 wk F: Difficulties with wire suspension at 35 wk	M: Hypoactive; rotorod deficits; unusual gait; hind limb clasping	Gait ataxia; loss of fine motor coordination
Stereotypic behaviors	Yes[a]	Yes	Not reported	Not reported	Hand wringing or flapping
Autonomic irregularities (hair changes, tremors, breathing)	Yes[a]	Yes	Yes	Yes	Yes
Seizures/abnormal EEG	Not reported	Not reported	Yes	Yes	Yes
Anxious behavior	M: Altered plus/zero maze behavior[a] F: Altered plus/zero maze behavior,[a] increased thigmotaxis[a]	Not reported	M: Less exploratory activity	M: More time in open arms	Yes
Cognitive performance	M: Impaired fear conditioning,[a] impaired object recognition[a] F: Normal spatial learning[a] and fear conditioning,[a] impaired object recognition[a]	Not reported	Not observed	M: Impaired cerebellar learning; both contextual and cued fear conditioning deficits	Mental retardation; loss of speech
Social interactions	Not reported	Not reported	HM: abnormal on resident intruder tests	Not reported	Some autistic traits; reduced social interactions

F, heterozygous females; M, hemizygous males.
[a] Reported in the current study.

N. A. Stearns et al. Neuroscience 146 (2007) 907–921

Chapter 1

Title:

"Expression of MeCP2 in post mitotic neurons rescues Rett Syndrome in mice".

Sandra Luikenhuis[*], Emanuela Giacometti[*], Caroline F. Beard[*], Rudolf Jaenisch[*†]

[*] Whitehead Institute for Biomedical Research, Massachusetts Institute of Technology, 9 Cambrigde Center, Cambridge, MA 02142

[†] To whom correspondence shout be addressed. Telephone (617) 258-5000, Fax (617) 258-6505, *jaenisch@wi.mit.edu*

Contributions: Emanuela Giacometti assisted in targeting the Tau Mecp2 construct into Es cells and generated Figures 2B and 2C-R. Caroline Beard was involved in the experimental design.

Data presented in this chapter have been published in *Proc Natl Acad Sci USA* (2004) **101**:6033-6038

Abstract

Mutations in *MECP2* are the cause of Rett syndrome (RTT) in humans, a neurodevelopmental disorder that affects mainly girls. MeCP2 is a protein that binds CpG dinucleotides and is thought to act as a global transcriptional repressor. It is highly expressed in neurons, but not in glia, of the postnatal brain. The timing of MeCP2 activation correlates with the maturation of the central nervous system and recent reports suggest that MeCP2 may be involved in the formation of synaptic contacts and may function in activity-dependent neuronal gene expression. Deletion or targeted mutation of *Mecp2* in mice leads to a Rett-like phenotype. Selective mutation of *Mecp2* in postnatal neurons leads to a similar although delayed phenotype, suggesting MeCP2 plays a role in postmitotic neurons. Here we test the hypothesis that the symptoms of RTT are exclusively caused by a neuronal MeCP2 deficiency by placing *Mecp2* expression under the control of a neuron-specific promoter. Expression of the *Mecp2* transgene in postmitotic neurons resulted in symptoms of severe motor dysfunction. Transgene expression in *Mecp2* mutant mice, however, rescued the RTT phenotype.

Introduction.

Rett-syndrome (RTT), a neurodevelopmental disorder, is a leading cause of mental retardation in females with an estimated prevalence of 1 in 10,000 to 15,000 female births. RTT patients develop normally until 6-18 month of age when they start to show symptoms including respiratory irregularities, progressive loss of motor skills, stereotypic hand movements, seizures, and features of autism. Examination of the brain reveals profound microencephaly due, at least in part, to smaller, more densely packed neurons. Other

abnormalities include a reduction in dendritic arborization (1, 2). In about 80 % of cases, RTT is associated with mutations in the X-linked *MECP2* gene that is subject to inactivation when located on the inactive X-chromosome (3). Therefore, heterozygous mutant females are mosaic for MeCP2 deficiency and show a wide range of phenotypes. Males, however, show a more severe phenotype usually involving encephalopathy, motor abnormalities and respiratory dysfunction. They rarely live beyond 2 years (2).

Mecp2 encodes a protein that binds specifically to methylated CpG dinucleotides and recruits chromatin remodeling complexes that contain the transcriptional repressor Sin3A and histone deacetylases 1 and 2 (4). In mouse, the protein localizes to highly methylated pericentromeric heterochromatin (5). Though MeCP2 is found in most tissues and cell types, highest expression levels are detected in the brain where it is primarily present in neurons but not in glia (5-7). The timing of *Mecp2* expression correlates with the maturation of the central nervous system (CNS) (5, 8) and recent reports suggest that MeCP2 may be involved in the formation of synaptic contacts (9). Although biochemical evidence suggests that MeCP2 acts as a global silencer, transcriptional profiling has failed to detect global changes in gene expression (10). A candidate approach has identified *BDNF*, a gene involved in neuronal survival, development, and plasticity, as a target for MeCP2 (11). These findings are consistent with MeCP2 playing a role in the maintenance and modulation of neuronal maturity. In particular, MeCP2 may function as a key regulator of activity-dependent neuronal gene expression.

Complete or partial deletion of *Mecp2* in mice leads to a neurological phenotype that is similar but less severe than human RTT (12, 13).

Heterozygous females remain healthy into adulthood. In contrast, *Mecp2* mutant males appear normal and healthy at birth but begin to show a phenotype that resembles the human condition at 3 to 8 weeks of age, and die at 6 to 10 weeks of age. Mutant brains show a reduction in brain weight and neuronal cell size but no obvious structural defects or signs of neurodegeneration. Conditional mutation of *Mecp2* in the neural progenitor cells at embryonic day 12 results in a phenotype identical to that of the null mutation (12). Mutation of *Mecp2* in the postnatal neurons of restricted regions in the brain leads to a similar although delayed neuronal phenotype, suggesting MeCP2 plays a role in postmitotic neurons (12). Here we test the hypothesis that the phenotype is exclusively caused by a neuronal MeCP2 deficiency by placing *Mecp2* expression under the control of a neuron-specific promoter. Overexpression of the *Mecp2* transgene in postmitotic neurons proved to be detrimental and lead to symptoms of severe motor dysfunction. Transgene expression in *Mecp2* mutant mice, however, resulted in a rescue of the RTT phenotype.

Materials and Methods

Gene targeting construct.

To introduce the *Mecp2* coding sequence as an in-frame fusion into exon 1 of the *tau* locus we first cloned a 3.8 Kb *Kpn*I/*EcoR*I fragment from pHV, which contains 14 Kb of *tau* genomic sequence (kindly provided by K. Tucker) into pBluescript (Stratagene) generating pTau-KR with a unique *Nco*I cloning site. Next we eliminated a unique *Spe*I site in the polylinker of pTau-KR by cutting the vector with *Spe*I, treating it with the DNA polymerase I Klenow fragment

(New England Biolabs) and religating it. We created pTau-KR-linker by introducing suitable restriction sites to allow the in-frame fusion. We inserted an adapter that destroyed the *Nco*I cloning site while introducing a new *Nco*I site that was shifted by 2 bp, plus a *Spe*I and an *EcoR*V site. The primers used were TAUadapt-F (5'-TTT GGT CAT GAT GCC ATG GAC TAG TCG ATA TCT CAT GAG ATT A-3') and TAU-link-R (5'-TAA TCT CAT GAG ATA TCG ACT AGT CCA TGG CAT CAT GAC CAA A-3'). The 1455 nucleotide-long coding sequence of *Mecp2* was amplified by PCR from IMAGE clone 1395411 (AI181668) and confirmed by sequencing. The PCR primers introduced a modified Kozak sequence including an *Nco*I site (ATTCC**ATG**G was changed to CCACC**ATG**G) and restriction sites that facilitated cloning. Primer RI-MeCP2-F (5'-cggaattccgccaccatggtagctgggatgttaggg-3') added an *EcoR*I site 5' of the sequence, and primer Xba-MeCP2-R (5'-gctctagagctcagctaactctctcggtcacg-3') added an *Xba*I site to the 3' end. To provide the construct with an SV40 late polyadenylation signal (SV40pA) we next cloned the *EcoR*I/*Xba*I MeCP2 fragment into the *EcoR*I/*Spe*I digested vector pZ12-I-PL2 (Ariad). MeCP2-SV40pA was released as an *Nco*I/*Spe*I fragment and cloned into pTAU-KR-linker creating pTAU-MeCP2pA. A neo^{R}-resistance selectable marker from pPGKNR was isolated using *EcoR*I and *Sal*I and overhangs were filled in using Klenow. This blunt-ended fragment was cloned into the unique *EcoR*V site of pTAU-MeCP2pA. The targeting vector pTAU-MeCP2pAneo was confirmed by sequencing.

Generation of mice.

The targeting vector was linearized with *Sac*II and electroporated into V6.5 (129 x C57BL/6) F1 embryonic stem (ES) cell lines. We picked 96

neomycin-resistant clones of which 63 were analyzed by Southern blots as described (14).The 5' external probe consisted of a 528bp PCR fragment amplified from pHV and was located 1.5 Kb upstream of the *Nco*I insertion site in exon 1. The primers were Tau5'-F (5'-GAG CTG CTG CCA TCT TCA C-3') and Tau5'-R (5'-TTT GAT GTG TGC CCT ACA GAA-3'). The 3' external probe consisted of a 600 bp *BamH*I/*EcoR*I genomic fragment (15) that was located 6.1 Kb downstream of the insertion site. An internal probe was used to test for additional non-homologous insertions and consisted of a 200 bp *Pst*I fragment from the neo^R ORF (15). Eleven clones were targeted correctly which corresponds to a targeting efficiency of 17%. Two clones were used to generate chimeras by injection into (DBA/2 x C57BL/6) F1 blastocysts as described (16). Chimeras were mated to C57BL/6 females and offspring were analyzed for germline transmission. The heterozygous knock-in strain (*Tau-Mecp2* ki/+) was maintained on a mixed background that was predominantly C57BL/6 but also contained some 129 contributed by the original ES cells used for targeting. To obtain rescued males, *Tau-Mecp2* ki/+ heterozygous males were mated to heterozygous $Mecp^{1lox/+}$ females (12) that had been backcrossed to C57BL/6. After germline transmission was confirmed animals were routinely genotyped by PCR. For the *tau* locus the primer set Tau138 (5'-CTG GCA GAT CTT CCC GTC TA-3'), Tau1078 **(**5'-TGC CTG ACA GAG TCC AGA TG-3') and Neo1323 (5'-AGG GGA TCC GTC CTG TAA GT-3') gave a 941 bp band for the wild-type allele and a 796 bp band for the ki allele. The *Mecp2* allele was determined using primers Nsi-5 (5'-CAC CAC AGA AGT ACT ATG ATC-3'), 2lox-3 (5'-CTA GGT AAG AGC TCT TGT TGA-3') and Nsi-3 (5'-ATG CTG ACA AGC TTT CTT CTA-3'), which generated a 180 bp wild-type band and 300 bp band for the 1lox allele.

Immunoblot analysis.

Organs were routinely harvested and snap frozen in liquid N_2. Tissues were homogenized with a Polytron homogenizer (Biospec Products Inc.) in a lysis buffer containing 125 mM Tris, 1% SDS (pH 6.8) supplemented with a proteinase inhibitor cocktail (Roche). Protein concentrations were determined with a BCA protein assay kit (Pierce, Rockford, IL). Sample buffer containing bromophenol blue was added to final concentrations of 12.5% glycerol and 0.25% ß-mercaptoethanol. 40µg of protein (unless indicated otherwise) was loaded on 7.5% Tris-HCL acrylamide gels (Ready Gels, BIO-RAD), probed with an anti-MeCP2 rabbit polyclonal antibody (Upstate Biotech) or an anti-GAPDH rabbit polyclonal (Abcam) and visualized using the Amersham ECL system.

Immunohistochemistry.

Brains were harvested from 8 weeks old animals, weighed, immersion-fixed for 20 h in 10% phosphate buffered formalin and cryoprotected for 24 to 36 h in 30% sucrose and embedded in OCT. A series of 15 µm sagittal sections were slide mounted and stored at -20˚C. For immunohistochemistry slides were blocked in 5% normal goat serum and incubated with rabbit antibody raised against the C-terminal peptide of MeCP2 (11) at a dilution of 1:500 and a mouse anti neuron specific nuclear protein (NeuN, Chemicon) at a dilution of 1:200. The MeCP2 antibody was detected with a FITC conjugated goat anti-rabbit IgG and the NeuN antibody with a Rhodamine conjugated donkey anti-mouse IgG (both from Jackson Imunoresearch), both at a dilution of 1:500. Sections were finally rinsed in PBS/DAPI (1:10000) and mounted in Vectashield

(Vector laboratories). Images were taken with Leica fluorescence microscope under 20x magnification.

RNA samples and RNase Protection assay.

Embryo heads and adult brains were harvested, snap frozen in liquid N_2 and subsequently extracted with RNA-Bee (TEL-Test, INC.). Embryos were isolated from *Tau-Mecp2* ki/+ females mated with *Tau-Mecp2* ki/+ males. Embryos of the correct genotype were identified by PCR genotyping using DNA extracted from embryos (10.5 to 15.5 d.p.c.), yolk sac (9.75 d.p.c.) or tail tips.

For the RNase protection assay the probe template was generated by PCR from genomic DNA obtained from a transgenic mouse with primers TauExon1-27F (5'-GCCAGGAGTTTGACACAATG-3') and MeCP2-282R (5'-CATACATAGGTCCCCGGTCA-3'). The PCR product was cloned into the vector pCR2.1-TOPO (TOPO TA Cloning Kit, Invitrogen) and subcloned as a PstI Fragment into the transcription vector pSP72 (Promega). In vitro transcription was carried out with the Maxiscript T7 Kit (Ambion,). UTP$\propto P^{32}$ (3,000 Ci/mmol, 10 mCi/ml, Amersham Pharmacia) was diluted 1:10 with unlabeled nucleotide and the probes were gel-purified. 2000 cpm of probe and 10 µg of total RNA was used in the assay according to the manufacturer's specification (Ambion RPA III kit). The samples were resolved on a 6% acrylamide (1:30 bisacrylamide) and quantified by phosphor imaging.

Spontaneous activity measurements.

Motor activity was measured using an infrared beam activated movement-monitoring chamber (Opto-Varimax-Mini-A, Columbus Instruments). For each experiment, a mouse was placed in the chamber at least 3 hours before recordings started. Movement was monitored during the normal 12 h dark cycle (7 pm to 7 am).

Results

Expression of MeCP2 from the *tau* locus.

In order to express MeCP2 specifically in post-mitotic neurons we designed a targeting construct that places *Mecp2* expression under the control of the promoter of the microtubule-binding-protein, Tau. Tau protein is strongly expressed in neurons (17) and the endogenous *tau* locus has been used previously to drive neuron-specific expression of EGFP (15). Homozygous animals mutant for *tau* have been shown to be phenotypically indistinguishable from wild-type littermates (18). A cDNA containing the *Mecp2* coding sequence including a modified Kozak sequence (19) was placed into exon 1 of the *tau* gene in-frame with the endogenous initiation codon thereby creating a fusion protein that contains the first 31 amino acids of Tau (Tau-MeCP2, Fig. 1A). The targeting construct was introduced into V6.5 embryonic stem cells by electroporation and 63 neomycin-resistant clones were analyzed. Eleven clones were targeted correctly and two of these (Fig. 1B) were used to generate germ line-transmitting chimeras.

To examine and compare the expression pattern of Tau-MeCP2 and endogenous MeCP2, we determined their protein levels in various adult mouse tissues by immunoblot analysis (Figure 2A, B). We found that Tau-MeCP2 expression in the brain was 2-4-fold higher than endogenous MeCP2 (Fig. 2A, lanes 4 to 9). Endogenous MeCP2 was expressed highly in lung and spleen, and moderately in kidney and heart and liver (Fig 2B, wt). Tau-MeCP2 protein expression was high in lung and kidney, and was low in heart (Fig. 2B, R). Very low expression in liver and spleen was detectable after long exposure times.

MeCP2 localizes to highly methylated centromeric heterochromatin (20), and immunohistochemical analysis revealed the typical punctate nuclear MeCP2 staining pattern in wild-type brains (Fig. 2C). This pattern was not detectable in *Mecp2* mutant animals. Instead a faint diffuse nuclear staining was observed which probably arose from the detection of the truncated MeCP2 protein (Fig. 2G) (12). The deletion of exon 3 encompasses most of the methyl-CpG-binding domain (MBD) but the C-terminal epitope including the nuclear localization sequence (NLS) remains largely intact (12). We found that in *Mecp2* mutant mice heterozygous for the *Tau-Mecp2* transgene (rescued animals) MeCP2 distribution was indistinguishable from wild-type MeCP2 (Fig. 2K) suggesting correct localization of the fusion protein. This was to be expected, because the MBD and the NLS have both been shown to be necessary and possibly sufficient for the specific localization of MeCP2 (20). The axonal localization signal of Tau is located in the 3' untranslated region (UTR) and therefore not part of the Tau-MeCP2 mRNA (21). In addition we found that all MeCP2-positive cells were double labeled with an antibody against the neuron-specific marker protein

NeuN (22) (Fig.2E, M, Q) indicating that endogenous MeCP2 as well as Tau-MeCP2 were detectable only in neuronal cells (Fig. 2F, N, R).

Timing of Tau-MeCP2 expression.

In order to quantify the relative expression of *Mecp2* and *Tau-Mecp2* during embryonic development we carried out an RNase protection assay (RPA) on embryos harvested between 9.75 and 15.5 days past coitum (d.p.c.). The probe (RPA) was designed to span the *Tau-Mecp2* junction including 82 bp of *tau* exon 1 and 164 bp of the *Mecp2* cDNA. This allowed the detection of the *Tau-Mecp2* RNA as well as the endogenous *Mecp2* and *tau* transcripts (Fig. 3A). *Mecp2* RNA was detectable as early as 9.75 d.p.c. with levels steadily increasing until they reached adult levels at 15.5 d.p.c (Fig. 3B, compare lane 5 with lanes 6 and 9). *Tau-Mecp2* expression followed closely that of endogenous *tau* with RNA being present starting at 10.5 d.p.c. and, like *Mecp2*, reaching maximum expression levels at 15.5 d.p.c (Fig. 3B, compare lane 5 with lanes 6 and 9). The timing of *Tau-Mecp2* expression therefore appeared to closely mimic that of *Mecp2*.

Quantification of expression levels revealed that in 15.5 d.p.c. embryonic heads as well as in adult brains the amount of *Mecp2* RNA appeared to be similar to *Tau-Mecp2* RNA. On the protein level, however, Tau-MeCP2 was 2-4 times more abundant (Fig. 2A) suggesting a difference in either translation efficiency of the transcripts or protein stability.

Overexpression of MeCP2 is detrimental.

Wild-type animals heterozygous for the transgene were fertile and healthy with no obvious phenotypic abnormalities. In contrast, wild-type as well as *Mecp*2 mutant animals homozygous for the transgene suffered from profound motor dysfunction including side-to-side swaying, tremors and gait ataxia. There was no reduction in brain weight in animals at 2 to 4 month of age (data not shown). Animals were of normal weight at birth, but by weaning age pups were severely runted and up to 60% smaller than wild-type littermates (Fig. 4B). The condition improved when animals were fostered in small groups, indicating that the failure to thrive was largely due to their inability to compete with littermates for food. Once the animals reached weaning age the phenotype appeared to be stable, but they remained small and do not mate. By 9 month ataxia and tremors appeared to have intensified. The animals were emaciated, had a disheveled look, and developed additional problems such as cataracts and lesions. The lesions were probably caused by excessive stereotypic scratching. However, no premature death was observed. Preliminary data suggest that *Mecp2*-mutant animals homozygous for the transgene were slightly less affected compared to *Mecp2* wild-type animals homozygous for the transgene as judged by weight and appearance (data not shown). The phenotype was specific and not due to the lack of Tau protein because animals homozygous for other transgenes targeted to exon 1 of the *tau* locus were phenotypically normal (15 and unpublished data).

Immunohistochemical analysis of brain sections revealed a punctate MeCP2 staining pattern (Fig. 2M) suggesting that the level of Tau-MeCP2 overexpression had no effect on Tau-MeCP2 localization in adult mice. Previous reports detected diffuse nuclear MeCP2 staining at 10 d.p.c. which became

increasingly punctate through 16.5 d.p.c. (5). Our results suggest that MeCP2 dosage is critical and that overexpression of MeCP2 4- to 6 -fold above wild-type level is detrimental to the health of the animal.

Expression of MeCP2 in postmitotic neurons rescues the RTT phenotype.

MeCP2 mutant mice die on average around 10 weeks of age(12). In contrast, mutant animals heterozygous for the transgene were healthy and fertile and in various crosses passed on all alleles at the expected Mendelian ratios (data not shown). They were phenotypically indistinguishable from their wild-type littermates and displayed no RTT-like symptoms (Fig. 4A). A distinct feature of *Mecp2* mutant animals are weight abnormalities, and in agreement with previous reports (13) *Mecp2* mutant animals were severely underweight from four to five weeks (Fig4C). In contrast, the weight of rescued animals was indistinguishable from that of wild-type littermates throughout postnatal development (Fig. 4C).

Human RTT syndrome, as well as the *Mecp2* mutant mouse phenotype, are characterized by a decrease in head growth and neuronal cell size as well as increased cell packing density throughout the brain (12, 23-25). As published previously we found a 14 - 18 % reduction in brain weight in 8 to 13 week old *Mecp2* mutant animals. In contrast, rescued animals showed no difference in brain weight compared to wild-type littermates, even when brains were harvested as late as 5 months of age (Fig.4D). Hypoactivity is another characteristic of *Mecp2* mutant mice (12, 13, 26). We tested exploratory response as well as total nocturnal activity by placing animals in cages equipped with an infrared beam movement detector. The age of the mice tested ranged

from 4 to 6.5 months, long after the onset of RTT symptoms in *Mecp2* mutant mice and in all cases after *Mecp2* mutant littermates had died. In both behavioral tests rescued animals were indistinguishable from wild-type littermates (Fig. 4E).

In summary, our data indicate that rescued animals do not display any of the common RTT phenotypes that have been described for *Mecp2* mutant animals. Therefore expression of *Mecp2* in postmitotic neurons is sufficient to alleviate the RTT phenotype, even at slightly elevated protein levels.

Discussion.

Mutation of the methyl-binding protein MeCP2 leads to RTT in humans, and increasing evidence suggests that this disorder is primarily caused by a defect in neuronal maintenance and maturation. In a mouse model, loss of MeCP2 expression leads to a RTT-like phenotype including tremors, heavy breathing, hypoactivity and smaller brain size associated with smaller, more densely packed neurons. After the onset of symptoms at 4 to 6 weeks of age and progressive physical deterioration, the animals typically die around 10-12 weeks of age (12, 13). Deletion of *Mecp2* exon 3 encoding most of the methyl-binding domain in neural progenitor cells produces a phenotype that is indistinguishable from the germline mutation. In contrast, loss of MeCP2 function in postmitotic neurons of the postnatal brain led to a delayed onset of symptoms by up to 3 months (12). MeCP2 is primarily expressed in mature neuronal populations (5-7) with an expression pattern that follows the maturation of the CNS (5). Recent studies suggest that MeCP2 may be important for the maintenance and modulation of synapses (9). In addition, neurons of

RTT individuals appear to show a reduction in dendritic complexity (27). Also, recent experiments in Xenopus revealed a specific function of MeCP2 in early neural development (28).

Here we provide functional evidence for the requirement of MeCP2 in postmitotic neurons by placing the *Mecp2* cDNA under the control of the endogenous promoter of the microtubule-binding-protein, Tau. By introducing the cDNA into exon 1 of the *tau* gene in-frame with the endogenous start codon we created a fusion protein that contained the first 31 amino acids of Tau (Tau-MeCP2). Tau-MeCP2 was expressed at a level 2-4-fold higher than endogenous MeCP2, and the onset of expression correlated closely with endogenous *tau* expression being first detectable at 10.5 d.p.c. In agreement with previous reports, endogenous *Mecp2* RNA was detectable at 9.75 d.p.c. Immunohistochemical analysis of brain sections revealed that Tau-MeCP2 localized like endogenous MeCP2 to heterochromatic foci of postmitotic neurons in adult mice.

One copy of the *Tau-Mecp2* transgene led to the complete rescue of all assessed phenotypes in *Mecp2* mutant animals. They had a normal lifespan and showed normal physical development as judged by weight. The rescued animals had normal brain weight and showed no signs of hypoactivity, tremors or any other physical symptoms typically associated with RTT, even at an advanced age of 6 month or more. We therefore conclude that expression of MeCP2 in postmitotic neurons is sufficient to alleviate the phenotype in MeCP2 mutant mice. Our data strongly suggest that the RTT phenotype is caused by lack of MeCP2 in the brain. Nevertheless, we cannot fully exclude a contribution of MeCP2 in some peripheral tissues, because the physiological basis of some

symptoms in Rett patients as well as in *Mecp2* mutant animals still remains to be determined.

It has been reported previously that there is no obvious correlation between MeCP2 protein and RNA levels in adult tissues, suggesting that *Mecp2* translation may be postranscriptionally regulated (5). The endogenous *Mecp2* sequence contains a 182 bp 5' UTR and a highly conserved 8.5 Kb 3' UTR with alternative polyadenylation (pA) signals. Depending on which pA signal is used, either a 1.9 Kb or a 10 kb transcript is produced. In the brain the 10 Kb transcript is the predominant one (29). In our experiments, the *Tau-Mecp2* construct did not include either of the untranslated regions. Since both the short and the long transcript have similar half-lives (29) it is possible that the 3'UTR contains regulatory elements important for translation efficiency. In fact, the *Mecp2* 3'UTR has recently been predicted to contain potential target sequences for microRNAs (miRNAs), which confer posttranslational repression (30).

Moderate overexpression of MeCP2 in wild-type mice heterozygous for *Tau-Mecp2* had no adverse effect. In contrast, homozygosity for the transgene led to severe motor dysfunction in a wild-type as well as a *Mecp2* mutant background. The result was an impaired ability to compete with littermates for food, leaving the pups severely runted. Symptoms included tremors, gait ataxia and side-to side swaying. These observations suggest that neurons can tolerate a 2 to 3-fold higher level of MeCP2 expression but that higher expression levels result in obvious detrimental consequences. Interestingly, *Mecp2* mutant animals homogzygous for the transgene showed a slightly less severe phenotype, which emphasizes the importance of MeCP2 dosage.

We found that MeCP2 expression was dispensable through early embryonic development. In agreement with this, previous studies described that MeCP2 expression was undetectable before 9.5 d.p.c on the RNA or protein level indicating that it plays no essential role in early embryonic development (5, 31). Moreover, we find that MeCP2 is not necessary for neurogenesis, despite the fact that MeCP2 appears to be expressed in some neuronal precursor cells of the rodent brain (32). The delayed phenotype of the conditional mutant observed after postnatal loss of MeCP2 function in postmitotic neurons may be attributable to the fact that the expression of CamKII-driven Cre recombinase used in this experiment is limited to certain parts of the postnatal brain including the forebrain, hippocampus and brainstem. It is only marginally active in the cerebellum, a region where *Mecp2* mRNA is highly expressed (32). In contrast, loss of MeCP2 function in neural progenitor cells affects essentially all neurons. It is also possible that the abatement of the phenotype of CamKII-Cre mutants is due to the presence of MeCP2 in neurons during prenatal development or the lack of Cre expression in a crucial cell type.

Our results are consistent with MeCP2 playing no essential role in the early stages of brain development. It is possible in fact, that neurons are functionally normal in the young postnatal patient, and that neural dysfunction becomes manifest only later due to prolonged MeCP2 deficiency. If correct, therapeutic strategies could be aimed at preventing postnatal dysfunctions from developing in *MECP2* mutant neurons.

Acknowledgments.

We thank members of the Jaenisch lab for discussions and critical comments on the manuscript. We also thank K. Tucker for providing reagents, J. Dausman for blastocyst injections, R. Flannery for animal care, and A. Caron (MIT Center for Cancer Reasearch histology facility) for technical support. This work was conducted using the W. M. Keck biological imaging facility at the Whitehead Institute and was supported by NIH grant CA87869 to R.J. and the Rett Syndrome Research Foundation.

References

1. Zoghbi, H. Y. (2003) *Science* **302,** 826-30.
2. Kriaucionis, S. & Bird, A. (2003) *Hum Mol Genet* **12 Spec No 2,** R221-7.
3. Amir, R. E., Van den Veyver, I. B., Wan, M., Tran, C. Q., Francke, U. & Zoghbi, H. Y. (1999) *Nat Genet* **23,** 185-8.
4. Nan, X., Ng, H. H., Johnson, C. A., Laherty, C. D., Turner, B. M., Eisenman, R. N. & Bird, A. (1998) *Nature* **393,** 386-9.
5. Shahbazian, M. D., Antalffy, B., Armstrong, D. L. & Zoghbi, H. Y. (2002) *Hum Mol Genet* **11,** 115-24.
6. Akbarian, S., Chen, R. Z., Gribnau, J., Rasmussen, T. P., Fong, H., Jaenisch, R. & Jones, E. G. (2001) *Neurobiol Dis* **8,** 784-91.
7. Coy, J. F., Sedlacek, Z., Bachner, D., Delius, H. & Poustka, A. (1999) *Hum Mol Genet* **8,** 1253-62.
8. Mullaney, B. C., Johnston, M. V. & Blue, M. E. (2004) *Neuroscience* **123,** 939-49.
9. Cohen, D. R., Matarazzo, V., Palmer, A. M., Tu, Y., Jeon, O. H., Pevsner, J. & Ronnett, G. V. (2003) *Mol Cell Neurosci* **22,** 417-29.
10. Tudor, M., Akbarian, S., Chen, R. Z. & Jaenisch, R. (2002) *Proc Natl Acad Sci U S A* **99,** 15536-41.
11. Chen, W. G., Chang, Q., Lin, Y., Meissner, A., West, A. E., Griffith, E. C., Jaenisch, R. & Greenberg, M. E. (2003) *Science* **302,** 885-9.
12. Chen, R. Z., Akbarian, S., Tudor, M. & Jaenisch, R. (2001) *Nat Genet* **27,** 327-31.
13. Guy, J., Hendrich, B., Holmes, M., Martin, J. E. & Bird, A. (2001) *Nat Genet* **27,** 322-6.

14. Sambrook, J., Fritsch, E.F. & Maniatis, T. (1989) *Molecular Cloning: A Laboratory Manual* (Cold Spring Harbor Laboratory Press, Cold Spring Harbor, New York).

15. Tucker, K. L., Meyer, M. & Barde, Y. A. (2001) *Nat Neurosci* **4,** 29-37.

16. Hogan, B., Beddington, R., Costantini, F., & Laciy, E. (1994) *Manipulating the Mouse Embryo: A Laboratory Manual* (Cold Spring Harbor Laboratory Press, Cold Spring Harbor, New York).

17. Binder, L. I., Frankfurter, A. & Rebhun, L. I. (1985) *J Cell Biol* **101,** 1371-8.

18. Harada, A., Oguchi, K., Okabe, S., Kuno, J., Terada, S., Ohshima, T., Sato-Yoshitake, R., Takei, Y., Noda, T. & Hirokawa, N. (1994) *Nature* **369,** 488-91.

19. Kozak, M. (1986) *Cell* **44,** 283-92.

20. Nan, X., Tate, P., Li, E. & Bird, A. (1996) *Mol Cell Biol* **16,** 414-21.

21. Aronov, S., Aranda, G., Behar, L. & Ginzburg, I. (2001) *J Neurosci* **21,** 6577-87.

22. Mullen, R. J., Buck, C. R. & Smith, A. M. (1992) *Development* **116,** 201-11.

23. Jellinger, K., Armstrong, D., Zoghbi, H. Y. & Percy, A. K. (1988) *Acta Neuropathol (Berl)* **76,** 142-58.

24. Hagberg, G., Stenbom, Y. & Engerstrom, I. W. (2001) *Brain Dev* **23 Suppl 1,** S227-9.

25. Bauman, M. L., Kemper, T. L. & Arin, D. M. (1995) *Neuropediatrics* **26,** 105-8.

26. Shahbazian, M., Young, J., Yuva-Paylor, L., Spencer, C., Antalffy, B., Noebels, J., Armstrong, D., Paylor, R. & Zoghbi, H. (2002) *Neuron* **35,** 243-54.

27. Armstrong, D., Dunn, J. K., Antalffy, B. & Trivedi, R. (1995) *J Neuropathol Exp Neurol* **54,** 195-201.

28. Stancheva, I., Collins, A. L., Van den Veyver, I. B., Zoghbi, H. & Meehan, R. R. (2003) *Mol Cell* **12,** 425-35.

29. Reichwald, K., Thiesen, J., Wiehe, T., Weitzel, J., Poustka, W. A., Rosenthal, A., Platzer, M., Stratling, W. H. & Kioschis, P. (2000) *Mamm Genome* **11,** 182-90.

30. Lewis, B. P., Shih, I. H., Jones-Rhoades, M. W., Bartel, D. P. & Burge, C. B. (2003) *Cell* **115,** 787-98.

31. Kantor, B., Makedonski, K., Shemer, R. & Razin, A. (2003) *Gene Expr Patterns* **3,** 697-702.

32. Jung, B. P., Jugloff, D. G., Zhang, G., Logan, R., Brown, S. & Eubanks, J. H. (2003) *J Neurobiol* **55,** 86-96.

Figure Legends.

Figure 1. Targeting the *Mecp2* cDNA to the tau locus. A. Targeting strategy to insert the *Mecp2* cDNA and the neomycin resistance marker (NEO^R) into exon 1 of the *tau* locus. The upstream and downstream targeting arms are shown in light and dark grey, respectively. The locations of 5' and 3' external probes used for Southern blot analysis are indicated. **B.** Southern blot analysis of targeted ES cell clones (ki/+) after digestion with *BamH*I (left panel) and *Kpn*I (right panel). When hybridized with the 5' external probe, wild-type clones display a 9 Kb band. The correct targeting event results in a band-shift to 4.75 Kb for the targeted allele. Hybridization with the 3' external probe results in a 8.8 Kb wild-type band and a 12.5 Kb band for the targeted allele.

Figure 2. Expression of *Mecp2* from the *tau* locus. A. Immunoblot analysis of protein prepared from whole brain samples. As controls, 40 µg of protein were loaded from wild-type and MeCP2 mutant (MeCP2 KO) animals, and MeCP2 mutant animals heterozygous for the Tau-MeCP2 transgene (Rescue). The protein extract from a MeCP2 wild-type animal heterozygous for the transgene (Tau-MeCP2 ki/+) was loaded as serial dilutions as indicated. The Tau-MeCP2 fusion protein contains 31 amino acids of the Tau protein which results in a band shift. **B.** Endogenous MeCP2 (wild-type animal, wt) is highly expressed in the lung and spleen, and less in the liver, kidney and heart. Tau-MeCP2 expression (rescued animal, R) is high in lung and kidney. Low level expression is also detectable in the heart. In the liver and spleen Tau-MeCP2 is detectable only after long exposure times. **C-R.** Tau-MeCP2 expression is neuron-specific

in the brain and localizes to heterochromatic foci. Double labeled immuno-fluorescence of MeCP2 (green) and neuron-specific nuclear protein (NeuN, red) from wild-type (C-F), MeCP2 KO (G-J), rescued (K-N) and Tau-MeCP2 homozygous (Tau-MeCP2 ki/ki, O-R) hippocampi of adult animals. Punctate MeCP2 staining is detectable in wild-type animals (C) as well as animals carrying the Tau-MeCP2 transgene (K, O). Inserts in panels C, G, K, O show enlargements of a small number of cells to illustrate MeCP2 staining. Endogenous MeCP2 as well as Tau-MeCP2 expression overlaps with NeuN immunoreactivity (F, N, R). Only weak diffuse MeCP2 staining is present in MeCP2 null cells (G). Nuclear DAPI stain is shown in blue (E, I, M, Q).

Figure 3. Timing of *Tau-Mecp2* expression. A. Probe design for the RNase protection assay. The probe overlaps the *Tau-Mecp2* junction of the transgene and consists of 82 bp of *tau* sequence and 164 bp of *Mecp2* cDNA sequence (26 bp of exon 2 and 138 bp of exon 3). **B.** RNase protection assay. RNA was extracted from embryos (9.75 d.p.c) and embryonic heads (10.5 to 15.5 d.p.c.) of *Mecp2* wild-type animals heterozygous for the *Tau-Mecp2* transgene (lanes 1 - 5), or from brains of adult control animals (lanes 6 - 9). Lane 10 shows the no sample control, and lane 11 is 15% loading of the no RNase control. Wild-type *Mecp2* RNA is detectable as two bands that probably represent different splice products (lanes 1 - 6 and 9). No *Mecp2* signal is detectable in animals carrying the mutant *Mecp2* allele that lacks exon 3 (lanes 7 and 8). The ratio of *Tau-Mecp2* RNA expression to endogenous *Mecp2* RNA as quantitated by phosphorimaging is given below the gel.

Figure 4. Expression of MeCP2 in postmitotic neurons rescues the RTT phenotype, but overexpression of MeCP2 is detrimental. A. Rescued animals are indistinguishable from their wild-type litter mates. Animals are shown at 8 weeks of age. **B.** *Mecp2* wild-type animals heterozygous for *Tau-Mecp2* (*Tau-Mecp2* ki/+) show normal physical development. *Mecp2* overexpressing animals (*Tau-Mecp2* ki/ki) have a normal birth weight but progressively lose weight so that animals are up to 60% smaller than wild-type littermates at weaning age. **C.** Neuronal expression of MeCP2 rescues the weight-loss phenotype. *Mecp2* null animals start to lose weight at about 5 weeks of age. The weight of rescued as well as *Tau-Mecp2* ki/+ animals is comparable to that of wild-type littermates. **D.** Rescued animals have a brain weight comparable to wild-type littermates. In contrast, *Mecp2* mutant animals show a 15 - 18 % reduction in brain weight. **E.** Spontaneous activity of rescued animals is comparable with the activity of wild-type littermates as measured by an infrared beam activated movement detector.

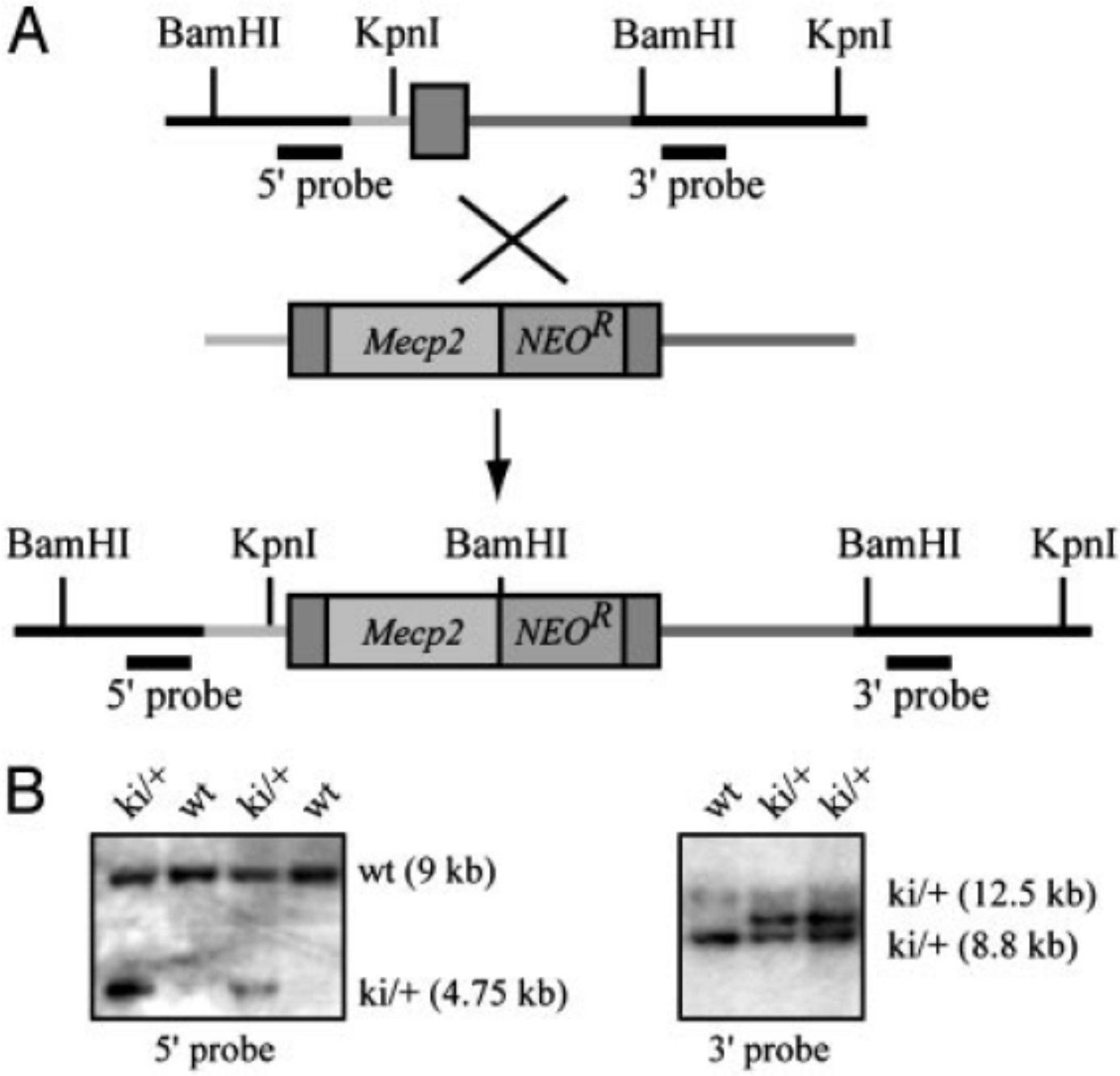

Fig. 1.Targeting the MeCP2 cDNA to the tau locus. (A) Targeting strategy to insert the Mecp2 cDNA and the neomycin resistance marker (NEOR) into exon 1 of the tau locus. The upstream and downstream targeting arms are shown in light and dark gray, respectively. The locations of 5 and 3 external probes used for Southern blot analysis are indicated. (B) Southern blot analysis of targeted embryonic stem cell clones (ki) after digestion with BamHI (Left) and KpnI (Right). When hybridized with the 5 externalprobe, wild-type clones display a 9-kb band. The correct targeting event results in a band-shift to 4.75 kb for the targeted allele. Hybridization with the 3 external probe results in a 8.8-kb wild-type band and a 12.5-kb band for the targeted allele.

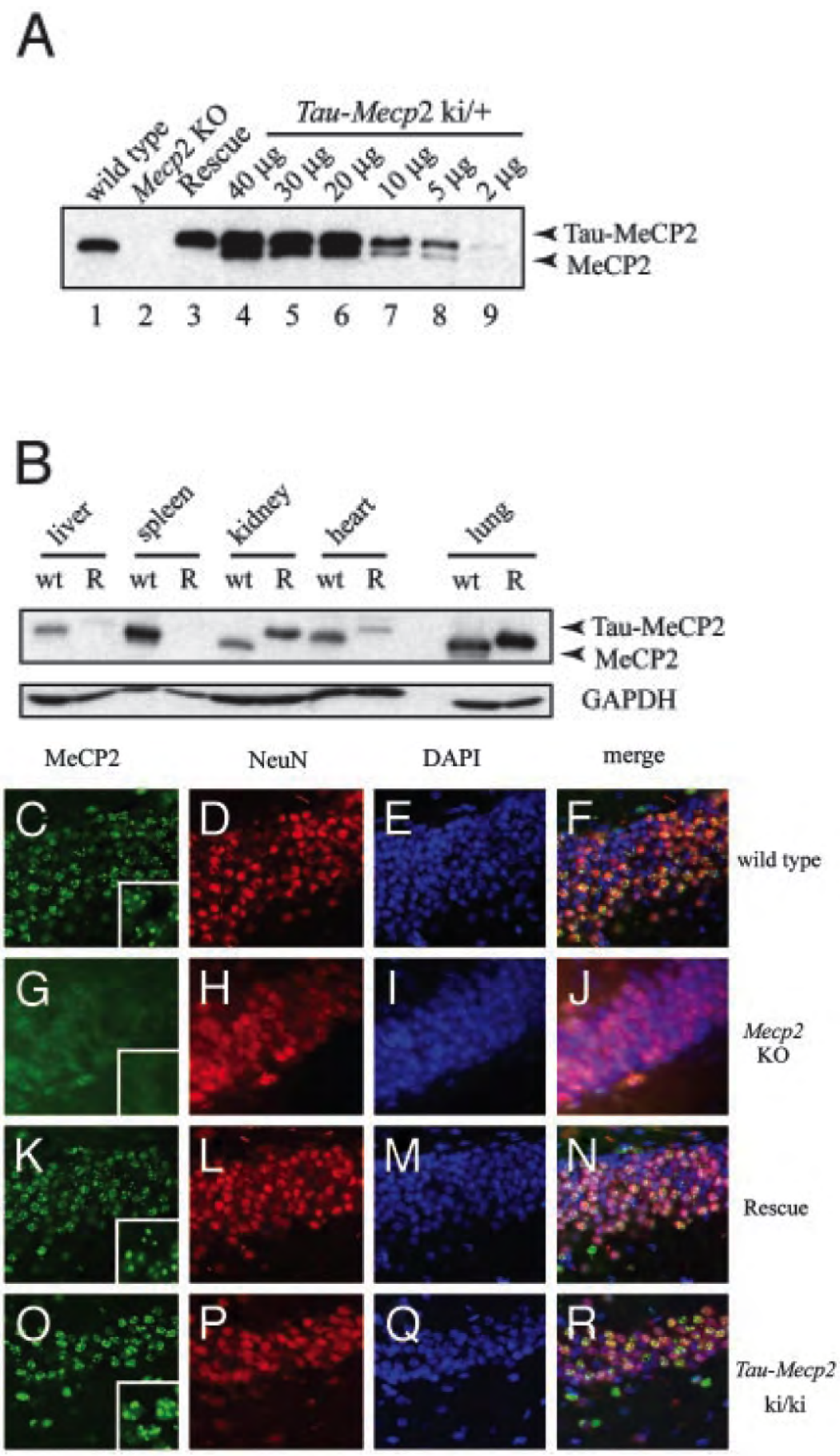

Fig. 2. Expression of MeCP2 from the tau locus. (A) Immunoblot analysis ofprotein prepared from whole brain samples. As controls, 40 g of proteinwere loaded from wild-type and Mecp2 mutant (Mecp2 KO) animals, and Mecp2 mutant animals heterozygous for the Tau-Mecp2 transgene(Rescue). The protein extract from a Mecp2 wild-type animal heterozygous for the transgene (Tau-Mecp2 ki) was loaded as serial dilutions as indicated. The Tau-MeCP2 fusion-protein contains 31 aa of the Tau protein, which results in a band shift. (B) Endogenous MeCP2 (wild-type animal, wt) is highly expressed in the lung and spleen,and less in the liver, kidney, and heart. Tau-MeCP2 expression (rescued animal, R) is high in lung and kidney. Low-level expression is also detectable in the heart. In the liver and spleen Tau-MeCP2 is detectable only after long exposure times. (C–R) Tau-MeCP2 expression is neuron-specific in the brain and localizes to heterochromatic foci. Double labeled immuno-fluorescence of MeCP2 (green) and neuron-specific nuclear protein (NeuN, red) from wild-type (C–F), Mecp2 KO (G–J), rescued (K–N) and Tau-Mecp2 homozygous (Tau-Mecp2 ki ki, O–R) hippocampi of adult animals are shown. Punctate MeCP2 staining is detectable in wild-type animals (C) as well as animals carrying the Tau-Mecp2 transgene (K and O). Insets in C, G, K, and O show enlargements of a small number of cells to illustrate MeCP2 staining. Endogenous MeCP2 as well as Tau-MeCP2 expression overlaps with NeuN immunoreactivity (F, N, and R). Only weak diffuse MeCP2 staining is present in Mecp2 null cells (G). Nuclear 4 ,6-diamidino-2-phenylindole (DAPI) stain is shown in blue (E, I, M, and Q).

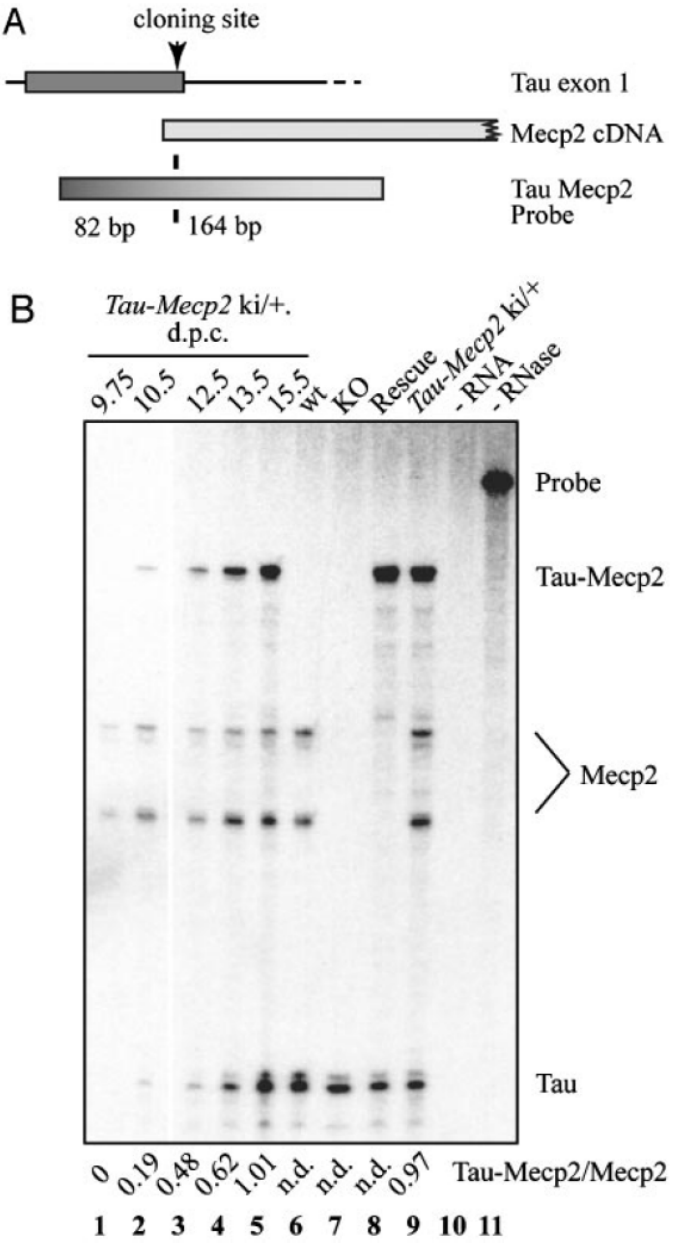

Fig.3. Timing of Tau-Mecp2 expression. (A) Probe design for the RNase protection assay. The probe overlaps the Tau-Mecp2 junction of the transgene and consists of 82 bp of Tau sequence and 164 bp of Mecp2 cDNA sequence (26 bp of exon 2 and 138 bp of exon 3). (B) RNase protection assay. RNA was extracted from embryos (9.75 dpc) and embryonic heads (10.5–15.5 dpc) of Mecp2 wild-type animals heterozygous for the Tau-Mecp2 transgene (lanes 1–5), or from brains of adult control animals (lanes 6–9). Lane 10 shows the no sample control, and lane 11 is 15% loading of the no RNase control. Wild-type Mecp2RNAis detectable as two bands that probably represent different splice products (lanes 1–6 and 9). No Mecp2 signal is detectable in animals carrying the mutant Mecp2 allele that lacks exon 3 (lanes 7 and 8). The ratio of Tau-Mecp2 RNA expression to endogenous Mecp2 RNA as quantitated by phosphorimaging is given below the gel.

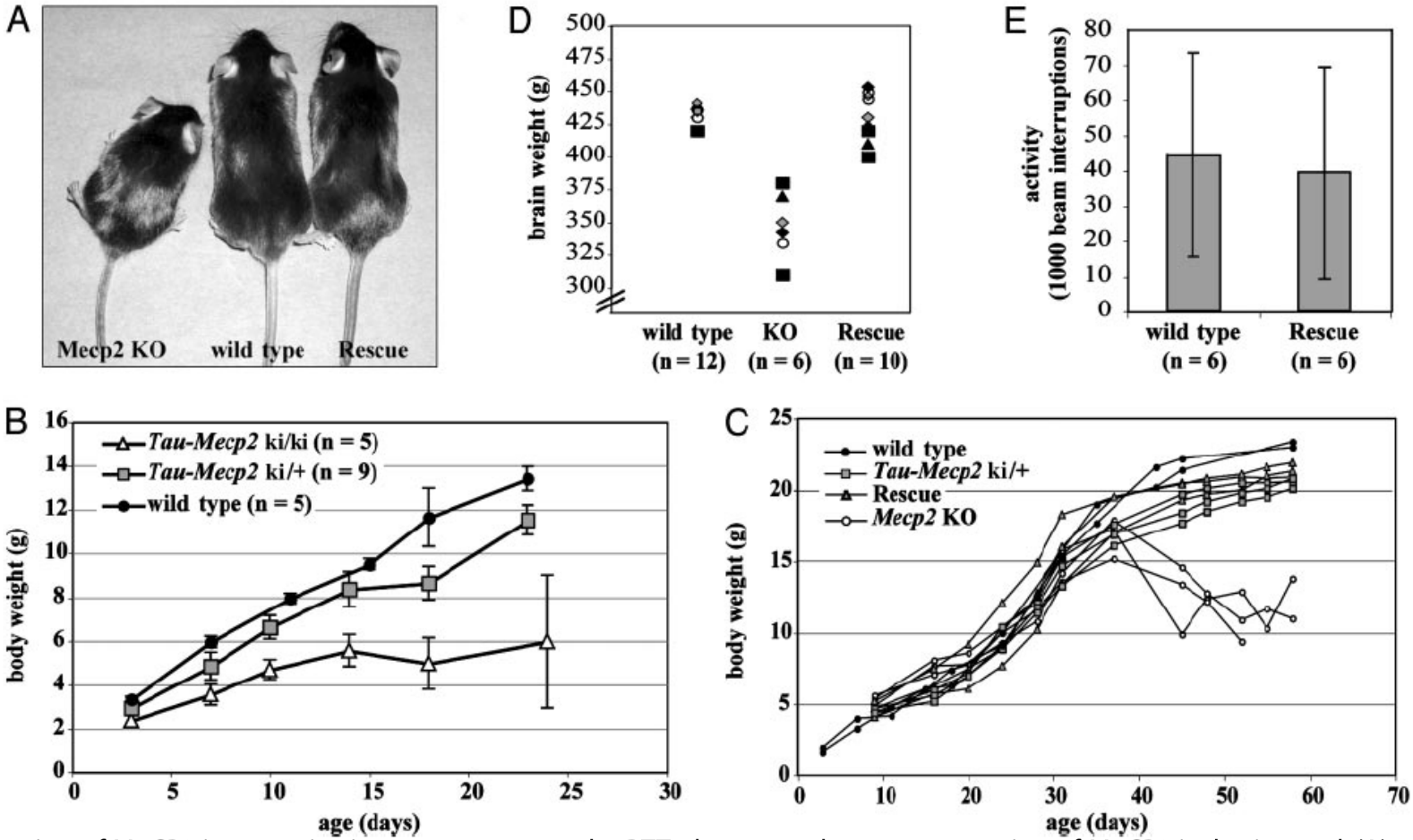

Fig. 4. Expression of MeCP2 in postmitotic neurons rescues the RTT phenotype, but overexpression of MeCP2 is detrimental. (A) Rescued animals are indistinguishable from their wild-type littermates. Animals are shown at 8 weeks of age. (B) Mecp2 wild-type animals heterozygous for Tau-Mecp2 (Tau-Mecp2ki) show normal physical development. Mecp2 overexpressing animals (Tau-Mecp2 ki ki) have a normal birth weight, but progressively lose weight so that animals are up to 60% smaller than wild-type littermates at weaning age. (C) Neuronal expression of MeCP2 rescues the weight-loss phenotype. Mecp2 null animals start to lose weight at 5 weeks of age. The weight of rescued as well as Tau-Mecp2 ki animals is comparable to that of wild-type littermates. (D) Rescued animals have a brain weight comparable to wild-type littermates. In contrast, Mecp2 mutant animals show a 15–18% reduction in brain weight. (E) Spontaneous activity of rescued animals is comparable with the activity of wild-type littermates as measured by an infrared beam activated movement detector.

Chapter 2

Title:

Partial rescue of MeCP2 deficiency by postnatal activation of MeCP2.

Emanuela Giacometti[1], Sandra Luikenhuis [3], Caroline Beard[1], Rudolf Jaenisch[1,2].

[1]Whitehead Institute for Biomedical Research, 9 Cambridge Center, Cambridge, MA 02142. [2]Massachusetts Institute of Technology, Department of Biology, Cambridge, MA 02139. [3]Magen Biosciences, 790 Memorial Drive Cambridge, MA 02139.

Contributions: Sandra Luikenhuis generated the LSLMecp2 transgenic mouse, Caroline Beard was involved in the experimental design.

Data presented in this chapter have been published in *Proc Natl Acad Sci USA* (2007) **104**(6):1931-6

Abstract.

In humans mutations in the X-linked *MECP2* gene, are the cause of Rett syndrome (RTT), a neurodevelopmental disorder that affects mainly girls. MeCP2 binds to methylated CpGs and is thought to act as a transcriptional repressor. In male mice, deletion or targeted mutation of *Mecp2* leads to lethality and causes a neuronal phenotype. Selective mutation of *Mecp2* in postnatal neurons results in a similar although delayed phenotype, suggesting that the symptoms are caused by MeCP2 deficiency in postmitotic neurons. In agreement with this idea, expression of a Mecp2 transgene in postmitotic neurons of *Mecp2* null mutant mice resulted in the phenotypical rescue of the symptoms. To assess whether postnatal activation of MeCP2 in mutant animals could also affect the progression of the disorder, we constructed a conditionally active Mecp2 "rescue transgene" which was activated between P0 and P30. The Mecp2 transgene was under the control of the CAGGS promoter and was activated using brain specific Cre-mediated recombination. Our results indicate that post-natal, neuron-specific activation of MeCP2 as late as 2 to 4 weeks of age significantly prolonged the lifespan of mutant animals and delayed the onset of neurologic symptoms.

Introduction.

Rett syndrome (RTT) is an X-linked neurological disorder that predominantly affects girls (1). First signs of illness include deceleration of head growth between 2-4 months of age. Affected individuals usually develop full-

blown symptoms between the ages of 1 and 4 years. The disorder is characterized by social withdrawal, loss of motor skills and gait ataxia. Many affected individuals develop stereotypic hand movement and autonomic dysfunctions such as irregular respiration. All RTT subjects have severe mental retardation.

Mutations in the X-linked *MECP2* gene (methyl-CpG binding protein 2) account for nearly 80% of RTT cases (2-5). To study the RTT etiology, we and others established mouse models by engineering *Mecp2* gene deletions (6-8). Conditional mutations have shown that although MeCP2 is also expressed outside the nervous system, deficiency in neurons is responsible for the phenotype (7). Electrophysiological analyses demonstrated that MeCP2 deficiency shifts the balance between excitation and inhibition in cortical neurons (9) and, more recently, MeCP2 has been implicated in regulating RNA splicing (10). Male mutant mice develop normally until 4-5 weeks of age, when RTT-like symptoms become manifest including reduced brain weight, decreased CA2 neuron size, hindlimb clasping, and impaired locomotor function (6, 7). A recent study showed that postnatal loss of MeCP2 in the forebrain is sufficient to cause many of the behavioral aspects of RTT in mice (11).

Given the strong biochemical evidence that MeCP2 binds methylated CpGs and functions in establishing or maintaining a repressive chromatin state by recruiting histone deacetylases (12-14) and H3 K9 methylating enzymes (15) it is surprising that only few differences in gene expression were observed between wt and mutant (16-20). Among the identified targets of MeCP2 are glucocorticoid regulated genes (19), *Hairy 2* (21), and *Bdnf*. *Bdnf (*Brain-derived-

neurotrophic-factor), the first identified target gene, is repressed in resting neurons by binding of MeCP2 to the neuronal specific promoter region. Resting neurons from *Mecp2* null animals have slightly higher BDNF expression (22-24) whereas calcium influx triggers MeCP2 phosphorylation leading to *Bdnf* activation (25). Recent *in vivo* data suggested a functional interaction between the two genes since over-expression of BDNF was shown to extend the lifespan, to partially rescue locomotor defects, and to reverse the electrophysiological deficits of MeCP2 deficient animals (24, 26). MeCP2 has also been implicated in the regulation of imprinted genes such as *Ube3a* (27), *Gabrb3* (28) and *Dlx5* (29), although some of these claims have been challenged (30). Thus, in spite of the great insights derived from those studies it remains unclear whether Rett syndrome is the result of misregulation of few key genes, such as *Bdnf*, or whether it is caused by misregulation of multiple genes each with an incremental contribution to the phenotype.

Because overt symptoms become manifest only at 1-2 years of age in RTT females and at 4-5 weeks of age in male *Mecp2* mutant mice, it would be important to know whether the behavioral and physiological symptoms are due to abnormal brain development or to neuronal dysfunction caused by MeCP2 deficiency in mature neurons. If MeCP2 plays an ongoing critical role in mature CNS neurons and only prolonged deficiency leads to neuronal dysfunctions, it may be possible to restore these functions by reactivating MeCP2 or by affecting expression of other genes in adult neurons. Indeed, previous results have demonstrated that a *Tau* promoter driven reactivation of a Mecp2 transgene in postmitotic neurons rescued the MeCP2 deficient phenotype in mice (31). These

experiments did not address the possibility that activation of MeCP2 at later ages could affect the course of the disorder. Here we use Cre-mediated recombination in Mecp2 -/y mice to show that activation of MeCP2 as late as 2-4 weeks of age can delay lethality and the onset of symptoms.

Results.

Generation of the CAGGS Lox-Stop-Lox Mecp2 transgene.

To investigate whether the phenotype in MeCP2 deficient mice could be affected by post-natal, brain-specific reactivation of MeCP2, we engineered a conditional rescue transgene. MeCP2 is present in two isoforms: e1 and e2 (32-34). These isoforms have a slightly different N-terminal region and are expressed at different levels but have been demonstrated to be functionally equivalent in mice as brain expression of the e2 isoform alone rescued the phenotype of Mecp2 -/y mice (31). We used the mouse Mecp2e2 cDNA placed downstream of a Stop cassette containing a neo resistance gene and three polyadenylation signals (Fig. 1A). The synthetic CAGGS promoter, a hybrid promoter-enhancer containing the b-actin enhancer and the CMV early promoter (35), was placed upstream of the Stop cassette. Because the Stop cassette was flanked by LoxP sites (36), Cre mediated recombination would result in expression of MeCP2e2 from the CAGGS promoter. C10 ES cells were used to target the transgene to the modified *Col1a1* locus by frt/Flpe recombinase-mediated site-specific integration (37) and the targeted ES cells

were injected into blastocysts to generate CAGGS LoxP-Stop-LoxP (LSL) Mecp2 mice.

To test whether the LSL element repressed the transgene expression, CAGGS LSL Mecp2 transgenic mice were crossed with *Mecp2 +/-* mice (7) to generate animals carrying the *Mecp2* null allele as well as the conditional rescue construct. Western analysis of extracts from brain, lung and spleen of transgenic mice (CAGGS LSL Mecp2; *Mecp2* -/y) failed to detect MeCP2 protein (Fig. 1C) indicating that the LSL cassette efficiently repressed expression of the transgene.

Brain specific activation of the rescue transgene by Cre mediated recombination.

We crossed the *Mecp2*+/-; CAGGS LSL Mecp2 mice with various Cre transgenic lines to test whether removal of the STOP cassette would result in activation of the CAGGS Mecp2 transgene. Four different lines were used that expressed Cre recombinase during embryogenesis (Nestin Cre and *Tau* Cre) or during postnatal life (CamKinaseII Cre 93 and 159). The nestin Cre line activates the recombinase at E 10 in precursors of neurons and glia (7, 38) whereas the *Tau* Cre line activates the enzyme in postmitotic neurons (31, 39). In the CamKinaseII Cre line 93 (C93) the recombinase is activated in the postnatal forebrain, hippocampus, midbrain and brainstem, reaching maximum expression at around P21 (40) whereas in the CamKinaseII Cre line 159 (C159)

Cre starts to be expressed in forebrain only at around P15 and reaches maximal activity at ~P30 (41). The main characteristics of the Cre lines used are summarized in Fig. 1B.

To assess Mecp2 transgene expression we performed western blot analysis on total brain extracts from 6 weeks old animals. As shown in Fig. 1D (lane 1), wt mice expressed the two MeCP2 isoforms e1 and e2 at a ratio of 9 to 1 as reported previously (33, 34) whereas only the e2 form was expressed from the CAGGS Mecp2 transgene (lanes 3 to 6). Mice carrying the Nestin (lane 3) or the *Tau* transgene (lane 4) expressed MeCP2 at a similar level as wt mice whereas C93 double transgenic animals (lane 5) had much lower MeCP2 expression. No MeCP2 protein was detected in total brain extracts from mice carrying the C159 transgene (lane 6). We also performed western analysis on specific sub-regions of the brain (Fig. 1E and F). The level of MeCP2 in frontal cortex, hippocampus and cerebellum of Nestin Cre and *Tau* Cre mice was similar to the level of MeCP2 in wt mice (Fig.1E). Total MeCP2 levels in animals carrying the C93 Cre or the C159 Cre were similar or reduced, respectively, as compared to wt mice and no expression was found in the cerebellum (Fig. 1F).

To evaluate MeCP2 expression in single cells we performed immunohistochemical analysis on brain sections. Staining for the Neuronal-specific Nuclear protein (NeuN) and MeCP2 was used to determine the fraction of neurons that had activated the transgene in different brain regions. Fig. 2D shows that CAGGS MeCP2 staining was nuclear and localized to heterochromatin dense areas (inset ii, arrowheads) whereas NeuN showed both nuclear and cytoplasmic staining (inset i). We quantified the number of neurons that

expressed the Mecp2 transgene. As shown in Figs. 2 B-D, 70-90% of the neurons expressed CAGGS MeCP2 throughout the entire brain in Nestin Cre and *Tau* Cre animals. In contrast, CamKinaseII driven Cre was activated only to specific areas of the forebrain: Cre93 and Cre159 expressed MeCP2 in ~ 50% of frontal cortical neurons, C93 expressed MeCP2 in all regions of the hippocampus (CA1, CA2, CA3, DG) while expression in the C159 animals was restricted to the dentate gyrus. No MeCP2 protein was found in the cerebellum of these mice (representative images for all 3 regions are shown as supporting information on the PNAS web site in Fig. 5S). We also noticed some variability between different CAGGS MeCP2 expressing cells: the majority had wt levels of MeCP2 but ~20% of the cells had higher or lower than endogenous MeCP2 signal (data not shown).

The results shown in figure 1 and 2 indicate that the CAGGS Mecp2 transgene was activated by all Cre transgenes though the level and the anatomical distribution of MeCP2 expression differed between the four tested Cre lines. In the following discussion the *Mecp2* null mutant animals carrying the CAGGS Mecp2 transgene in combination with one of the different Cre transgenes will be referred to as "rescued" mice and the corresponding transgene combination as "rescue transgenes".

Cre-mediated expression of MeCP2 significantly delays lethality and progression of symptoms.

Mecp2 null mice develop symptoms between 4-6 weeks and die around 10-12 weeks of age (7, 24). Fig. 3A shows that Nestin Cre and *Tau* Cre mediated activation of Mecp2 increased the life span of *Mecp2* mutants to more than 8 months. Also, a smaller but significant increase in life span by about 4 weeks was observed when the Mecp2 transgene was activated by C93 and C159 Cre (Fig. 3B).

Mecp2 mutant animals progressively lose motor coordination starting at 4 weeks and become severely lethargic. To assess whether activation of MeCP2 would affect the progressive behavioral alterations characteristic of the disorder we tested nocturnal activity by placing animals in cages equipped with an infrared beam movement detector. Figs. 3C-E show the results of baseline activity of mice at different ages. As expected there was no difference in nocturnal activity at 4-5 weeks in any of the genotypes (3C). At 6-15 weeks of age *Mecp2* null mice were significantly less active than wt mice (3D). Rescued mice carrying the Nestin Cre, the *Tau* Cre or the C93 transgenes were as active as wt mice. C159 double rescued mice were more active than *Mecp2* null mutant mice but less active than the other genotypes. MeCP2 -/y animals (white bar) start to deteriorate, become uncoordinated and hypoactive, while all mutant mice carrying the rescue transgenes had nocturnal baseline activities very similar to wt level (black bar). No *Mecp2* null mutant animals survived beyond 15 weeks of age and all other genotypes showed less activity than wt mice (3E).

These results suggest that Cre mediated activation of the Mecp2 transgene significantly prolonged the life span and delayed behavioral

deterioration. The extent of rescue was, however, directly correlated with the time and level of Cre transgene activation. Early activation of Cre in most neurons (Nestin Cre and *Tau* Cre) led to the most efficient rescue. Importantly, postnatal activation of MeCP2 between 1-2 weeks of age by the C93 Cre driven transgene led to a significant rescue of symptoms whereas later activation of Cre between 2-4 weeks, as in C159, was less efficient.

Physical development and brain growth are normal in rescued animals.

In addition to motor dysfunction, *Mecp2* mutant animals display decreased brain weight, smaller neurons and become obese with age (7). Fig. 4A shows that body weight of mutant animals carrying any rescue transgene combination was indistinguishable from that of wild-type (black line) littermates, while MeCP2 deficient animals tended to gain weight (red line). Consistent with this finding, rescued animals showed no significant difference in brain weight when compared to wild-type littermates (Fig. 4B). Finally, no significant decrease in neuronal cell size in hippocampus and cortex was seen in the C93 rescued animals while *Mecp2* null mutants have smaller sized neurons (7) (Fig. 4C). Representative images from the hippocampi of these mice are shown as supporting information on the PNAS web site in Fig. 6S.

Discussion.

An unresolved issue in Rett syndrome is whether the manifestation of overt symptoms can be affected by restoring MeCP2 expression in postnatal

neurons. Previous results showed that *Tau* promoter-driven activation of MeCP2 in post-mitotic mutant neurons prevents development of an obvious phenotype, consistent with the conclusion that RTT is not a developmental disorder but rather is caused by MeCP2 deficiency in mature neurons (31). However, these experiments did not resolve the important question of whether later reactivation of MeCP2 in postnatal life could affect the phenotype progression. Here we show that induction of a Mecp2 transgene in postnatal mutant animals delayed onset of symptoms and time of death.

To achieve activation of MeCP2 in postnatal neurons we constructed a conditionally active rescue transgene by placing a LoxP-Stop-LoxP cassette in front of the Mecp2e2 cDNA. MeCP2 was activated by crossing the conditional transgene into different Cre lines that induced recombination during early development (Nestin Cre and *Tau* Cre), at 2 weeks (C93) or between 2-4 weeks of age (C159). Immunohistochemistry indicated that the Nestin and *Tau* Cre transgenes activated Mecp2 in all regions of the brain whereas expression of the CamKinaseII Cre transgenes was restricted to a smaller fraction of cells in a given region and was not detected in the cerebellum.

Mecp2 null animals are characterized by severe motor impairment and lethargy beginning at around 4 weeks of age and death at 8-12 weeks of age. These phenotypes were significantly delayed when the Mecp2 rescue transgenes were activated. The extent of the rescue seemed to depend on the timing of Mecp2 activation and on the fraction of neurons that had undergone Cre-mediated recombination. Thus, Nestin Cre and *Tau* Cre-mediated MeCP2

activation extended the life span of mutant mice to 8 months whereas the C93 and C159 transgenes extended life span by ~ 4 weeks. A significant improvement of basal nocturnal activity was found in mutant animals carrying the rescue transgenes. Finally, anatomical alterations typical for RTT syndrome such as a decreased brain weight and neuronal cell size were not seen in rescued animals.

The most important conclusion from these results is that reactivation of MeCP2 in mutant animals even as late as 2 to 4 weeks of age can result in a significant amelioration of RTT-like symptoms. However, full restoration of the phenotype was not achieved with any of the rescue transgenes, even when the transgene was activated early in development in progenitor cells (Nestin Cre) or at a time when neurons become postmitotic (*Tau* Cre). Inappropriate expression of MeCP2 probably contributed to this partial rescue. The immunohistochemical data indicated that temporal and spatial expression of the transgene varied considerably depending on the Cre line used with 80% of cells expressing MeCP2 in brains of the Nestin and *Tau* rescued mice and only 10% expressing MeCP2 in the brains of C159 animals. Insufficient or no activation may have occurred in thalamus, cerebellum, brain stem and medulla (CamKinaseII Cre lines) that may be important for the RTT phenotype. For example the cerebellum plays an important role in the integration of sensory perception and motor output and deficiencies in the medullar respiratory network could be the cause of fatal breathing irregularities in *Mecp2* null mice (42). Lack of expression of Mecp2 in these areas may have contributed to the reduced motor activity and viability of the CamKinaseII Cre rescued animals. In addition CAGGS promoter

driven Mecp2 expression may have been inappropriate, (too low or too high) in a given neuron, compared to wt levels. Overexpression of MeCP2 has been shown to have detrimental effects on CNS function both in humans and mice (31, 43-45). We note that expression of MeCP2 from the *Tau* locus (31) fully rescued the phenotype yet expression of Cre from the same locus was not sufficient to achieve complete rescue in our system. Cre mediated excision is a stochastic event that does not happen at the same time in all cells because it depends both on the level of Cre enzyme and the availability of the flanking LoxP sites. This may have created mosaicism within the neuronal population. Direct expression from the *Tau* locus may have resulted in a higher fraction of neurons expressing appropriate levels of MeCP2 emphasizing the limitations of the Cre system.

A major unresolved issue in the pathogenesis of RTT is whether the disorder is caused by dysfunction of postnatal neurons at a time when symptoms become apparent or whether it is a prenatal developmental disorder with postnatal phenotypic manifestation in the CNS. Our results are consistent with the notion that the physical deterioration of null mice can be rescued by reactivation of MeCP2 even at an age when overt symptoms are about to commence. This implies that newborn RTT individuals might not have irreversible neuronal damage and that pathological alterations of neurons may occur only later in life. If correct, this presumption would encourage developing therapeutic strategies aimed at affecting the course of the RTT by reversing gene expression abnormalities caused by MeCP2 deficiency. While it would be difficult to reverse a mutation in the *Mecp2* gene it may be possible to modulate the activity of downstream genes that have been shown to impact the phenotype

progression, such as *Bdnf* (24). Identification of such downstream genes should further advance our understanding of the molecular basis of Rett Syndrome.

Methods.

Generation of the conditional Mecp2 LSL transgene.

We cloned a NcoI/SpeI Mecp2e2 cDNA pA fragment from (31) into pBluscript. The CAGGS promoter (35) was inserted into the SalI-EcoRI site upstream of Mecp2pA. The LoxP-Stop-LoxP neo resitance cassette was cloned into the EcoRI site between the CAGGS and the Mecp2pA (36). The whole CAGGS LSL Mecp2 pA fragment was released from pBluscript with a SalI digest, blunted and inserted into the EcoRV sie of pKATGfrt plasmid (37). We targeted the *Cola1* locus in C10 cells (37). Hygromycin resistant ES clones were analyzed by Southern blot (37). Positively targeted clones were injected into C57Bl/6-DBA2 blastocysts. Chimeric offspring were bred to C57Bl/6 mice and screened for germline transmission.

Mating schemes and genotyping.

Male mice homozygous for the LSL transgene were mated to *Mecp2* +/- females from the germline null colony (7) to obtain LSL/+; *Mecp2* +/- females which were then mated to males carrying the Cre transgene. Genotyping for the *Mecp2*

locus and for the Cre was done as previously published (7, 40). Genotyping for the *Col1a1* locus was done as (24).

Isolation of frontal cortex, hippocampus and cerebellum.

For forebrain samples, the forebrain was separated from the mid- and hindbrain by a coronal cut along the rostral border of the superior colliculi. For hippocampus samples: the cerebellum was removed and the brains were cut mid-sagittally; under a dissecting microscope, the anterior border of the hippocampus was identified as the fimbria hippocampi; dorsally, the hippocampal white matter was carefully separated from overlying cerebral cortex along the alveus; and, finally, the subiculum was bisected in the middle to release the hippocampal gray matter. For brain weight analysis, brains were freshly isolated and weighed.

Immunoblot analysis.

Organs were harvested and snap frozen in liquid nitrogen. Tissues were homogenized with a Polytron in a lysis buffer containing 125 mM Tris and 1% SDS (pH 6.8) supplemented with a proteinase inhibitor mix (Roche). Protein concentrations were determined by BCA (Pierce). Sample buffer was added to a final concentrations of 12.5% glycerol and 0.25% 2-mercaptoethanol. A total of 50 mg of protein was loaded on 4-12% Nu-Page Gel, probed with an anti-MeCP2 rabbit polyclonal antibody (Upstate Biotechnology cat. 07-013) or anti-

GAPDH rabbit polyclonal (Abcam) and visualized using the Amersham Pharmacia ECL.

Immunohistochemistry.

Brains were perfused with 4% paraformaldehyde in 0.1 M phosphate buffer (pH 7.4), post-fixed in 4% paraformaldehyde overnight at 4°C, washed in PBS, processed by TISSUE-TEK VIP machine (Miles Scientific), and imbedded in paraffin. Five microns serial sections were deparaffinized and treated with 10 mg/ml proteinaseK in 50mM Tris, 5mM EDTA for 10 minutes at RT. Slides were blocked in 5% normal goat serum and incubated with anti-MeCP2 polyclonal (23) and mouse anti-NeuN (Chemicon) at a dilution of 1:200. The primary antibodies were detected with a Rhodamine-conjugated goat anti-rabbit IgG or with FITC-conjugated donkey anti-mouse IgG (Jackson ImmunoResearch), both at a dilution of 1:500. Sections were finally rinsed in PBS DAPI and mounted in Vectashield (Vector laboratories). Images were taken with a Leica fluorescence microscope at 40X magnification.

Nuclear size measurements.

For nuclear size measurement, brains were perfused and imbedded in paraffin as described above. Four microns serial coronal sections were prepared and stained as described above. Digital pictures from the hippocampus (CA1-CA2) and somatosensory cortex LV were taken and the nuclear area (arbitrary unit) of the neuron was determined by tracing the outline of the nucleus in the DAPI

channel, using OpenLab. Neurons were identified by NeuN staining and the results are expressed as the fraction of NeuN positive cells that showed MeCP2 signal. Images were collected from at least 2 animals (8 weeks old) per genotype, 200 cells per animal were counted.

Spontaneous activity measurements.

Motor activity was measured using an infrared beam-activated movement-monitoring chamber (Opto-Varimax-MiniA, Columbus Instruments). For each experiment, a mouse was placed in the chamber at least 3h before recordings started. Movement was monitored during the normal 12h dark cycle (7 p.m. to 7 a.m.). A total of 7 wt mice, 4 transgenic controls, 4 NestinCre, 4 *Tau* Cre, 7 CamkII93 Cre and 5 CamkII159 Cre double transgenic mice were used. One dark cycle per animal per time point was collected.

Acknowledgments.

The authors acknowledge the excellent technical assistance of Jessica Dausman, Ruth Flannery and Dong Dong Fu. We also thank George Bell for the statistical analysis, Grant Welstead, Qiang Chang and Heinz Linhart for critical reading of the manuscript. The work was supported by a pre-doctoral fellowship from the Boehringer Ingelheim Foundation to EG, by the Rett Syndrome Research Foundation, and by NIH grants R01-HD045022, R37-CA084198 and R01-CA087869.

References.

1. Hagberg, B. & Hagberg, G. (1997) *Eur Child Adolesc Psychiatry* **6 Suppl 1,** 5-7.

2. Amir, R. E., Van den Veyver, I. B., Wan, M., Tran, C. Q., Francke, U., & Zoghbi, H. Y. (1999) *Nat Genet* **23,** 185-188.

3. Van den Veyver, I. B. & Zoghbi, H. Y. (2000) *Curr Opin Genet Dev* **10,** 275-279.

4. Wan, M., Lee, S. S., Zhang, X., Houwink-Manville, I., Song, H. R., Amir, R. E., Budden, S., Naidu, S., Pereira, J. L., Lo, I. F.*, et al.* (1999) *Am J Hum Genet* **65,** 1520-1529.

5. Xiang, F., Buervenich, S., Nicolao, P., Bailey, M. E., Zhang, Z., & Anvret, M. (2000) *J Med Genet* **37,** 250-255.

6. Guy, J., Hendrich, B., Holmes, M., Martin, J. E., & Bird, A. (2001) *Nat Genet* **27,** 322-326.

7. Chen, R. Z., Akbarian, S., Tudor, M., & Jaenisch, R. (2001) *Nat Genet* **27,** 327-331.

8. Shahbazian, M., Young, J., Yuva-Paylor, L., Spencer, C., Antalffy, B., Noebels, J., Armstrong, D., Paylor, R., & Zoghbi, H. (2002) *Neuron* **35,** 243-254.

9. Dani, V. S., Chang, Q., Maffei, A., Turrigiano, G. G., Jaenisch, R., & Nelson, S. B. (2005) *Proc Natl Acad Sci U S A* **102,** 12560-12565.

10. Young, J. I., Hong, E. P., Castle, J. C., Crespo-Barreto, J., Bowman, A. B., Rose, M. F., Kang, D., Richman, R., Johnson, J. M., Berget, S.*, et al.* (2005) *Proc Natl Acad Sci U S A* **102,** 17551-17558.

11. Gemelli, T., Berton, O., Nelson, E. D., Perrotti, L. I., Jaenisch, R., & Monteggia, L. M. (2006) *Biol Psychiatry* **59,** 468-476.

12. Lewis, J. D., Meehan, R. R., Henzel, W. J., Maurer-Fogy, I., Jeppesen, P., Klein, F., & Bird, A. (1992) *Cell* **69,** 905-914.

13. Nan, X., Campoy, F. J., & Bird, A. (1997) *Cell* **88,** 471-481.

14. Klose, R. J. & Bird, A. P. (2006) *Trends Biochem Sci* **31,** 89-97.

15. Fuks, F., Hurd, P. J., Wolf, D., Nan, X., Bird, A. P., & Kouzarides, T. (2003) *J Biol Chem* **278,** 4035-4040.

16. Traynor, J., Agarwal, P., Lazzeroni, L., & Francke, U. (2002) *BMC Med Genet* **3,** 12.

17. Tudor, M., Akbarian, S., Chen, R. Z., & Jaenisch, R. (2002) *Proc Natl Acad Sci U S A* **99,** 15536–15541.

18. Matarazzo, V. & Ronnett, G. V. (2004) *Proc Natl Acad Sci U S A* **101,** 7763–7768.

19. Nuber, U. A., Kriaucionis, S., Roloff, T. C., Guy, J., Selfridge, J., Steinhoff, C., Schulz, R., Lipkowitz, B., Ropers, H. H., Holmes, M. C.*, et al.* (2005) *Hum Mol Genet* **14,** 2247–2256.

20. Ballestar, E., Ropero, S., Alaminos, M., Armstrong, J., Setien, F., Agrelo, R., Fraga, M. F., Herranz, M., Avila, S., Pineda, M.*, et al.* (2005) *Hum Genet* **116,** 91–104.

21. Vetter, M. L. (2003) *Dev Cell* **5,** 359–360.

22. Martinowich, K., Hattori, D., Wu, H., Fouse, S., He, F., Hu, Y., Fan, G., & Sun, Y. E. (2003) *Science* **302,** 890–893.

23. Chen, W. G., Chang, Q., Lin, Y., Meissner, A., West, A. E., Griffith, E. C., Jaenisch, R., & Greenberg, M. E. (2003) *Science* **302,** 885–889.

24. Chang, Q., Khare, G., Dani, V., Nelson, S., & Jaenisch, R. (2006) *Neuron* **49,** 341–348.

25. Zhou, Z., Hong, E. J., Cohen, S., Zhao, W. N., Ho, H. Y., Schmidt, L., Chen, W. G., Lin, Y., Savner, E., Griffith, E. C.*, et al.* (2006) *Neuron* **52,** 255–269.

26. Sun, Y. E. & Wu, H. (2006) *Neuron* **49,** 321-323.

27. Makedonski, K., Abuhatzira, L., Kaufman, Y., Razin, A., & Shemer, R. (2005) *Hum Mol Genet* **14,** 1049-1058.

28. Samaco, R. C., Hogart, A., & LaSalle, J. M. (2005) *Hum Mol Genet* **14,** 483-492.

29. Horike, S., Cai, S., Miyano, M., Cheng, J. F., & Kohwi-Shigematsu, T. (2005) *Nat Genet* **37,** 31-40.

30. Jordan, C. & Francke, U. (2006) *Hum Mol Genet* **15,** 2210-2215.

31. Luikenhuis, S., Giacometti, E., Beard, C. F., & Jaenisch, R. (2004) *Proc Natl Acad Sci U S A* **101,** 6033-6038.

32. Quenard, A., Yilmaz, S., Fontaine, H., Bienvenu, T., Moncla, A., des Portes, V., Rivier, F., Mathieu, M., Raux, G., Jonveaux, P.*, et al.* (2006) *Eur J Med Genet* **49,** 313-322.

33. Mnatzakanian, G. N., Lohi, H., Munteanu, I., Alfred, S. E., Yamada, T., MacLeod, P. J., Jones, J. R., Scherer, S. W., Schanen, N. C., Friez, M. J.*, et al.* (2004) *Nat Genet* **36,** 339-341.

34. Kriaucionis, S. & Bird, A. (2004) *Nucleic Acids Res* **32,** 1818-1823.

35. Niwa, H., Yamamura, K., & Miyazaki, J. (1991) *Gene* **108,** 193-199.

36. Soriano, P. (1999) *Nat Genet* **21,** 70-71.

37. Beard, C., Hochedlinger, K., Plath, K., Wutz, A., & Jaenisch, R. (2006) *Genesis* **44,** 23-28.

38. Dubois, N. C., Hofmann, D., Kaloulis, K., Bishop, J. M., & Trumpp, A. (2006) *Genesis* **44,** 355-360.

39. Tucker, K. L., Meyer, M., & Barde, Y. A. (2001) *Nat Neurosci* **4,** 29-37.

40. Fan, G., Beard, C., Chen, R. Z., Csankovszki, G., Sun, Y., Siniaia, M., Biniszkiewicz, D., Bates, B., Lee, P. P., Kuhn, R.*, et al.* (2001) *J Neurosci* **21,** 788-797.

41. Minichiello, L., Korte, M., Wolfer, D., Kuhn, R., Unsicker, K., Cestari, V., Rossi-Arnaud, C., Lipp, H. P., Bonhoeffer, T., & Klein, R. (1999) *Neuron* **24,** 401-414.

42. Viemari, J. C., Roux, J. C., Tryba, A. K., Saywell, V., Burnet, H., Pena, F., Zanella, S., Bevengut, M., Barthelemy-Requin, M., Herzing, L. B.*, et al.* (2005) *J Neurosci* **25,** 11521-11530.

43. Van Esch, H., Bauters, M., Ignatius, J., Jansen, M., Raynaud, M., Hollanders, K., Lugtenberg, D., Bienvenu, T., Jensen, L. R., Gecz, J.*, et al.* (2005) *Am J Hum Genet* **77,** 442-453.

44. Meins, M., Lehmann, J., Gerresheim, F., Herchenbach, J., Hagedorn, M., Hameister, K., & Epplen, J. T. (2005) *J Med Genet* **42,** e12.

45. Collins, A. L., Levenson, J. M., Vilaythong, A. P., Richman, R., Armstrong, D. L., Noebels, J. L., David Sweatt, J., & Zoghbi, H. Y. (2004) *Hum Mol Genet* **13,** 2679-2689.

Figure Legends.

FIG.1 Schematic representation of the rescue construct.

A. Mecp2e2 cDNA (white box), CAGGS promoter (dark grey box), stop cassette (light grey box), LoxP sites (black boxes). The construct was targeted to the *Col1a1* locus. Expression of Cre will loop out the stop cassette allowing the expression of MeCP2e2. **B** Characteristics of the Cre lines used. **C.** Western blot analysis of tissue from wt (lanes 1), transgenic (CAGGS LSL Mecp2; *Mecp2* -/y, lanes 2) and *Mecp2* -/y (KO) mice (lane 3). No MeCP2 signal was detected in brain, lung and spleen of null animals containing the CAGGS LSL Mecp2 transgene. Anti-GAPDH as loading control. **D.** Western blot of total brain extracts of 6 weeks old animals. Lane 1, endogenous MeCP2 in wt brain. The higher, stronger band corresponds to MeCP2e1 and the lower fainter band corresponds to the MeCP2e2. Lane2: *Mecp2* -/y (KO); CAGGS LSL Mecp*2*. Lane 3,4: Nestin and *Tau* Cre rescued animals respectively. Lane 5-6: C93 and C159 rescued mice. **E-F.** Western blot analysis of CAGGS MeCP2 expression in cortex

(Co), hippocampus (Hi) and cerebellum (Ce). *Tau* and Nestin Cre activate the transgene in all areas (E, lanes 4 to 9) while C93 and C159 activate Mecp2 in cortex and hippocampus (F, lanes 4, 5,7 and8) but not in cerebellum (F, lanes 6 and 9). E, F lanes 1-3: endogenous MeCP2.

FIG.2 Expression of the CAGGS Mecp2 in different areas of the brain.

A. LV cortical neurons from a C93 rescued animal. CAGGS MeCP2 localizes in heterochromatin rich areas of the nucleus (arrowheads in inset ii). NeuN (Neuronal Nuclear-specific marker in green (i) and MeCP2 in red (ii), merge (iii). **B-D.** Percentage of neurons expressing CAGGS MeCP2. For each genotype (mice were at least 3 months old) we analyzed LV of the cortex (M1-S1) (2B), hippocampal CA1/ CA2 boundary (2C) and cerebellum (2D). Nestin (N) and *Tau* Cre (T) rescued animals expressed MeCP2 in 70 to 90% of neurons in all brain regions surveyed. C93 rescued mice had MeCP2 expression in 50% of the neurons in cortex and hippocampus. C159 rescued mice had maximum expression in the cortex (60% of neurons), but little or no expression elsewhere. No MeCP2 positive cells were found in the cerebellum of C93 and C159 rescued animals. In wt mice 100% of neurons express MeCP2 while no expression was observed in *Mecp2* -/y mice (data not shown). At least 100 cells per animal were included in the count. "n" is the number of animals analyzed for each genotype.

FIG.3 Rescued animals have higher probability of survival than *Mecp2* null littermates.

Kaplan-Meier survival curves were generated by plotting the percentage of live mice (Y axis) against number of days after birth (X axis). "n": number of animals analyzed. **A.** Nestin (N) and *Tau* (T) Cre double transgenic animals lived up to 280 days while control mice died within 106 days after birth. **B.** C93 and C159 mice lived up to 140 and 160 days, respectively. (C159 vs. null: log rank test p=0.0431; C93 vs. C159 p=0.725). **C-E.** Spontaneous nocturnal activity was measured by placing the animals in cages equipped with a movement detector (infrared beam). On the Y axis the number of beam interruptions over 10 hours, each bar represents a different genotype. Animals were monitored before 5 weeks (C), during the symptomatic stage (5 to 15 weeks) (D), and later than 15 weeks (E). No significant difference between wt (black bar), mutant (white bar) and rescued mice was found in animals younger than 4 weeks of age. Between 5 and 15 weeks of age the *Mecp2* mutant animals became hypoactive while rescued animals maintained normal levels of activity. At later age (E) the rescued animals showed lower activity that wt controls. Wt, KO, N, T, C93, C159 as in 3A-B

FIG.4 Rescued animals have normal physical development and brain weight.

A. Body weight in grams. We followed the weight of wt (black line) and rescued animals and found no significant difference, while null mutants animals (red line) became overweight starting at 5 weeks. By 8 weeks they were significantly overweight compared to wt and rescued subjects. Nestin Cre*: purple line (n=4), *Tau* Cre*: yellow line (n=3), C93*: green line (n=5), C159*: blue line (n=5), wt : black line (n=4), KO*: red line (n=4) (**Mecp2* -/y; CAGGS LSL Mecp2). **B.** Brain weights in grams. White circles represent wt and red triangles represent *Mecp2*

null (*) brains. Green and yellow squares represent brains from C93 (*) rescued animals and *Tau* Cre * rescued animals, respectively. Paired t-test wt vs. transgenic p= 0.000110 (using the first 4 time points); wt vs. C93 p= 0.0788 **C.** Neurons of C93 double transgenic animals have a normal nuclear size. Two months old C93 Cre double transgenic (grey bar), control wt (black bar) and null transgenic (white bar) littermates were analyzed for the comparison. Images were taken from the primary motor cortex (layer V) at 40X magnification and measurements from at least 200 cells were used for each bar. The animals used for the analysis were 8 weeks old. Wt, KO, C93 as described above.

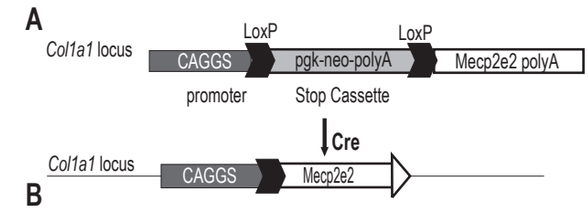

B

Promoter:	Expression starts at:	Active in :	Cell type:
Nestin (N)	E 10	All brain	neurons and glia
Tau (T)	E 9.5	All brain	post-mitotic neurons
CamKinaseII 93 (C93)	P0-P15	cortex, gray matter, hyppocampus	mature neurons
CamKinaseII 159 (C159)	P15-P30	frontal cortex, DG	mature neurons

C

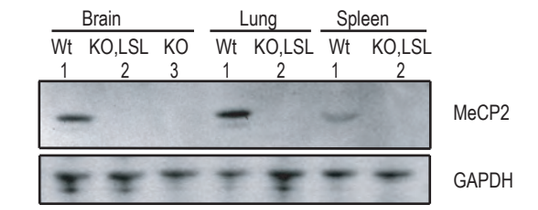

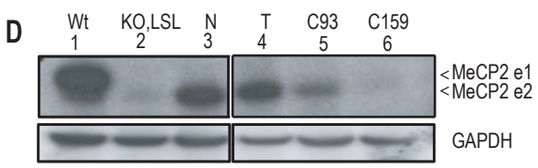

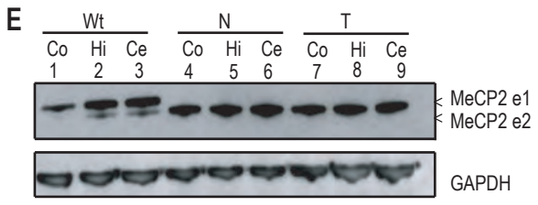

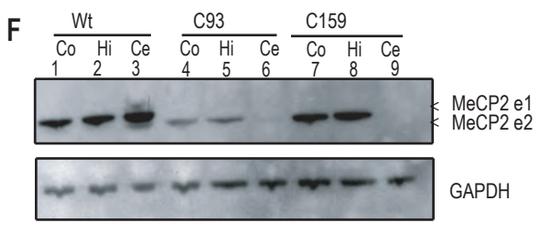

Figure 1. Schematic representation of the rescue construct. A. Mecp2e2 cDNA (white box), CAGGS promoter (dark grey box), stop cassette (light grey box), LoxP sites (black boxes). The construct was targeted to the Col1a1 locus. Expression of Cre will loop out the stop cassette allowing the expression of MeCP2e2. B Characteristics of the Cre lines used. C. Western blot analysis of tissue from wt (lanes 1), transgenic (CAGGS LSL Mecp2; Mecp2 -/y, lanes 2) and Mecp2 -/y (KO) mice (lane 3). No MeCP2 signal was detected in brain, lung and spleen of null animals containing the CAGGS LSL Mecp2 transgene. Anti-GAPDH as loading control. D. Western blot of total brain extracts of 6 weeks old animals. Lane 1, endogenous MeCP2 in wt brain. The higher, stronger band corresponds to MeCP2e1 and the lower fainter band corresponds to the MeCP2e2. Lane2: Mecp2 -/y (KO); CAGGS LSL Mecp2. Lane 3,4: Nestin and Tau Cre rescued animals respectively. Lane 5-6: C93 and C159 rescued mice. E-F. Western blot analysis of CAGGS MeCP2 expression in cortex (Co), hippocampus (Hi) and cerebellum (Ce). Tau and Nestin Cre activate the transgene in all areas (E, lanes 4 to 9) while C93 and C159 activate Mecp2 in cortex and hippocampus (F, lanes 4, 5,7 and8) but not in cerebellum (F, lanes 6 and 9). E, F lanes 1-3: endogenous MeCP2.

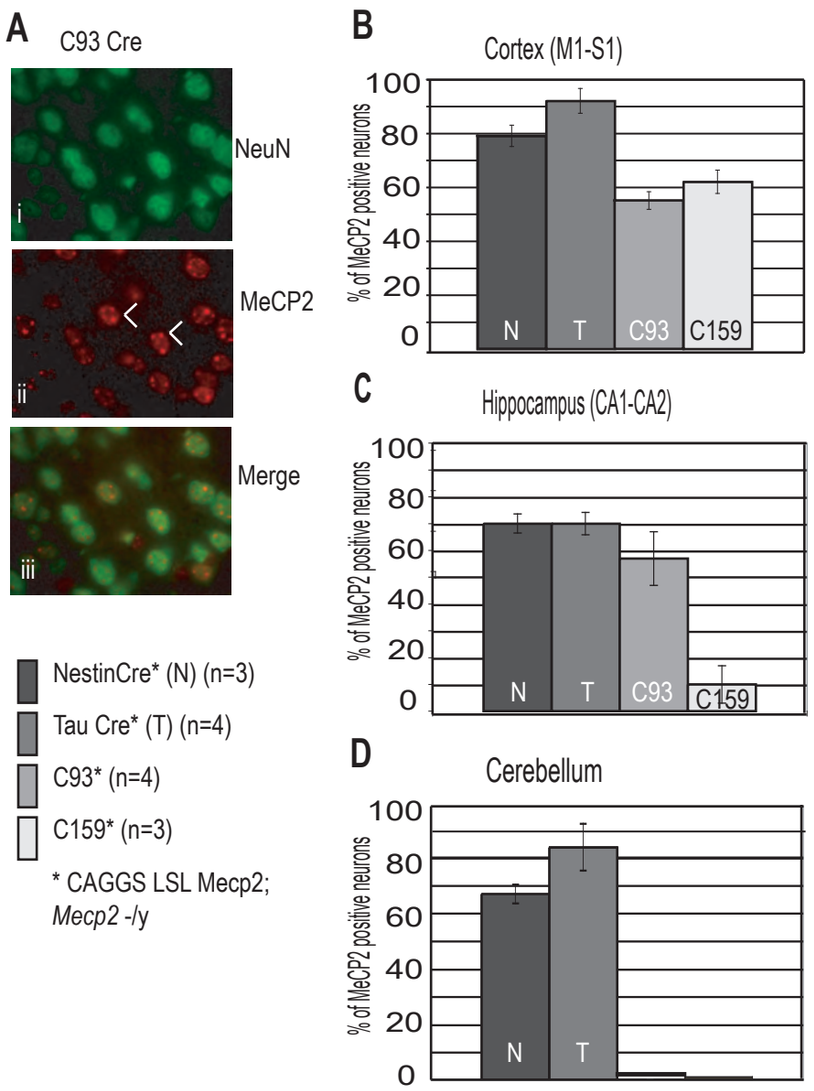

Figure2. Expression of the CAGGS Mecp2 in different areas of the brain. A. LV cortical neurons from a C93 rescued animal. CAGGS MeCP2 localizes in heterochromatin rich areas of the nucleus (arrowheads in inset ii). NeuN (Neuronal Nuclear-specific marker in green (i) and MeCP2 in red (ii), merge (iii). B-D. Percentage of neurons expressing CAGGS MeCP2. For each genotype (mice were at least 3 months old) we analyzed LV of the cortex (M1-S1) (2B), hippocampal CA1/ CA2 boundary (2C) and cerebellum (2D). Nestin (N) and Tau Cre (T) rescued animals expressed MeCP2 in 70 to 90% of neurons in all brain regions surveyed. C93 rescued mice had MeCP2 expression in 50% of the neurons in cortex and hippocampus. C159 rescued mice had maximum expression in the cortex (60% of neurons), but little or no expression elsewhere. No MeCP2 positive cells were found in the cerebellum of C93 and C159 rescued animals. In wt mice 100% of neurons express MeCP2 while no expression was observed in Mecp2 -/y mice (data not shown). At least 100 cells per animal were included in the count. "n" is the number of animals analyzed for each genotype.

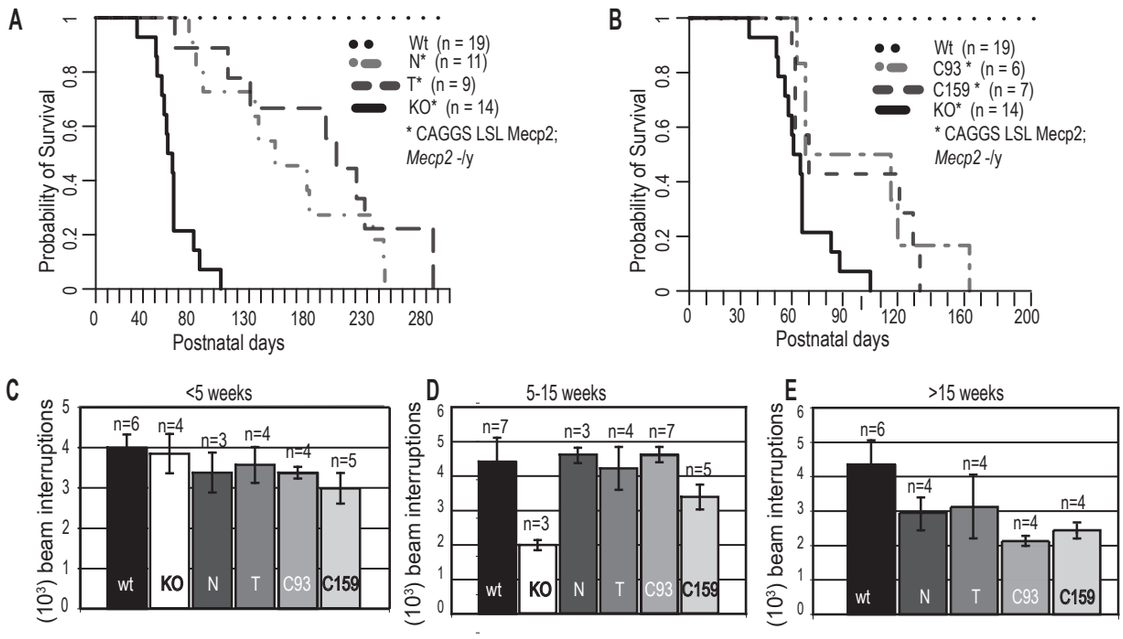

Figure 3. Rescued animals have higher probability of survival than Mecp2 null littermates. Kaplan-Meier survival curves were generated by plotting the percentage of live mice (Y axis) against number of days after birth (X axis). "n": number of animals analyzed. A. Nestin (N) and Tau (T) Cre double transgenic animals lived up to 280 days while control mice died within 106 days after birth. B. C93 and C159 mice lived up to 140 and 160 days, respectively. (C159 vs. null: log rank test p=0.0431; C93 vs. C159 p=0.725). C-E. Spontaneous nocturnal activity was measured by placing the animals in cages equipped with a movement detector (infrared beam). On the Y axis the number of beam interruptions over 10 hours, each bar represents a different genotype. Animals were monitored before 5 weeks (C), during the symptomatic stage (5 to 15 weeks) (D), and later than 15 weeks (E). No significant difference between wt (black bar), mutant (white bar) and rescued mice was found in animals younger than 4 weeks of age. Between 5 and 15 weeks of age the Mecp2 mutant animals became hypoactive while rescued animals maintained normal levels of activity. At later age (E) the rescued animals showed lower activity that wt controls. Wt, KO, N, T, C93, C159 as in 3A-B

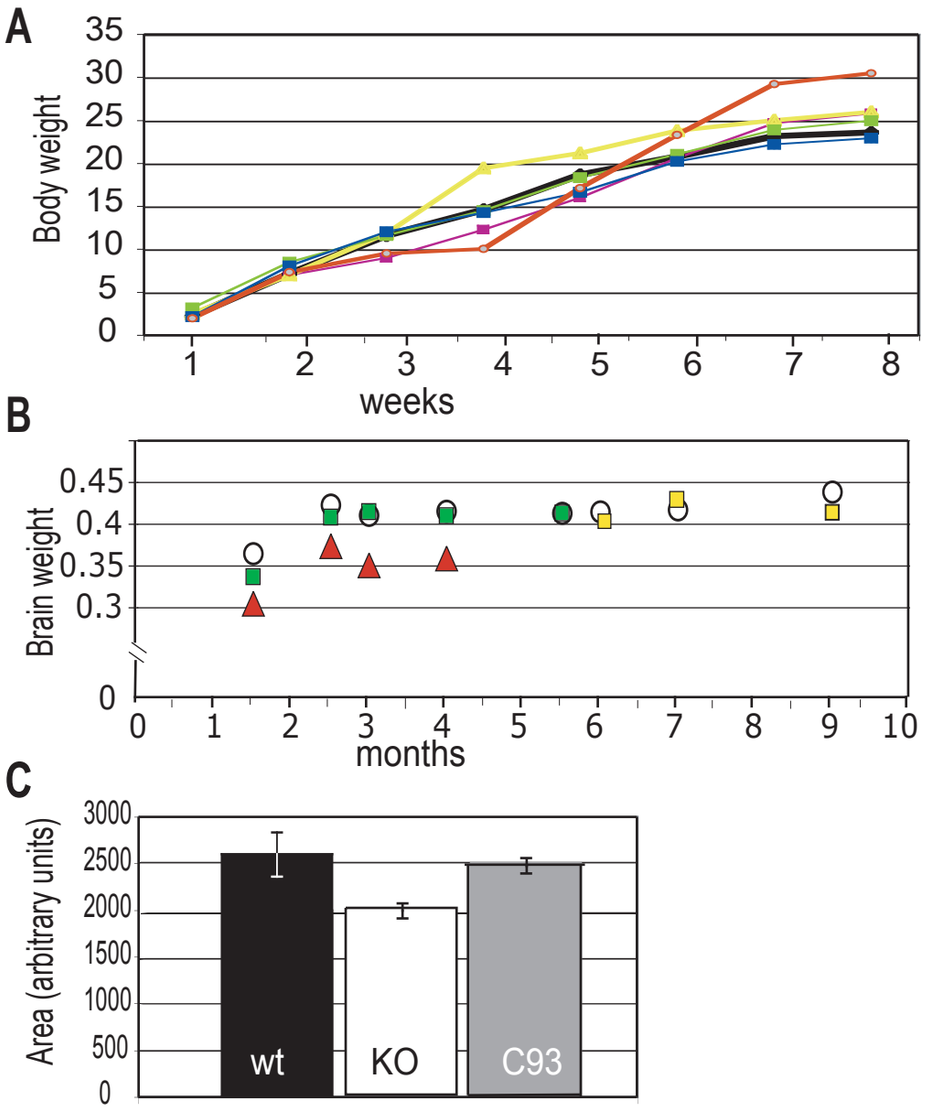

Figure 4. Rescued animals have normal physical development and brain weight. A. Body weight in grams. We followed the weight of wt (black line) and rescued animals and found no significant difference, while null mutants animals (red line) became overweight starting at 5 weeks. By 8 weeks they were significantly overweight compared to wt and rescued subjects. Nestin Cre*: purple line (n=4), Tau Cre*: yellow line (n=3), C93*: green line (n=5), C159*: blue line (n=5), wt : black line (n=4), KO*: red line (n=4) (*Mecp2 -/y; CAGGS LSL Mecp2). B. Brain weights in grams. White circles represent wt and red triangles represent Mecp2 null (*) brains. Green and yellow squares represent brains from C93 (*) rescued animals and Tau Cre * rescued animals, respectively. Paired t-test wt vs. transgenic p= 0.000110 (using the first 4 time points); wt vs. C93 p= 0.0788 C. Neurons of C93 double transgenic animals have a normal nuclear size. Two months old C93 Cre double transgenic (grey bar), control wt (black bar) and null transgenic (white bar) littermates were analyzed for the comparison. Images were taken from the primary motor cortex (layer V) at 40X magnification and measurements from at least 200 cells were used for each bar. The animals used for the analysis were 8 weeks old. Wt, KO, C93 as described above.

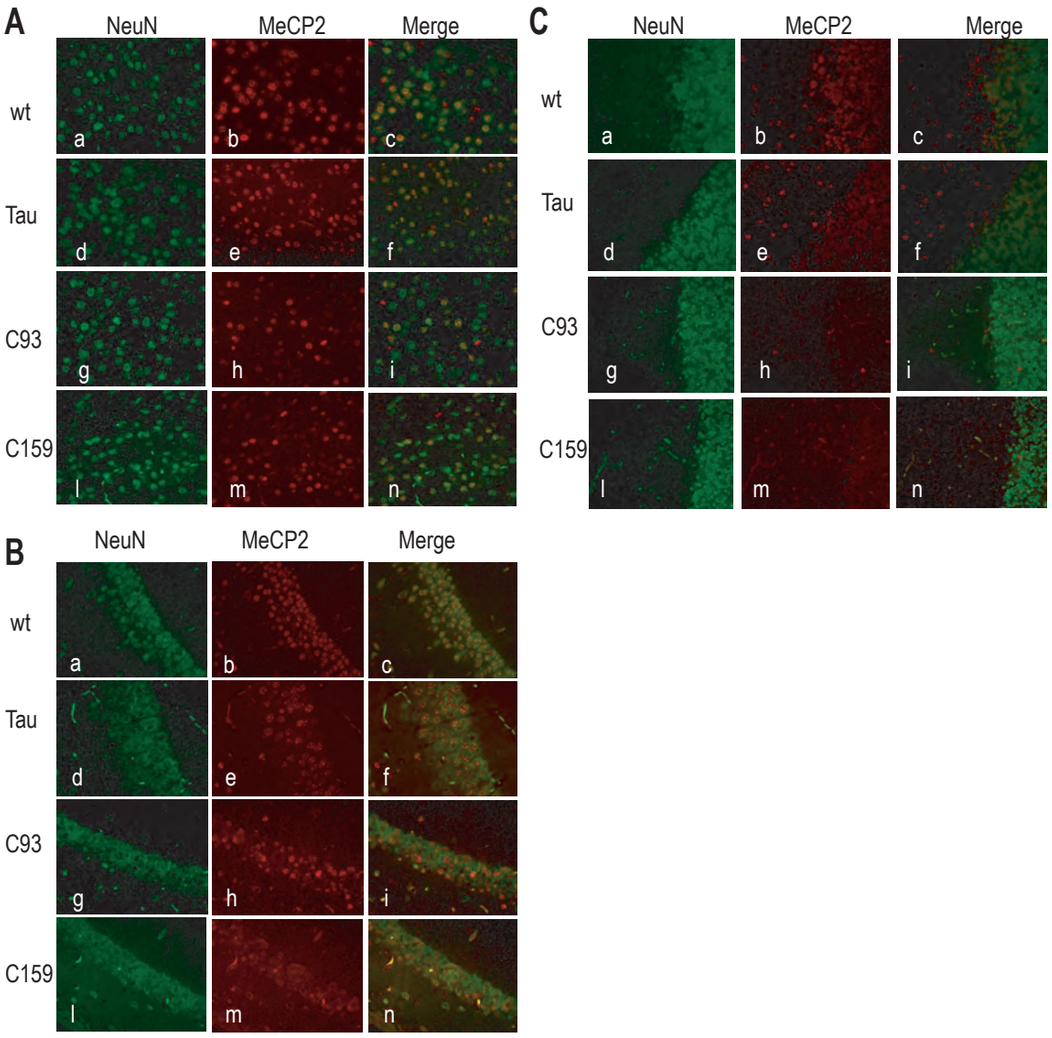

Figure 5S. Expression of the CAGGS Mecp2 in different areas of the brain. A–C. Representative images from primary somatosensory cortex layer V (2A), hippocampal CA1/CA2 boundary (2B) and cerebellum (2C) of wt animals (a, b, c,), Tau Cre (d,e,f) C93 Cre (g, h, i) and C159 (l, m. n) rescued animals. Sections were stained for NeuN (Neuronal Nuclear-specific marker in green (a, d, g, l) and for MeCP2 in red (b, e, h, m). Merge of the two channels is shown in c, f, i, n.

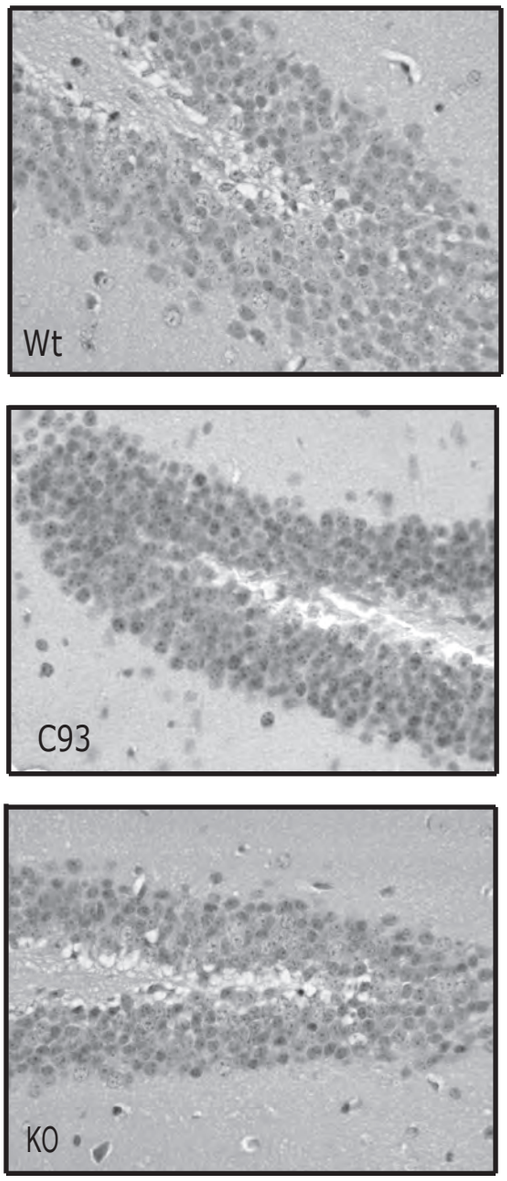

Figure 6S. Neurons of C93 double transgenic animals have a normal nuclear size. Images from the hippocampus (dentate gyrus) of wt, KO*, and C93* rescued animals. Nuclei were visualized with haematoxylin and eosin stain. (*Mecp2 -/y; CAGGS LSL Mecp2)

Chapter 3

"Insulin growth factor 1 derived peptide partially rescues Rett-like symptoms in MeCP2 mutant mice"

Emanuela Giacometti[1*], Daniela Tropea[2*], Nathan R. Wilson[2*],

Dong Dong Fu[1], Ruth Flannery[1], Mriganka Sur[2#], Rudolf Jaenisch[1,3#]

[1]Whitehead Institute for Biomedical Research, 9 Cambridge Center, Cambridge, MA 02142

[2]Picower Institute for Learning and Memory and Department of Brain and Cognitive Sciences, Massachusetts Institute of Technology, 43 Vassar Street, Cambridge, MA 02139

[3]Department of Biology, Massachusetts Institute of Technology, 77 Massachusetts Avenue, Cambridge, MA 02139

* These authors contributed equally to the work.

Abstract::

Rett Syndrome is a severe form of X-linked mental retardation caused by mutations in the gene coding for methyl CpG-binding protein 2 (MECP2). Here we tested whether treatment of Mecp2 mutant mice with (1-3)IGF-1, a 3 amino acid active fragment of insulin-like growth factor 1 (IGF-1), would affect the severity and progression of the Rett-like disease. Mecp2 mutant mice exhibited reduced synaptic potentials and persistent cortical plasticity indicative of immature synapses, along with decreased levels of the postsynaptic protein PSD-95 in cortical neurons. We show that systemic treatment with (1-3)IGF-1 extends life span, improves locomotor function and partially restores the reduced synaptic function and delayed maturation. In addition, the PI3K/Akt/PSD-95 pathway is significantly up-regulated in treated mice. Our results suggest (1-3)IGF-1 as a strong candidate for pharmacological treatment of Rett Syndrome and potentially of other CNS disorders caused by delayed synapse maturation.

Introduction:

Rett Syndrome is an X-linked neurological disorder that affects 1 in 10,000-15,000 live births[1]. The disorder is characterized by seemingly normal postnatal development followed by a sudden growth deceleration associated with progressive loss of acquired motor and language skills, stereotypic hand movements, muscle hypotonia, autonomic dysfunctions and severe cognitive impairment. Patients live into adulthood but are severely debilitated and require

full-time care. Unfortunately, there is no specific treatment for Rett Syndrome and management is mainly symptomatic and individualized.

The causative mutation in 85% of Rett patients resides on the gene coding for methyl CpG-binding protein 2 (MECP2)[2]. MeCP2 is thought to act as a global transcriptional silencer through selective binding to CpG-methylated sequences in the promoters of its target genes and subsequent recruitment of the Sin3A silencing complex[3]. While expressed in many tissues, it is strongly expressed in the central nervous system (CNS) following the onset of neuronal maturation and synaptogenesis[4,5]. Three mouse models with either absent[6,7] or truncated[8] MeCP2 have now been generated, and genetic experiments in these models have confirmed that the postnatal CNS-specific deletion of Mecp2 is sufficient to cause Rett-like symptoms[9]. Reciprocally, the expression of MeCP2 protein in null mice even at a very late stage of the disease can rescue the phenotype[10,11]. Much effort has been directed at identifying the genes mis-regulated in the absence of MeCP2[12], and until now the best characterized target of MeCP2 regulation is the brain derived neurotrophic factor BDNF[13]. MeCP2-null mice have lower levels of BDNF than wild type, and over-expression of BDNF relieves a host of symptoms in MeCP2-null mice[14], as well as in other models of CNS disorders[15,16]. However, despite this protein's potentially versatile therapeutic applications, non-invasive (intravenous or intra-peritoneal) administration of BDNF is hampered by its poor efficiency in crossing the brain capillary endothelial wall (the blood-brain barrier).

A second pleiotrophic growth factor with similar promise in CNS therapy, and the additional ability to cross the blood-brain barrier, is insulin-like growth factor 1 (IGF-1). IGF-1 is widely expressed in the CNS during normal

development, predominately by neurons[17], and studies of IGF-1 null and over-expressing mice have demonstrated that this molecule, similar(ly) to / as with BDNF, strongly promotes neuronal cell survival, synaptic maturation and function[18]. Moreover, IGF-1 is a modulator of functional plasticity in the developing cortex[19], and shares key intersecting intracellular pathways with BDNF such as the PI3K/Akt pathway[20]. The biological action of IGF-1 is mediated by the binding of IGF binding proteins (IGFBP 1-6) which modulate IGF-1's half life and affinity for the IGF-1 receptor. Interestingly, Itoh et al. recently reported that the binding protein IGFBP3 is a target of MeCP2 regulation that is up-regulated in MeCP2 null mice and Rett patients[21]. IGF-1 is cleaved by acid proteases into 2 peptides: (des)-IGF-1, and the N-terminal tri-peptide glycine-proline-glutamate, (1-3)IGF-1[21]. Of these products, (1-3)IGF-1 is of particular interest as it crosses the blood brain barrier more efficiently than IGF-1[22] while retaining strong neuro-protective efficacy[23-25]. Thus, given a) the established attractiveness of BDNF for the treatment of Rett Syndrome, b) the similarity of BDNF and IGF-1 in promoting neuronal and synaptic growth and survival, and c) the ability of IGF-1 and in particular (1-3)IGF-1 to cross the blood-brain barrier, we decided to investigate the ability of (1-3)IGF-1 to ameliorate Rett-like symptoms in a mouse model of the disease.

Results:

(1-3)IGF-1 administration improves life span and behavioral performance in a mouse model of Rett syndrome.

MeCP2 -/y mice develop Rett-like symptoms beginning at 4-6 weeks of age, at which they progressively become lethargic, develop gait ataxia, have

tremors, and die between 10 and 12 weeks of age (wild-type mice live for 1-1.5 years)[7]. To test the effectiveness of (1-3)IGF-1 treatment on the progression of these symptoms, we treated MeCP2 null animals from 2 weeks of age with daily intra-peritoneal injections of (1-3)IGF-1 (see **Methods**), while observing the life-expectancy and motor activity of treated animals compared to vehicle-injected controls. First, compared to vehicle-treated MeCP2 -/y littermates, MeCP2 -/y mice treated with (1-3)IGF-1 (**Fig. 1a**) showed a ~50% increase in life expectancy (an increase in the 0.5 probability survival rate from ca 60 days to 90 days), corresponding to a significant enhancement of survival (P = 0.54 * 10^-7, log rank test). Baseline nocturnal activity was also recorded, and results are shown in **Fig. 1b,c**. Before 6 weeks, MeCP2 -/y mice did not show obvious symptoms and there was no difference in activity between experimental groups (42003 ± 15870 beam crossings "wt" vs. 28337 ± 13691 crossings "wt-t" vs. 32412 ± 10843 crossings "ko-v" vs. 34601 ± 12336 crossings "ko-t"; $P > 0.05$, unpaired t-test; **Fig. 1b**). After 6 weeks however, MeCP2 -/y mice became progressively lethargic when compared to wild type littermates, and MeCP2 -/y animals treated with (1-3)IGF-1 showed a significant increase in activity levels compared with MeCP2 -/y littermates treated with vehicle (46786 ± 15601 beam crossings "wt" vs. 52353 ± 18355 crossings "wt-t" vs. 27215 ± 6893 crossings "ko-v" vs. 40455 ± 21592 crossings "ko-t"; P = 4.06 * 10^-5 "wt. vs. ko-v" and $P < 0.001$ "ko-v vs. ko-t", unpaired t-test; **Fig. 1c**).

Effects of (1-3)IGF-1 treatment on brain weight and neuronal cell size in the MeCP2 KO mouse.

One of the more consistent anatomical findings in Rett syndrome patients and MeCP2 null mice is a decreased brain weight and a reduction of soma size in neurons of the cortex and hippocampus[7]. Mutant mice with either ablated IGF-1[26], IGF1R mis-expression, or over-expression of IGFBPs also demonstrate brain growth retardation[27,28]. Conversely, transgenic mice over-expressing IGF-1 at 2 to 4 postnatal weeks exhibit a 5% increase in brain weight[29]. To investigate whether (1-3)IGF-1 treatment would also lead to a recovery of brain weight in the MeCP2 null mice, we collected brains from all experimental groups and measured brain weight and neuronal soma size. Following treatment with (1-3)IGF-1 in knockout animals, we observed an ~10% increase in average brain weight (0.41 ± 0.03 g "wt" vs. 0.42 ± 0.02 g "wt-t" vs. 0.33 ± 0.02 g "ko-v" vs. 0.36 ± 0.02 g "ko-t"; P = 4.02 * 10^-5 "wt. vs. ko-v" and P = 0.03 "ko-v vs. ko-t", unpaired t-test; **Fig. 2a**), with a modest but non-significant increase in the soma size of pyramidal neurons in layer 5 of sensorimotor cortex treated with (1-3)IGF-1 compared to vehicle-treated controls (20.31 ± 1.66 μm perimeter "wt" vs. 24.50 ± 0.85 μm "wt-t" vs. 18.60 ± 1.11 μm "ko-v" vs. 19.29 ± 0.63 μm "ko-t"; P = 0.19 "wt. vs. wt-t" and P = 0.62 "ko-v vs. ko-t", unpaired t-test; **Fig. 2b,c**).

Bradycardia in MeCP2-/y mice is partially rescued by (1-3)IGF-1 treatment.

Clinical and experimental evidence shows autonomic system dysfunctions such as labile breathing rhythms and reduced baseline cardiac vagal tone in Rett Syndrome patients[30]. A poor control of the feedback mechanisms that regulate blood pressure homeostasis through the sympathetic system, for example

hyperventilation-induced decrease in heart rate, is common in Rett patients and can cause life threatening cardiac arrhythmias[30,31]. The pathogenesis of the cardiac dysautonomia, although not well understood, suggests that immature neuronal connections in the brainstem could be the cause. To examine heart rate abnormalities in MeCP2 -/y mice and the effect of (1-3)IGF-1 treatment, we monitored real time cardiac pulse rate in non-anesthetized wild type and MeCP2 -/y animals treated with vehicle or (1-3)IGF-1. Wild type mice exhibited a regular distribution of heart rate measurements centered around 750 beats per minute (**Fig. 3a**). In contrast, MeCP2 -/y mice exhibited a very irregular heart rate, with frequent episodes of bradycardia (**Fig. 3b**). Treatment with (1-3)IGF-1 significantly reduced the occurrence of these episodes in MeCP2 -/y mice (**Fig. 3c**), as seen by aligning the cumulative distributions of heart rates observed in the three conditions ($P < 10^{-50}$ "wt vs. ko-v" and $P < 10^{-50}$ "ko-v vs. ko-t", Kolmogorov-Smirnov test; n = 114347 samples from 5 mice "wt" vs. 198021 samples from 5 mice "ko-v" vs. 241251 samples from 9 mice "ko-t"; **Fig. 3d**).

Effects of (1-3)IGF-1 on the synaptic physiology of MeCP2 mutant mice.

Recent studies have reported that neurons across multiple brain regions of MeCP2 -/y mice display a profound reduction in spontaneous activity as a consequence of reduced excitatory synaptic drive[14,32-34] and that this phenotype can be rescued by overexpression of BDNF[14]. Similarly, acute application of an IGF-1 derivate has been shown to elevate evoked excitatory postsynaptic current (EPSC) amplitudes by 40% in rat hippocampal cultures[35,36]. To thus test the efficacy of (1-3)IGF-1 in rescuing the MeCP2 -/y physiological phenotype, we acquired intracellular whole cell recordings in acute brain slices, measuring

excitatory synaptic drive (spontaneous EPSC amplitude and frequency) in layer 5 cortical neurons (**Fig. 4a**). Here, EPSCs recorded from -/y animals were significantly reduced in amplitude compared to EPSCs measured in wild-type animals (P = 2.30 * 10^-50, Kolmogorov-Smirnov test; n = 1543 events "wt" vs. 717 events "ko-v"; **Fig. 4b**). The trend was partially reversed in EPSCs recorded from MeCP2 -/y animals treated with (1-3)IGF-1, which were significantly larger in amplitude than EPSCs from MeCP2 -/y mice treated with vehicle (P = 1.22 * 10^-9, Kolmogorov-Smirnov test; n = 717 events "ko-v" vs. 1723 events "ko-t"; (**Fig. 4b**). These differences were also seen when averaging across cells (17.28 ± 1.98 pA "wt" vs. 6.82 ± 2.50 pA "ko-v" vs. 9.13 ± 2.13 pA "ko-t"; P = 0.02 "wt vs. ko-t" and 0.04 "ko-t vs. ko-v", unpaired t-test; n = 11 cells "wt", 6 cells "ko-v", 7 cells "ko-t"; **Fig. 4c**). Throughout these measurements, access resistance, leak, and cellular intrinsic excitability were also verified to be consistent across groups (data not shown). Quantifying EPSC intervals showed a slight increase in the interval between EPSC events (reduced EPSC frequency) between wild-type and MeCP2 -/y animals (P = 0.04, Kolmogorov-Smirnov test; n = 203 events "wt" vs. 113 events "ko-v"; **Fig. 4d**); though the EPSC frequency were not significantly different when the mean values for individual cells from different groups were compared (2.83 ± 0.37 Hz "wt" vs. 2.91 ± 0.80 Hz "ko-v" vs. 3.06 ± 0.56 Hz "ko-t"; P = 0.99 "wt vs. ko-t" and 0.32 "ko-t vs. ko-v", unpaired t-test; n = 11 cells "wt", 6 cells "ko-v", 7 cells "ko-t"; **Fig. 4e**). Our findings thus indicate that the reduction of excitatory synaptic drive in cortical cells of MeCP2 -/y mice, and its partial rescue following (1-3)IGF-1 treatment, are due in part to a change in EPSC amplitude as a consequence of a change in the strength of the synapses mediating excitatory transmission in this region.

MeCP2 deficiency leads to prolonged ocular dominance plasticity.

The timing of MeCP2 expression[4] and recent data from rescue experiments[10,11] suggest that MeCP2 deficiency might cause incomplete brain development and neuronal maturation[37,38]. In particular we hypothesized that neuronal and synapse development might be arrested in Rett Syndrome, consistent with the postnatal head growth deceleration and arrest of cognitive functions in girls with Rett syndrome at an age equivalent to 12 months or younger. To test this hypothesis we measured ocular dominance (OD) plasticity in the visual cortex of wild type or MeCP2 mutant mice. OD plasticity is an effective and reliable way to assess synaptic plasticity of the cortex *in vivo*[39], and relies on the ability of visual cortical circuitry to be modulated by unbalanced activity from the two eyes. Visual stimulation of either eye produces a response in the binocular portion of primary visual cortex (V1; **Supplementary Fig. 1ai**). Suturing one eye for a few days during a critical period of development leads to a reduction of synaptic drive from the closed eye, an increase of drive from the open eye, and hence a shift in the balance of cortical response toward the open eye[40] (**Supplementary Fig. 1bii-iii,d**). [In wild type animals the cortical response to the contralateral eye is dominant (**Supplementary Fig. 1aii-iii,c**), so that OD plasticity is commonly measured by suturing the contralateral eye]. This form of plasticity can be elicited in young animals (e.g., P28 mice) even with a brief period (4 days) of monocular deprivation (MD), while the same period of MD is unable to induce an OD shift in the cortex of mature animals (e.g., >P50 mice, where the rearrangement of synaptic connections requires longer periods of MD).

We reasoned that if synaptic development was arrested in MeCP2-deficient mice, synapses in visual cortex of adult mice would still be sensitive to brief MD (as in **Supplementary Fig. 1d**). To measure cortical responses elicited by stimulation of the eyes, we used optical imaging of intrinsic signals, a technique which detects level of deoxygenated hemoglobin, is related closely to neuronal activity, and is a highly sensitive and reliable measure of cortical plasticity[39,41] (see detailed description in **Methods**). Because adult MeCP2 -/y mice do not tolerate the anesthetic required for this analysis, we used MeCP2 heterozygous females which develop milder symptoms. **Fig. 5** shows that indeed adult wild type mice did not show OD plasticity after 4 days of MD (**Fig. 5a**, black traces; **Fig. 5b**, "P60, wt" and "wt MD" bars, ODI = 0.25 "wt" vs. 0.27 "wt MD"; N = 5 mice "wt", 5 mice "wt MD"; P = 0.16, one-tailed t-test) while age-matched MeCP2 mutants (+/-) showed a significant shift in the visually driven response in favour of the open eye (**Fig. 5a**, purple dotted traces; **Fig. 5b**, "P60, +/-" and "+/- MD" bars, ODI = 0.29 ± 0.06 "+/-" vs. -0.02 ± 0.08 "+/- MD"; N = 2 mice "+/-", 5 mice "+/- MD"; P = 0.04, one-tailed t-test). These results reveal the persistence of rapid synaptic plasticity following unbalanced visual drive in the adult MeCP2 mutant visual cortex – a feature that is typical of an immature cortex and is consistent with a deficit in synaptic maturation or stabilization following MeCP2 deficiency.

Ocular dominance plasticity in adult MeCP2 +/- mice is prevented by (1-3)IGF-1 treatment.

Developmental changes in OD plasticity are controlled in part by the activation of the IGF-1 pathway, and administration of (1-3)IGF-1 can abolish OD plasticity in wild type young mice[19]. We therefore tested if (1-3)IGF-1

treatment could stabilize the prolonged OD plasticity observed in adult MeCP2 mutants. Female MeCP2 +/- mice, aged P60 or more, were monocularly deprived for 4 days and treated concurrently with (1-3)IGF-1. **Fig. 5a,b** show that (1-3)IGF-1 treatment prevented the OD plasticity in the adult Mecp2 +/- mice (**Fig. 5a**, purple and red traces; **Fig. 5b**, "P60, +/- MD" and "+/- MD (1-3)IGF-1" bars, ODI = -0.02 ± 0.08 "+/- MD" vs. 0.24 ± 0.02 "+/- MD (1-3)IGF-1"; *N* = 5 mice "+/- MD", 5 mice "+/- MD (1-3)IGF-1"; *P* = 0.01, one-tailed t-test), suggesting that indeed (1-3)IGF-1 rapidly induces synapse stabilization or maturation in a mouse model of Rett Syndrome.

(1-3)IGF-1 treatment activates Akt in the brain.

The biological actions of IGF-1 are mediated by the activation of multiple signaling pathways including the phosphoinositide-3 kinase (PI3K) / Akt pathways. To investigate whether this IGF-1 pathway is activated in the (1-3)IGF-1 treated mice, brain tissue was collected at different time points after intra-peritoneal injection and protein extracts were used for western blot analysis. **Fig. 6a** (rows I and IV) shows an increase of phosphorylation of the serine 473 residue of Akt in animals treated with (1-3)IGF-1 (wt-t) versus controls (wt-v). Levels of total Akt were not affected (**Fig. 6a,** rows II and V). Akt was activated one to three hours after injection (**Fig. 6a**, row I) and remained upregulated for up to 24 hours (**Fig. 6a,** row IV). This time course suggests that Akt activation is mediated by direct action of (1-3)IGF-1 in the brain.

Interestingly, it has also been shown recently that BDNF, Akt and the post-synaptic density protein 95 (PSD-95) act together in mice to induce synaptic potentiation in visual cortical neurons[42]. Similarly, the application of insulin to rat hippocampal cultures induces up-regulation of PSD-95 via activation of the PI3k/Akt pathway[43]. PSD-95 is a highly abundant scaffolding protein which critically determines the strength of excitatory synapses[44]. It is therefore possible that the (1-3)IGF-1 induced potentiation of synaptic strength that we observed (**Fig. 4**) is mediated by activation of the Akt/PSD-95 pathway. To test this hypothesis, levels of PSD-95 protein were quantified by Western blot analysis in wild type and MeCP2 null mice treated with either vehicle or (1-3)IGF-1. As shown in **Fig. 6b**, MeCP2 -/y mice expressed lower than normal levels of PSD-95 (**Fig. 6b**, row I, lanes 6-11) and treatment with (1-3)IGF-1 significantly increased expression of PSD-95 in these animals (**Fig. 6b**, row IV, lanes 6-11). The expression levels of a presynaptic vesicle glycoprotein, synaptophysin, remained unchanged in all groups (**Fig. 6b**, rows II and V), indicating a specific effect of (1-3)IGF1 on components of postsynaptic signaling and synaptic function. Averaging across multiple mice revealed a similar trend, whereby MeCP2 -/y mice expressed similar levels of synaptophysin, but significantly lower levels of PSD-95 ($P = 0.02$, unpaired t-test; $n = 5$ mice "wt", 6 mice "ko"; **Fig. 6c**), and treatment with (1-3)IGF-1 also tended to increase expression of PSD-95 compared to treatment with a vehicle ($n = 5$ mice "wt", 6 mice "ko"; **Fig. 6d**). Thus, the weakening of synaptic function characteristic of the Rett mouse model[32-34], and its strengthening and stabilization that we observed following (1-3)IGF-1 treatment appear to be

mediated at least in part via the targeted modulation of the Akt / PSD-95 pathway.

Discussion:

In this study we provide evidence that (1-3)IGF-1 ameliorates symptoms of Rett Syndrome in a mouse model of the disease. Several lines of evidence support the hypothesis that MeCP2 mutant animals display features of immature circuitry in the CNS that persist into adulthood. First, visual cortex connections in adult MeCP2+/- mice display synaptic changes following monocular deprivation usually characteristic of young mice. Second, single neurons and synapses show a reduction in excitatory postsynaptic currents, indicating immaturity or instability of synaptic contacts. Third, PSD-95, a marker of mature functional synapses and their strength, is down-regulated in MeCP2 null brains. Meanwhile, treatment with the IGF-1 derivative (1-3)IGF-1 rescues these phenotypes, in a manner that is compatible with activation of the Akt / PSD-95 pathway and consequent fostering of synaptic stabilization. Systemic application of (1-3)IGF-1 also significantly improves life expectancy and baseline nocturnal activity in MeCP2 -/y mice. Furthermore, (1-3)IGF-1 relieves some of the autonomic dysfunctions characteristic of MeCP2 deficiency such as bradycardia.

Rett Syndrome is characterized by decreased brain weight, delayed physical development, autonomic dysfunctions and hypoactivity; over-expression of a neurotrophic factor in the mouse model has been shown to relieve some aspects of the disease progression[14]. IGF-1 is widely expressed in the central nervous system (CNS) during normal development[17] and strongly

promotes neuronal cell survival, synaptic maturation and function. The absence of the IGF-1 gene during murine brain development results in smaller cells with fewer processes[26] and in humans is associated with mental retardation[45]. After treating MeCP2 null animals with (1-3)IGF-1 or vehicle we found a substantial improvement in life expectancy and basal nocturnal activity in the (1-3)IGF-1 treated group. Although these effects were highly significant, it is important to stress that MeCP2 -/y mice treated with (1-3)IGF-1 still develop the full range of symptoms and die prematurely. The disease progression in mice, like in patients, involves an almost asymptomatic early period followed by a progressive deterioration from 4 to 8 weeks with death occurring usually between 10 and 12 weeks. (1-3)IGF-1 treated mice develop symptoms at the same age as vehicle treated controls but live significantly longer and maintain increased activity during the later phase of the disease. IGF-1 levels normally decrease with age, and artificially increasing levels of IGF-1 in rodents and humans has been associated with decreased muscle loss and improved mobility[46]. A similar effect might be mediated by (1-3)IGF-1 and might result in facilitated access of (1-3)IGF-1 treated mice to food and water. **Figure 2** shows that (1-3)IGF-1 treatment significantly increases brain weight in MeCP2 -/y mice, and bigger neuronal soma size partially accounts for this effect. It is possible that (1-3)IGF-1 treatment also increases dendritic outgrowth or adult neurogenesis[47,48], further contributing to the overall increase in brain weight.

Our results constitute the first functional evidence for the persistence of an immature state of cortical connections in the adult MeCP2 +/- brain. Female MeCP2 mutant mice have an almost normal life span (8-10 months), and develop milder symptoms much later in life than male mutant mice. The

pronounced effect on synaptic plasticity observed in the MeCP2 mutant female brain was therefore rather unexpected. Due to random X inactivation, approximately 50% of neurons in the brains of female MeCP2 +/- mice express wild type MeCP2 protein. This would argue for a dominant effect of the mutant neurons on the entire synaptic network, consistent with the results of earlier genetic rescue experiments, demonstrating that reactivation of MeCP2 expression in >70% of the neurons did not prevent development of symptoms in MeCP2 -/y mice[11]. We speculate that (1-3)IGF-1 reduces OD plasticity in adult mutant mice by stabilizing synaptic contacts, though it might also increase the number of synaptic connections. It appears that (1-3)IGF-1 acts rapidly in stabilizing synaptic contacts in the visual cortex as the mice used for the monocular deprivation experiments were treated only for 4 days prior to the optical imaging. We cannot exclude the possibility that (1-3)IGF-1 affects non-neuronal cells; for example (1-3)IGF-1 treatment could increase vascular density and glucose utilization in the brain or have additional effects in peripheral tissues. In the experiments described, (1-3)IGF-1 was administered to the mice via intra-peritoneal injections. It is possible that other delivery methods, such as intravenous infusion or ventricular delivery would be more effective and potentially could further improve the extent of rescue of the symptoms.

In conclusion we have shown that systemic delivery of (1-3)IGF-1 can significantly improve survival and behavior in MeCP2 mutant mice. We also provide direct evidence that MeCP2 deficiency leads to immature synaptic function and organization which can be partially rescued by (1-3)IGF-1 administration. The CNS effect of (1-3)IGF-1 could be mediated by activation of the PI3K/Akt/PSD-95 pathway. While further studies will be needed to unravel

the exact mechanism of (1-3)IGF-1 action, the results presented here point to a potential utility of (1-3)IGF-1 towards the treatment of Rett Syndrome.

Acknowledgments:

We thank Sam H. Horng, Orsolya Kuti and Jessie Dausmann for excellent technical assistance, Shomit Sengupta and Caroline Beard for useful scientific discussion and critical reading of the manuscript. We also thank George Bell for help with statistical analysis and Tom di Cesare for graphics support. This work was supported by a predoctoral fellowship from the Boheringer Ingelheim foundation to EG, Ruth Kirschstein National Research Service Award postdoctoral fellowships (F32-EYO17240 and F32-EY017500, NIH) to DT and NRW, grants from the Simons Foundation and Autism Consortium to MS, and grants from the Rett Syndrome Research Foundation and NIH (RO1-CA087869 and RO1-HD045022) to RJ.

FIGURE LEGENDS:

Figure 1: Survival and baseline activity are significantly increased in treated animals.

A. (1-3)IGF-1 treated MeCP2 -/y mice have longer life expectancy than vehicle treated controls. Kaplan-Meier survival curves for MeCP2 -/y mice treated with vehicle ("ko-v", red line) or (1-3)IGF-1 ("ko-t", green line). The X axis shows the days after birth, and the Y axis shows the probability of survival. MeCP2 -/y mice treated with (1-3)IGF-1 exhibited a significantly longer life expectancy that their vehicle treated littermates. MeCP2 -/y mice were given

daily IP injections of (1-3)IGF-1 (0.01 mg / g body weight / day) every day from 2 weeks of age onward. “n” is the number of mice per experimental group.

B. (1-3)IGF-1 treatment improves locomotor function in MeCP2 null mice. Baseline nocturnal activity was measured by placing animals in cages equipped with a movement detector (infrared beam). The Y axis shows the number of beam interruptions over 10 hours; each bar represents a different experimental group. Nocturnal activity was recorded weekly between 4 and 17 weeks of age. Data from 4-5 weeks and >6 week-old mice is shown in B and C respectively. As expected, MeCP2 -/y mice treated with vehicle (“ko-v”, red bar), showed significantly less activity that wild type (“wt”, black bar) littermates. MeCP2 -/y animals treated with (1-3)IGF-1 (“ko-t”, green bar) were more active than vehicle-treated animals (“ko-v”, red bar) but not as active as wild type littermates. Wt animals treated with (1-3)IGF-1 (“wt-t” grey bar) were not significantly more active than wild type. “n” = number of animals per group, error bars represent standard deviation.

Figure 2: (1-3)IGF-1 increases brain weight and pyramidal neuron soma size.

A. Postnatal (1-3)IGF-1 treatment increases brain weight. The value bars indicate the average brain weight (at P60) of each experimental group: wild type “wt”, wild type treated with (1-3)IGF-1 “wt-t”; MeCP2 -/y receiving vehicle "ko-v” or treated with (1-3)IGF-1 “ko-t”. Error bars represent standard error. “n” :number of animals per group. MeCP2 -/y mice had lower brain weight compared to wt mice, and MeCP2 -/y mice treated with (1-

3)IGF-1 had increased brain weight compared to vehicle-treated MeCP2 -/y littermates.

B. Effect of postnatal (1-3)IGF-1 treatment on cell size of layer 5 neurons in sensorimotor (S1) cortex. (1-3)IGF-1 modestly increases average soma size in MeCP2 -/y animals compared to vehicle treated animals. "n" = number of animals per group; at least 24 cells per animal were measured.

C. Representative images of layer 5 neurons in S1 in the 4 experimental groups. Scale bar represents 100 μm.

Figure 3: (1-3) IGF-1 reduces the frequency of bradycardia in MeCP2 null mice.

A. Pooled distribution of heart rates observed in beats per minute (bpm) in wt animals. The Y axis depicts the total number of observations within an experimental group for a given bpm value (X axis).

B. Heart rate in beats per minute in MeCP2 -/y animals (8 weeks old) receiving vehicle for 6 weeks.Heart rate in beats per minute in MeCP2 -/y (8 weeks old) animals treated with (1-3)IGF-1 for 6 weeks.

C. Cumulative distributions of heart rate measurements in the 3 groups. The MeCP2 -/y distribution (red) was left-shifted compared to the wild-type distribution (blue), indicating a significant reduction in the distribution of heart rates. The MeCP2-/y treated with (1-3) IGF1 distribution (green) was in-between the two curves, indicating a partial rescue of the MeCP2-/y phenotype towards a more normal wild-type distribution.

Figure 4: Increased amplitude of synaptic currents for layer 5 pyramidal neurons in (1-3)IGF-1 treated MeCP2 -/y animals.

A. Representative traces from recordings of spontaneous excitatory postsynaptic currents (EPSCs) in wild type (wt), MeCP2 -/y treated with vehicle (ko-v), or (1-3)IGF-1 (ko-t) for two weeks. Top traces depict a compressed view of spontaneous activity, and the bottom two traces show individual events with an expanded scale. Mice were 28-32 days old.

B. Cumulative distributions of EPSC amplitudes, across all cells measured, in wild type (wt), MeCP2 -/y plus vehicle (ko-v) or MeCP2 -/y plus (1-3)IGF-1 (ko-t). Distributions indicate an increased percentage of events with smaller amplitudes in ko-v vs. wild-type. (1-3)IGF-1 treatment partially but significantly reversed this trend.

C. Neurons' mean EPSC amplitude in wild-type (wt), MeCP2 -/y (ko-v), and MeCP2 -/y treated with (1-3)IGF-1 for two weeks (ko-t). Mean EPSC amplitude was significantly reduced in -/y neurons compared to wild-type. Compared to ko-v animals, mean EPSC amplitude was modestly but significantly increased in -/y animals treated with (1-3)IGF-1. All error bars are s.e.m.

D. Distributions of intervals between EPSC events, reflecting EPSC frequency, are subtly modified between wt, and ko-v and ko-t groups.

E. Group analysis of mean EPSC frequency across cells in each treatment does not indicate a significant change between groups. All error bars are s.e.m.

Figure 5: Visual cortex plasticity in adult MeCP2 heterozygous mice is prevented by (1-3)IGF-1.

A. Ocular Dominance Index (ODI) distributions from individual adult animals. Regions of analysis typically included 900-1300 pixels, and ODI values were derived from the optical signal intensity at each pixel driven by the two eyes (see **Methods**). The mean ODI value from each animal was used for the population analyses of part B.

B. i. Adult wild type (black lines) and MeCP2 +/- mice (purple lines) either with monocular deprivation of the contralateral eye (MD, dashed lines) or without MD (continuous lines).

ii. Adult MeCP2 +/- mice following MD, either untreated (dashed purple line) or treated with (1-3)IGF-1 (red continuous line). Untreated mice show a shift in visual drive, measured by the ODI, away from the closed eye and towards the open eye, similar to developing animals (see part B) - demonstrating extended plasticity and indicating the persistence of immature synapses into adulthood. (1-3)IGF-1 treatment during the period of MD abolishes this plasticity, preserving an ocular dominance profile typical of non-deprived animals.

C. Mean ODI values for developing wild type mice (~P28, left) and adult wild type mice (~P60, right). Positive ODI values indicate higher drive from the contralateral eye while negative values indicate higher drive from the ipsilateral eye (see part A). Wild type “wt”, wild type after monocular deprivation “wt MD”, MeCP2 +/- “ +/-“, MeCP2 +/- after monocular deprivation “+/- MD”, and MeCP2 +/- treated with (1-3)IGF-1 during monocular deprivation “+/- MD-t”. After MD, visual cortex in wild type adult animals is still dominated by the contralateral eye while in adult MeCP2+/- mice there is severe reduction of contralateral eye drive and a shift of ODI

towards the ipsilateral eye. Treatment with (1-3)IGF-1 in MeCP2 +/- mice during MD prevents the ocular dominance shift towards the ipsilateral eye. The ODI values for P28 wild type animals were taken from Tropea et al.[19]. Error bars represent standard error.

Figure 6: Western blot analysis of total brain tissue from different experimental groups.

A. Time course of Akt activation in the brain following intraperitioneal injections of (1-3)IGF-1. 8 week old wild type C57Bl6 male mice were injected with vehicle (wt-v) (first two lanes in each row) or with (1-3)IGF-1 (wt-t), and brain tissue was collected at the time points indicated at the top of each lane: 5 minutes to 3 hours in rows I-III and 1 to 24 hours in rows IV-VI. An increase in p-Akt signal can be seen at 2hr from IP injection (row I, last two lanes). Total Akt levels (row II and V) remain unchanged until 12 hours when there is a small increase (row V last two lanes). Equal loading was controlled with GAPDH (row III and VI).

B. MeCP2-/y (ko) mice have lower levels of post-synaptic density protein 95 (PSD-95) (row I, lanes 6-11) than wild type littermates (wt) (row I, lanes 1-5). Adult MeCP2 -/y animals injected for 2 weeks with (1-3)IGF-1 (ko-t) have higher levels of PSD-95 than vehicle injected age-matched -/y littermates (ko-v) (row IV lanes 6 to 11). Levels of the synaptic vesicle glycoprotein synaptophysin (synap.) remain unchanged in all groups (row II and V). Equal loading was controlled with actin (rows III and VI).

C-D. Quantification of the Immunoblot signal for PSD-95 and synaptophysin across all groups. Bar graphs represents average pixel

density across all animals in a given experimental group. The signal was normalized to actin. Error bars represent standard deviation.

Supplementary Figure 1: Optical imaging of intrinsic signals to measure ocular dominance plasticity in visual cortex.

A. Optical imaging of intrinsic signals can be used to derive the strength of drive from each eye in primary visual cortex (V1).
   i. Visual pathway schematic, showing inputs from each eye to V1.
   ii. Schematic of the optical imaging setup. An anesthetized mouse is placed in front of a monitor displaying a periodic drifting bar stimulus. The skull surface is illuminated with red light (630 nm), and imaged with a CCD camera.
   iii. Blood vessel pattern in the binocular region of V1 (white circle) with representative optical signal levels when the contralateral eye (left, red signal) or the ipsilateral eye (right blue signal) is stimulated. In wild type adult animals the signal from the contralateral eye is stronger than the one from the ipsilateral eye.
B. Shift in ocular dominance after monocular deprivation in a young mouse.
   i. Monocular eye lid suture for 4 days.
   ii. After the lid suture is removed, each eye is stimulated in turn and visual responses in V1 are recorded.
   iii. The short period of monocular deprivation causes a weakening of inputs from the deprived contralateral eye (red) and strengthening of inputs from the non-deprived ipsilateral eye (blue).

C-D. Schematic of signal intensity in the binocular region of V1

when each eye is stimulated under different conditions in wild-type animals. Red and blue circles represent intensity of optical signal driven by the contralateral and ipsilateral eyes, respectively. Ocular Dominance Index (ODI) distributions at right are derived from the relative strength of drive from each eye at each pixel. Three conditions are shown: a normal adult wild type mouse (C), a young mouse after 4 days of monocular deprivation (D) and an adult mouse after 4 days of MD. In a wild-type mouse, MD of the contralateral eye during development causes a shift in the signal intensity and ODI towards the open ipsilateral eye. Such plasticity is not seen after a similar period of MD in an adult animal.

MATERIALS AND METHODS:

Mice mating and genotyping: We used the MeCP2 germline null allele from Chen *et al.*[7]. Genotyping was performed as in Chen *et al*[7].

(1-3)IGF-1 treatment: For the survival measurements, the nocturnal activity analysis and the immunoblot analysis, (1-3)IGF-1 (Bachem Biosciences # H22468) was administered daily via intra-peritoneal injections (0.01 mg /g body weight, vehicle = saline, 0.01% BSA). The treatment was started at P15 and maintained throughout the course of the experiments. For intracellular physiology experiments, the mice were injected daily (0.01 mg / g body weight, vehicle = saline, 0.01% BSA) for 2 weeks, from P15 to P28-P32 when they were

used for acute slice preparation. For optical imaging experiments, mice were injected with (1-3)IGF-1 (0.02 mg / g body weight, vehicle = saline, 0.01% BSA) daily from the day of the lid suture to the day of imaging.

Nocturnal activity measurements: Spontaneous motor activity was measured by using an infrared beam-activated movement-monitoring chamber (Opto-Varimax-MiniA; Columbus Instruments, Columbus, OH). For each experiment, a mouse was placed in the chamber at least 3 h before recordings started. Movement was monitored during the normal 12-h dark cycle (7 p.m. to 7 a.m.). One dark cycle per animal per time point was collected.

Soma size measurements: For nuclear size measurement, brains from 8 weeks old animals, treated with (1-3)IGF-1 or vehicle from the P20, were perfused with 4% paraformaldehyde in 0.1 M phosphate buffer (pH 7.4), postfixed in 4% formaline overnight at 4°C, washed in PBS, processed with a TISSUE-TEK VIP machine (Miles Scientific, Naperville, IL), and imbedded in paraffin. 4 μm serial coronal sections were prepared and Nissel stained. Digital pictures from somatosensory cortex, layer V were taken, and the size of the nuclear area of the neuron was determined by tracing the outline of the nucleus in microns by using OpenLab software (Improvision, Waltham, MA). Digital picture collection and cell measurements were done blind to the genotype.

Heart rate measurements: Real time cardiac pulse rate was measured using a tail clip sensor (Mouse OX Oximeter, Oakmont, PA). Mice were not anesthetized but physically restrained in a fitted open plastic tube. Prior to the recording session

the tube was placed overnight in the cages housing the experimental animals to allow habituation. Body temperature was maintained at ~82-84°F throughout the recording time. We recorded 3 trials of 15 minutes for each mouse, mice were 8 weeks old and treated with either vehicle or (1-3)IGF-1 from P15.

Slice physiology preparation: Coronal sections (300 μm thick) at or near sensorimotor cortex were cut in < 4°C ACSF using a Vibratome. Slices were incubated at 37° C for 20 minutes after slicing, and at room temperature for the remainder of the experiment. Slices were transferred to a Warner chamber and recordings were taken from visually identified pyramidal neurons located in layer 5. Artificial cerebral spinal fluid (ACSF) contained 126 mM NaCl, 25 mM NaHCO3, 1 mM NaHPO4, 3 mM KCl, 2 mM MgSO4, 2 mM CaCl2, and 14 mM dextrose, was adjusted to 315-320 mOsm and 7.4 pH, and was bubbled with 95% O2 / 5% CO2. The intracellular pipette solution contained 100 mM potassium gluconate, 20 mM KCl, 10 mM HEPES, 4 mM MgATP, 0.3 mM NaGTP, and 10 mM Na-phosphocreatine.

Intracellular whole-cell recordings: Borosilicate pipettes (3-5 MΩ, WPI) were pulled using a Sutter P-80 puller (Sutter Instruments). Cells were visualized with an Achroplan 40x water-immersion lens with infrared-DIC optics (Zeiss) and detected with an infrared camera (Hamamatsu) projecting to a video monitor. Experiments were driven by custom acquisition and real-time analysis software written in Matlab (Mathworks, Natick, MA) using a Multiclamp 700B amplifier (Axon Instruments) connected to a BNC-2110 connector block and M-Series dual-channel acquisition card (National Instruments). Gigaseal and rupture was

achieved and whole-cell recordings were continuously verified for low levels of leak and series resistance. For each recording, a 5 mV test pulse was applied in voltage clamp ~10 times to measure input and series resistance. Then in current clamp ~10 pulses (500 ms, 40-140 pA at 10 pA increments), were applied to quantify evoked firing rates and cellular excitability. Access resistance, leak, and cellular intrinsic excitability were verified to be consistent across groups. Finally, spontaneous EPSCs under voltage clamp at -60 mV were sampled at 10 kHz and low-pass filtered at 1 kHz. Analysis was performed using a custom software package written in Matlab, with all events detected according to automated thresholds and blindly verified for each event individually by the experimenter.

Optical imaging of intrinsic signals:

Adult (>P60) wild type (SVEV or BL6) and MeCP2 (+/-) mutant females (BL6) were used for this experiment. The wild type control group was composed of both wild type littermates of MeCP2 +/- females or wild type age matched SVEV females. For monocular deprivation, animals were anesthetized with Avertin (0.016 ml / g) and the eyelids of one eye was sutured for 4 days. Prior to imaging, the suture was removed and the deprived eye re-opened. Only animals in which the deprivation sutures were intact and the condition of the deprived eye appeared healthy were used for the imaging session. For IGF-1 signaling activation, a solution containing (1-3)IGF-1 was injected intra-peritoneally (IP) daily for the entire period of deprivation. For the imaging sessions mice were anesthetized with urethane (1.5 g / kg; 20% of the full dosage was administered IP each 20-30 minutes up to the final dosage, 0.02 ml of cloroprothixene 1% was also injected together with the first administration). The skull was exposed

and a custom-made plate was glued on the head to minimize movement. The skull was thinned over V1 with a dremel drill and covered with an agarose solution in saline (1.5%) and a glass coverslip. During the imaging session, the animal was constantly oxygenated, its temperature maintained with a heating blanket and the eyes periodically treated with silicone oil; physiological conditions were constantly monitored. The anesthetized mouse was placed in front of a monitor displaying a periodic stimulus presented to either eye, monocularly; the stimulus consisted of a drifting vertical or horizontal white bar of dimensions 9°x72°, drifting at 9 sec/cycle, over a uniformly gray background. The skull surface was illuminated with a red light (630 nm) and the change of luminance was captured by a CCD camera (Cascade 512B, Roper Scientific) at the rate of 15 frames / sec during each stimulus session of 25 minutes. A temporal high pass filter (135 frames) was employed to remove the slow signal noise, after which the signal was computer processed in order to extract, at each pixel, the temporal Fast Fourier Transform (FFT) component corresponding to the stimulus frequency. The FFT amplitude was used to measure the strength of the visual evoked response to each eye. The ocular dominance index was derived from each eye's response (R) at each pixel as ODI = (Rcontra – Ripsi)/ (Rcontra + Ripsi). The binocular zone was defined as the region activated by the stimulation of the eye ipsilateral to the imaged hemisphere, and the most highly-activated pixels (between 900 and 1900) in response to this stimulation were used in the analysis.

Western blot analysis: Brains were harvested and snap frozen in liquid nitrogen. Tissues were then homogenized in a glass-glass tissue douncer in RIPA buffer

(50 mM HEPES-KOH, pH 7.4, 40mM NaCl, 2mM NaVO4, 50mM NaF, 10 mM Na-pyrophosphate, 10mM Na-beta-glycerophosphate, 1% Na-deoxycolate, 1% NP-40, and 0.1% SDS) supplemented with proteinase inhibitors (Roche, Indianapolis, IN). Protein concentrations were determined by BCA (Pierce, Rockford, IL). Sample buffer was added to a final concentration of 12.5% glycerol and 0.25% 2-mercaptoethanol. A total of 50 g of protein was loaded on 4-12% Nu-Page gels. The following antibodies were used: Akt (Cell Signaling #4685), p-Akt S473 (Cell Signaling #4058), anti-PSD-95 (Cell Signaling #2507), anti-synaptophysin (Abcam #b18008), anti-actin (Abcam #6276), anti-GAPDH (Abcam #8485) and visualized using ECL (Amersham Pharmacia).

References:

1. Chahrour, M. & Zoghbi, H.Y. The story of rett syndrome: from clinic to neurobiology. *Neuron* **56**, 422-37 (2007).
2. Amir, R.E. et al. Rett syndrome is caused by mutations in X-linked MECP2, encoding methyl-CpG-binding protein 2. *Nat Genet* **23**, 185-8 (1999).
3. Nan, X. et al. Transcriptional repression by the methyl-CpG-binding protein MeCP2 involves a histone deacetylase complex. *Nature* **393**, 386-9 (1998).
4. Shahbazian, M.D., Antalffy, B., Armstrong, D.L. & Zoghbi, H.Y. Insight into Rett syndrome: MeCP2 levels display tissue- and cell-specific differences and correlate with neuronal maturation. *Hum Mol Genet* **11**, 115-24 (2002).
5. Cohen, D.R. et al. Expression of MeCP2 in olfactory receptor neurons is developmentally regulated and occurs before synaptogenesis. *Mol Cell Neurosci* **22**, 417-29 (2003).
6. Guy, J., Hendrich, B., Holmes, M., Martin, J.E. & Bird, A. A mouse Mecp2-null mutation causes neurological symptoms that mimic Rett syndrome. *Nat Genet* **27**, 322-6 (2001).
7. Chen, R.Z., Akbarian, S., Tudor, M. & Jaenisch, R. Deficiency of methyl-CpG binding protein-2 in CNS neurons results in a Rett-like phenotype in mice. *Nat Genet* **27**, 327-31 (2001).

8. Shahbazian, M. et al. Mice with truncated MeCP2 recapitulate many Rett syndrome features and display hyperacetylation of histone H3. *Neuron* **35**, 243–54 (2002).

9. Gemelli, T. et al. Postnatal loss of methyl-CpG binding protein 2 in the forebrain is sufficient to mediate behavioral aspects of Rett syndrome in mice. *Biol Psychiatry* **59**, 468–76 (2006).

10. Guy, J., Gan, J., Selfridge, J., Cobb, S. & Bird, A. Reversal of neurological defects in a mouse model of Rett syndrome. *Science* **315**, 1143–7 (2007).

11. Giacometti, E., Luikenhuis, S., Beard, C. & Jaenisch, R. Partial rescue of MeCP2 deficiency by postnatal activation of MeCP2. *Proc Natl Acad Sci U S A* **104**, 1931–6 (2007).

12. Tudor, M., Akbarian, S., Chen, R.Z. & Jaenisch, R. Transcriptional profiling of a mouse model for Rett syndrome reveals subtle transcriptional changes in the brain. *Proc Natl Acad Sci U S A* **99**, 15536–41 (2002).

13. Chen, W.G. et al. Derepression of BDNF transcription involves calcium-dependent phosphorylation of MeCP2. *Science* **302**, 885–9 (2003).

14. Chang, Q., Khare, G., Dani, V., Nelson, S. & Jaenisch, R. The disease progression of Mecp2 mutant mice is affected by the level of BDNF expression. *Neuron* **49**, 341–8 (2006).

15. Cepeda, C. et al. Increased GABAergic function in mouse models of Huntington's disease: reversal by BDNF. *J Neurosci Res* **78**, 855-67 (2004).

16. Kells, A.P. et al. AAV-mediated gene delivery of BDNF or GDNF is neuroprotective in a model of Huntington disease. *Mol Ther* **9**, 682-8 (2004).

17. Bondy, C.A. Transient IGF-I gene expression during the maturation of functionally related central projection neurons. *J Neurosci* **11**, 3442-55 (1991).

18. Liu, J.P., Baker, J., Perkins, A.S., Robertson, E.J. & Efstratiadis, A. Mice carrying null mutations of the genes encoding insulin-like growth factor I (Igf-1) and type 1 IGF receptor (Igf1r). *Cell* **75**, 59-72 (1993).

19. Tropea, D. et al. Gene expression changes and molecular pathways mediating activity-dependent plasticity in visual cortex. *Nat Neurosci* **9**, 660-8 (2006).

20. Zheng, W.H. & Quirion, R. Comparative signaling pathways of insulin-like growth factor-1 and brain-derived neurotrophic factor in hippocampal neurons and the role of the PI3 kinase pathway in cell survival. *J Neurochem* **89**, 844-52 (2004).

21. Itoh, M. et al. Methyl CpG-binding protein 2 (a mutation of which causes Rett syndrome) directly regulates insulin-like growth factor

binding protein 3 in mouse and human brains. *J Neuropathol Exp Neurol* **66**, 117-23 (2007).

22. Baker, A.M. et al. Central penetration and stability of N-terminal tripeptide of insulin-like growth factor-I, glycine-proline-glutamate in adult rat. *Neuropeptides* **39**, 81-7 (2005).
23. Sizonenko, S.V., Sirimanne, E.S., Williams, C.E. & Gluckman, P.D. Neuroprotective effects of the N-terminal tripeptide of IGF-1, glycine-proline-glutamate, in the immature rat brain after hypoxic-ischemic injury. *Brain Res* **922**, 42-50 (2001).
24. Guan, J. et al. Neuroprotective effects of the N-terminal tripeptide of insulin-like growth factor-1, glycine-proline-glutamate (GPE) following intravenous infusion in hypoxic-ischemic adult rats. *Neuropharmacology* **47**, 892-903 (2004).
25. Saura, J. et al. Neuroprotective effects of Gly-Pro-Glu, the N-terminal tripeptide of IGF-1, in the hippocampus in vitro. *Neuroreport* **10**, 161-4 (1999).
26. Cheng, C.M. et al. Insulin-like growth factor 1 is essential for normal dendritic growth. *J Neurosci Res* **73**, 1-9 (2003).
27. Schneider, M.R., Lahm, H., Wu, M., Hoeflich, A. & Wolf, E. Transgenic mouse models for studying the functions of insulin-like growth factor-binding proteins. *Faseb J* **14**, 629-40 (2000).
28. Lee, K.H., Calikoglu, A.S., Ye, P. & D'Ercole, A.J. Insulin-like growth factor-I (IGF-I) ameliorates and IGF binding protein-1 (IGFBP-1)

exacerbates the effects of undernutrition on brain growth during early postnatal life: studies in IGF-I and IGFBP-1 transgenic mice. *Pediatr Res* **45**, 331-6 (1999).

29. Ye, P. et al. Astrocyte-specific overexpression of insulin-like growth factor-I promotes brain overgrowth and glial fibrillary acidic protein expression. *J Neurosci Res* **78**, 472-84 (2004).
30. Julu, P.O. et al. Characterisation of breathing and associated central autonomic dysfunction in the Rett disorder. *Arch Dis Child* **85**, 29-37 (2001).
31. Acampa, M. & Guideri, F. Cardiac disease and Rett syndrome. *Arch Dis Child* **91**, 440-3 (2006).
32. Chao, H.T., Zoghbi, H.Y. & Rosenmund, C. MeCP2 Controls Excitatory Synaptic Strength by Regulating Glutamatergic Synapse Number. *Neuron* **56**, 58-65 (2007).
33. Dani, V.S. et al. Reduced cortical activity due to a shift in the balance between excitation and inhibition in a mouse model of Rett syndrome. *Proc Natl Acad Sci U S A* **102**, 12560-5 (2005).
34. Nelson, E.D., Kavalali, E.T. & Monteggia, L.M. MeCP2-dependent transcriptional repression regulates excitatory neurotransmission. *Curr Biol* **16**, 710-6 (2006).
35. Ramsey, M.M., Adams, M.M., Ariwodola, O.J., Sonntag, W.E. & Weiner, J.L. Functional characterization of des-IGF-1 action at

excitatory synapses in the CA1 region of rat hippocampus. *J Neurophysiol* **94**, 247-54 (2005).

36. Xing, C. et al. Effects of insulin-like growth factor 1 on synaptic excitability in cultured rat hippocampal neurons. *Exp Neurol* **205**, 222-9 (2007).

37. Kaufmann, W.E., Taylor, C.V., Hohmann, C.F., Sanwal, I.B. & Naidu, S. Abnormalities in neuronal maturation in Rett syndrome neocortex: preliminary molecular correlates. *Eur Child Adolesc Psychiatry* **6 Suppl 1**, 75-7 (1997).

38. Johnston, M.V., Jeon, O.H., Pevsner, J., Blue, M.E. & Naidu, S. Neurobiology of Rett syndrome: a genetic disorder of synapse development. *Brain Dev* **23 Suppl 1**, S206-13 (2001).

39. Hofer, S.B., Mrsic-Flogel, T.D., Bonhoeffer, T. & Hubener, M. Prior experience enhances plasticity in adult visual cortex. *Nat Neurosci* **9**, 127-32 (2006).

40. Gordon, J.A. & Stryker, M.P. Experience-dependent plasticity of binocular responses in the primary visual cortex of the mouse. *J Neurosci* **16**, 3274-86 (1996).

41. Smith, S.L. & Trachtenberg, J.T. Experience-dependent binocular competition in the visual cortex begins at eye opening. *Nat Neurosci* **10**, 370-5 (2007).

42. Yoshii, A. & Constantine-Paton, M. BDNF induces transport of PSD-95 to dendrites through PI3K-AKT signaling after NMDA receptor activation. *Nat Neurosci* **10**, 702-11 (2007).

43. Lee, C.C., Huang, C.C., Wu, M.Y. & Hsu, K.S. Insulin stimulates postsynaptic density-95 protein translation via the phosphoinositide 3-kinase-Akt-mammalian target of rapamycin signaling pathway. *J Biol Chem* **280**, 18543-50 (2005).

44. El-Husseini, A.E., Schnell, E., Chetkovich, D.M., Nicoll, R.A. & Bredt, D.S. PSD-95 involvement in maturation of excitatory synapses. *Science* **290**, 1364-8 (2000).

45. van Dam, P.S. et al. Growth hormone, insulin-like growth factor I and cognitive function in adults. *Growth Horm IGF Res* **10 Suppl B**, S69-73 (2000).

46. Rudman, D. et al. Effects of human growth hormone in men over 60 years old. *N Engl J Med* **323**, 1-6 (1990).

47. Aberg, M.A. et al. IGF-I has a direct proliferative effect in adult hippocampal progenitor cells. *Mol Cell Neurosci* **24**, 23-40 (2003).

48. Aberg, M.A., Aberg, N.D., Hedbacker, H., Oscarsson, J. & Eriksson, P.S. Peripheral infusion of IGF-I selectively induces neurogenesis in the adult rat hippocampus. *J Neurosci* **20**, 2896-903 (2000).

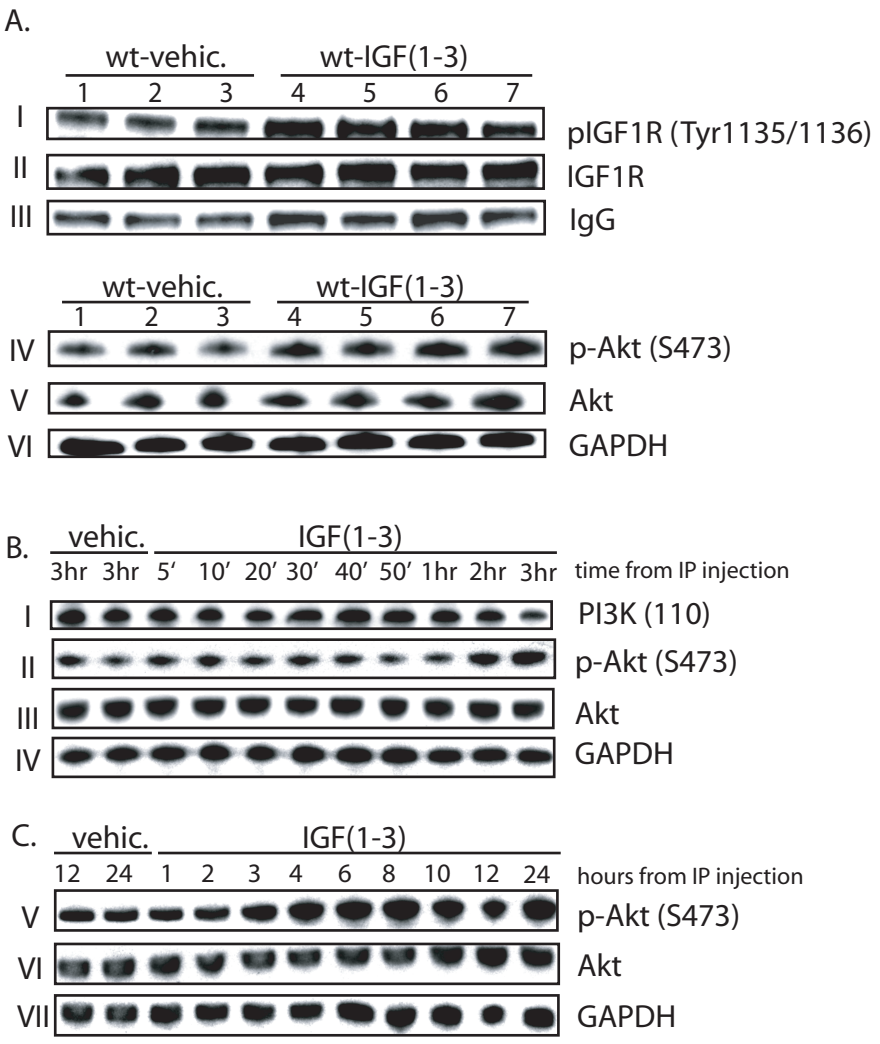

Figure 1. A. IGF1R activation. Western blot analysis of brain tissue from wild type mice injected with vehicle (lane 1–3) or (1–3)IGF1 (lane4–7). Equal amounts of total protein from whole brains extracts was used to immunoprecipitate IFGR1. IGF1R immunoprecipitates were blotted either with anti IGF1R (row II) or with a anti phospho IGF1R (IGF1RTy1135/1136/IRSbTyr1150/1151) (row I).IgG signal was used as loading control. Row IV–VI :whole brain extracts Lanes 4–7 show increased Akt Ser 473 phosphorilation compared to samples in lanes 1–3 while total Akt is unchanged: row IV. Row V: GAPDH was used as loading control. B–C. Time course of Akt activation after (1–3)IGF1 injection. Whole brain protein samples from (1–3)IGF1 were obtained at various time points indicated at the top of each lane: 5 minutes to 3hours (row I–IV) or 1hour to 24 hours (row V–VII) after IP injection and blotted with anti PI3K p110 (row I), p–Akt (rows I,V) or total Akt (rows II,VI). GAPDH was used a loading control (rows IV and VII). Protein from vehicle injected mice was collected at 3, 12, 24hours.

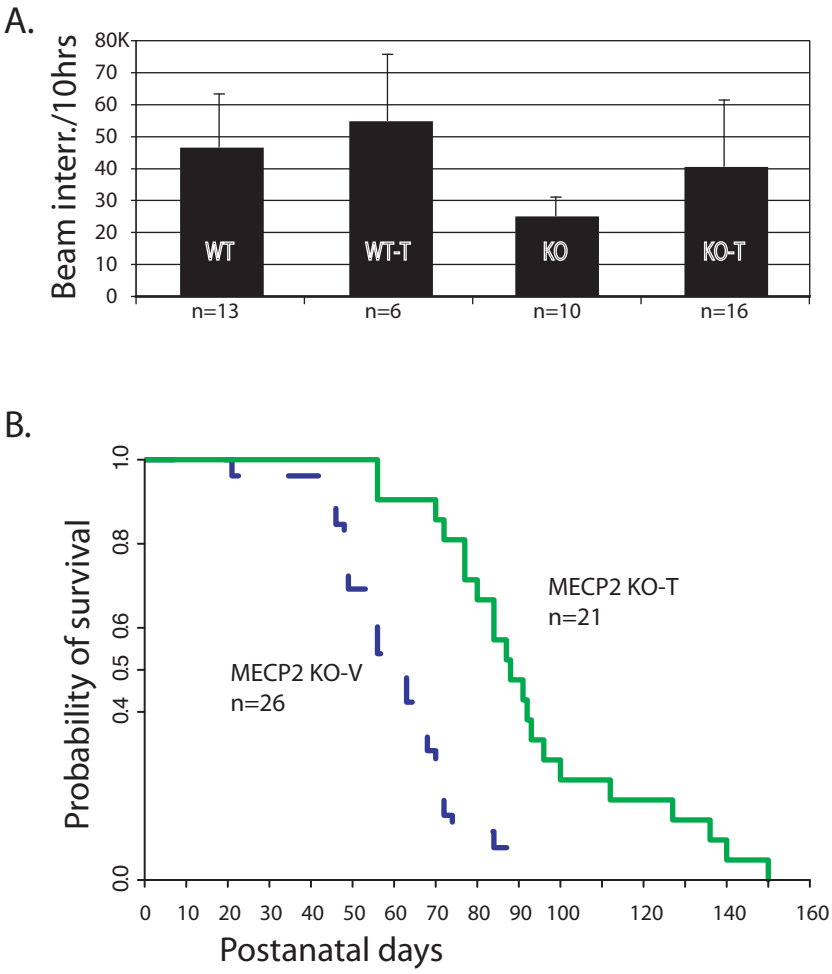

Figure 2. A. Baseline nocturnal activity was measured by placing animals in cages equipped with a movement detector (infrared beam). On the y axis the number of beam interruptions over 10 hours, each bar represents a different experimental group. Nocturnal activity was recorded weekly between 4 and 17 weeks of age. Data from 8 weeks old mice is shown here. As expected KO vehicle treated show significantly less activity that wt littermates (p=8.08E-04). MeCP2 1l/y (KO-T) animals treated with (1-3)IGF1 were more active than MeCP2 1l/y (KO) mice treated with vehicle (p=5.37E-05) but not as active as wild type (WT) littermates (p=0.026). Wt animals treated with (1-3)IGF1 (WT-T) were not significantly more active than wilt type vehicle treated(p=0.56). n is the number of animals used.

B. Kaplan-Meier survival curves for MeCP2 ko mice treated with vehicle (KO-V) or (1-3)IGF1 (KO-T). On the x axis the days after birth and on the Y axis the probably of survival. MeCP2 KO treated mice have a longer life expectancy that their vehicle treated litter mates (p=0.54e-07). MeCp22 Ko mice were given daily IP injections of (1-3)IGF1 (0.001 mg/gm body weight/day) every day from 2 weeks of age onward.

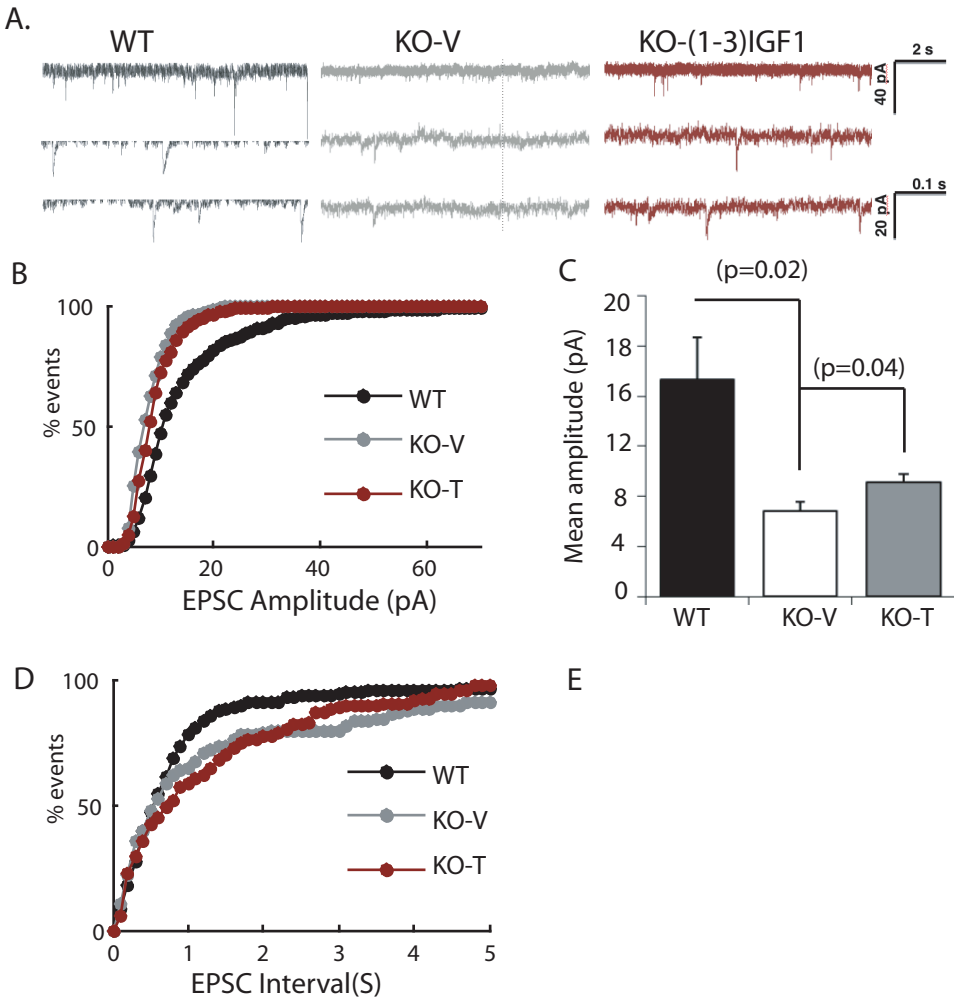

Figure 3. A. Representative traces from recordings of spontaneous excitatory postsynaptic currents (EPSCs) in either wild type (WT) or knockout treated with vehicle (V) or (1–3) IGF–1 for two weeks. Top traces depict a compressed view of spontaneous activity, and the bottom two traces show individual events with an expanded scale. B. Distributions of EPSC amplitudes,across all cells mesured, in wild type and knockout vehicle or (1–3) (IGF–1) trea, indiccate a increased percentage of evnets with smaller amplitudes (p=2.3e--5o,Kolmogorov–Smirnov) in Ko animals versus wild type . (1–3) IGF–1treatment partially reversed this trend (p=1.2e–9,Kolmogorov–Smirnov) C. Mean EPSC amplitude in wild–type (n=11 cells, 5 animals, 1543 events), untreated knockout (n=6 cells, 2 animals, 717 events), and knockout tissue treated with (1–3) IGF–1 for two weeks (n=7 cells, 3 animals, 1723 events). Mean EPSC amplitude was significantly reduced in knockout neurons (*, P=0.02 paired t–test). Compared to knockout animals, mean EPSC amplitude was mdestly increased in knockout animals treated with (1–3) IGF–1 (P=0.04 paired t–test). D. Distributions of EPSC intervals between events, pooling equal numbers of events from each recorded cell, are subtly modified between WT, and KO and KO+T groups. WT intervals are subtly but significantly longer compared to KO and KO+T intervals. E. However, group analysis of mean EPSC frequency does not indicate a significant change between groups.

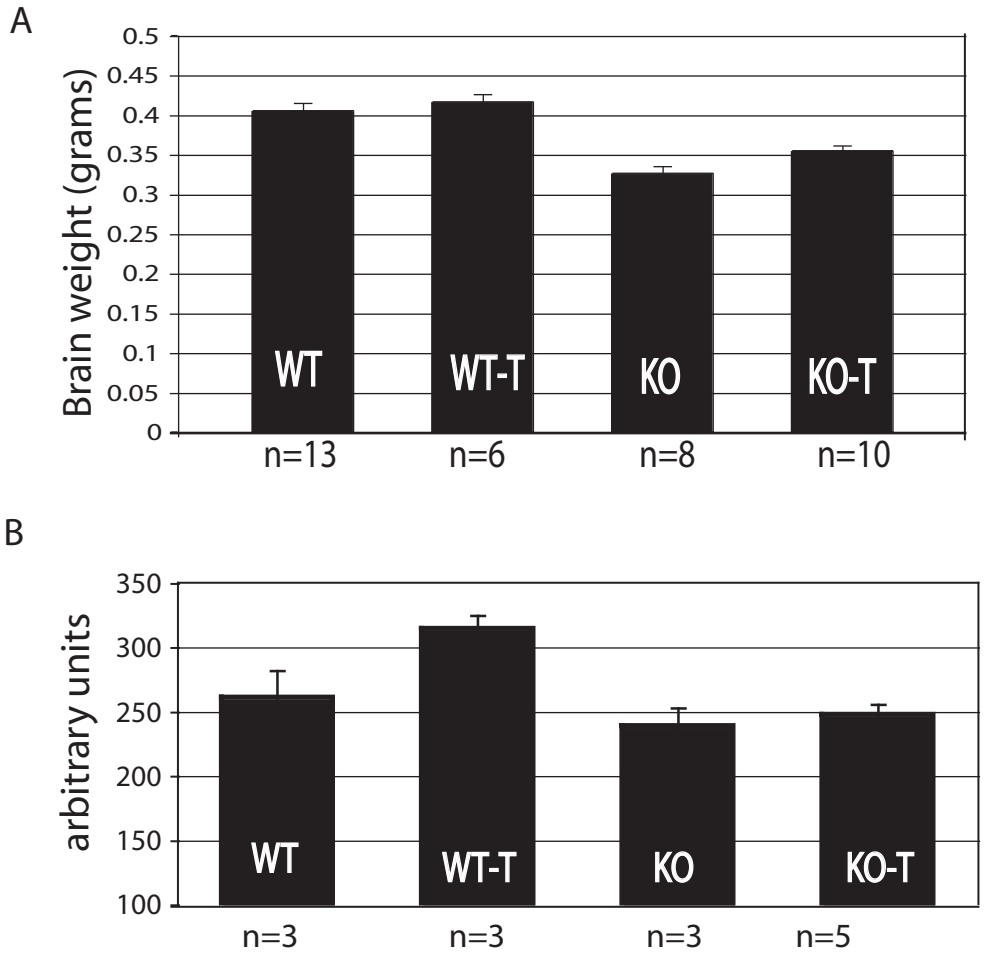

Figure 4. A. Brain weight. Postnatal (1-3)IGF1treatment increases brain weight. The value bars indicate the average brain weight of each experimental group. The error bars represent the standard error. "n" :number of animals per group. MeCP21l/y treated with (1-3)IGF1 (KO-T) had an increased brain weight compared to vehicle treated MeCP21l/y (KO) littermates (0.355 gr vs 0.326 gr p=0.032). Same was observed for (1-3)IGF1 wild type (WT) versus vehicle treated wt mice (WT-V)(0.421 gr vs o.410 gr p=0.021). All animals were older than P60. B. Cell size. (1-3)IGF1modestly increaseaverage soma size in cortical (S1, LV) neruons.

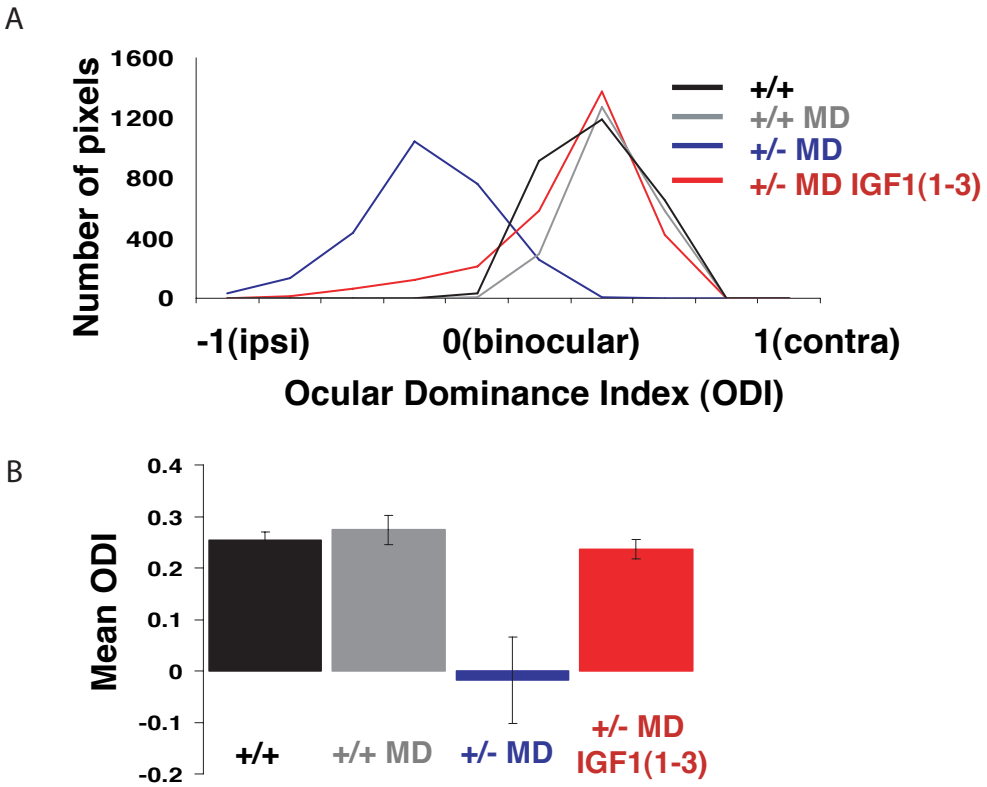

Figure 5. ODI mesures in MeCP2 mutant animals and controls after monocular deprivation.

A. Representative Ocular Dominance Index (ODI) plots from the binocular zone of mice from the 3 experimental groups. Dotted grey line: wild type mice after 4 days of deprivation; straight blue line: Mecp2 mutant mice, deprived for 4 days, straight red line: Mecp2 mutant mice, deprived for 4 days and treated with IGF1(1–3). Each experimental group contains data from at least 5 animals. B. Mean and Standard Deviation of the Ocular Dominance Index (ODI) for the 4 groups of mice, the bar graphs are representative of data collected from at least 5 animals per group. We also collectedcontro data from wild type animals, non treated and non monuclraly deprived (data not shownn).

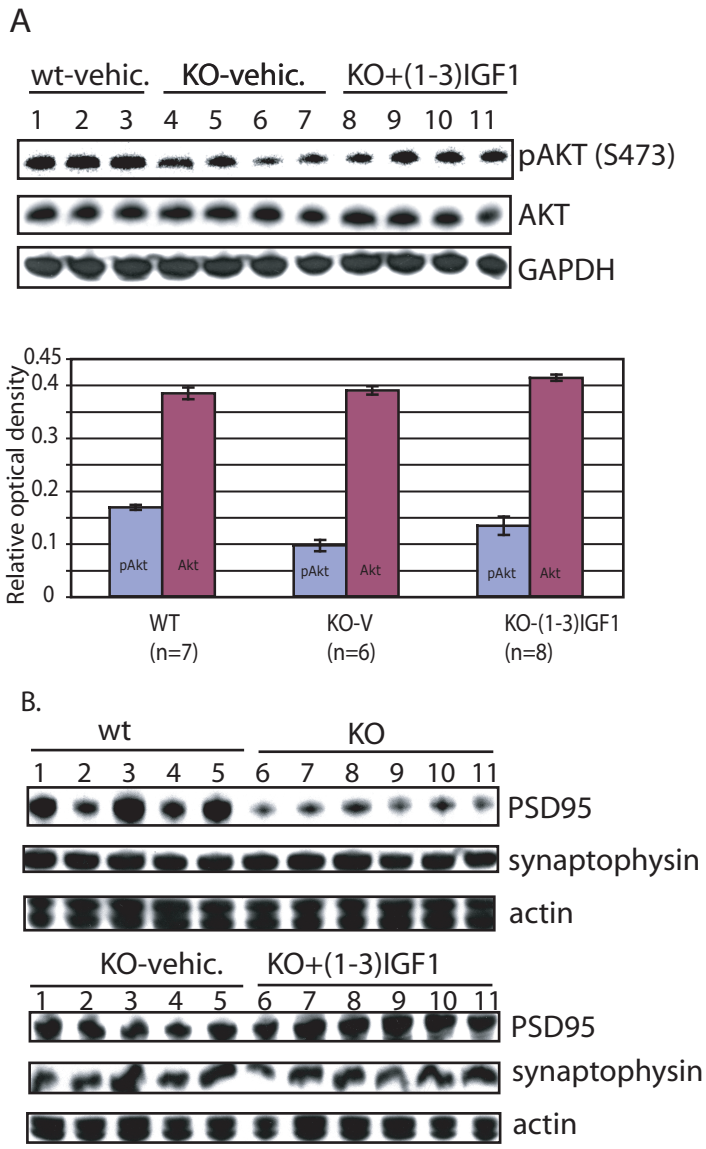

Figure 6. A. Levels of phosphorilated Akt (row I) increases in MeCP2 -/y animals treated with (1-3)IGF-1. Sample westernblot on total brain extracts (top) and average signal quantification of at least 3 blots (bottom). "n"=total number of mice in each experimental group. Signal intensities were normalized to the GPDH signal. Blue and red bar represents the signal quantification for the phospho-Akt anitbody and total Akt respectively. B. IGF1(1-3) treatment increases the expression of PSD95 but not of synaptophysin.

Perspectives

Relevance of the over-expression model.

The data described in Chapter two show that two-three folds level of over-expression of MeCP2 in the brain can lead to severe motor dysfunction. The TauMeCP2 Ki/Ki mice were runted due to an impaired ability to compete with littermates for food. Symptoms included tremors, gait ataxia, and side-to side swaying. In our observations the symptoms were quite different from the Rett like phenotype displayed by the *Mecp2* 1l/y mice. A subsequent publication by Collins et al. using transgenic mice that over express (human) *MECP2,* MeCP2(Tg1), confirmed these observations. Detailed neurobehavioral and electrophysiological studies of the MeCP2 (Tg1) mouse demonstrated onset of phenotypes quite different from the classical MeCP2 knock out model. These mice displayed enhanced motor and contextual learning and enhanced synaptic plasticity in the hippocampus during the first 10 weeks of age; after 20 weeks of age, however, these mice developed seizures, became hypoactive and approximately 30% of them died by 1 year [165]. These data demonstrate that MeCP2 levels must be tightly regulated in vivo, and that even mild over expression of this protein is detrimental. Furthermore, these results suggested the possibility that duplications or gain-of-function mutations in MECP2 might underlie some cases of X-linked delayed-onset neurobehavioral disorders [165]. Indeed using an X-chromosome DNA array with a resolution of 80 kb to screen patients with suspected X-linked mental retardation (XLMR) for X-chromosomal aberrations showed a duplication at Xq28 in a small cohort of these patients.

Genotype-phenotype correlation pointed to the duplication of MECP2 as the underlying cause of severe mental retardation [166].

Functional redundancy of MeCp2e1 and MeCP2e2.

The presence of two isoforms of *Mecp2* with differential tissue expression could suggest the existence of distinct functions for each isoform. For example, the MeCP2e1 N-terminus contains a conserved serine residue that is absent in MeCP2e2 and which could be a target of BDNF induced phosphorylation. It may be of future interest to determine the functional significance of differing MeCP2 N-termini by the creation of isoform-specific gene disruptions in mice. Nevertheless the data presented in chapter one demonstrates that MeCP2e2, which is normally expressed at very low level in the brain, is sufficient to rescue the phenotype, arguing for a complete functional redundancy of the two isoforms.

Transcriptional regulation of MeCP2 expression.

It has been reported previously that there is no obvious correlation between MeCP2 protein and RNA level in adult tissues, suggesting that *Mecp2* translation may be post-transcriptionally regulated [105]. The endogeous *Mecp2* sequence contains a 182 bp 5' UTR and a highly conserved 8.5 KB 3' UTR with alternative (pA) polyadenylation signals. Depending on which pA is used, either a 1.9 Kb or a 10Kb transcript is produced. The long transcript predominates in the brain whereas the shorter form is expressed in visceral organs and muscle [167]. In the experiments presented in chapter one, the Tau

-Mecp2 construct did not include either of the untranslated regions and showed an unexpectedly high expression level. Klein et al. (2007) have identified a potential target sequence for microRNAs mediated posttranslational regulation in the 3'UTR of the *Mecp2* gene. In particular they have shown that mir132, a CREB (camp response element binding protein) induced microRNA, is necessary and sufficient to regulate MeCP2 protein levels in neurons. Antisense oligonucleotide mediated reduction of **mir132** causes increased expression of MeCP2 protein (not mRNA) and interestingly it specifically increases BDNF III transcripts levels [168].

Complete reversal of symptoms.

Chapter two presented evidence that postnatal activation of MeCP2 in the forebrain is sufficient to significantly delay the onset of symptoms but was not sufficient to completely rescue the phenotype. So while on one side the data supported the hope that indeed post-natal treatment could be effective, it left some questions unanswered. For example, in the experiments presented in Chapter 2, the number of cells expressing the Mecp2 rescue transgene varied between 0 to 70%, so could 100% expression lead to a complete reversal of symptoms? Moreover the rescue transgene was activated no later than 3 weeks after birth. This is shortly before the mice show overt symptoms. Would later activation, 4 to 8 weeks still be effective? When is the latest time point possible? These questions have been addressed in a recent publication by Guy et al. [164]. In this study a stop cassette flanked by LoxP sites was placed upstream of the endogenous *Mecp2* gene. To control the removal of the stop cassette and

therefore *Mecp2* gene reactivation, Guy et al. also introduced a transgene expressing the Cre-recombinase, estrogen receptor fusion protein (cre-ER). Upon delivery of tamoxifen (TM) the cytoplasmic Cre-Er protein translocates to nucleus and loops out the Stop cassette allowing **expression of MeCP2 at wild type levels and in all tissues** where it is normally expressed from the endogenous promoter. Using this inducible MeCP2 deletion system Guy et al. were able to show that reactivation of the *Mecp2* gene even in a fully symptomatic mouse leads to a complete reversal of the phenotype.

This complete reversibility is consistent with the notion that no permanent damage at the structural and molecular levels is caused by the absence of MeCP2. Moreover it shows that MeCP2 function is required at all times for maintenance of mature neuron function.

Implications of the rescue experiments.

The most important implication of the rescue studies is that RS does not cause permanent damage to the CNS structure both in terms of architecture and anatomy but also at the molecular level. MeCP2 deficient neurons remain proficient to carry out their normal function even at advanced stages of disease and can resume normal activity once MeCP2 is reintroduced or once we develop another means of intervention that will compensate for the loss of MeCP2. The fact that MeCP2 can be re-introduced and completely rescue the RS phenotype also means that the DNA methylation pattern that recruits MeCP2 to its correct targets is established and maintained properly in its absence, and that all the other cofactors or protein complexes that mediate its downstream activity are

also present and functional. The possibility of reintroducing functional MeCP2 protein in patients through gene therapy is certainly being considered. Gene therapy is unarguably the definitive way to treat genetic diseases. Although a straightforward concept in theory, in practice gene therapy has proven difficult to realize even when directed to easily accessed somatic cell systems. Gene therapy for diseases in which the CNS is the target organ presents even greater challenges because of fact that neurons are non-dividing cells and are difficult to access. From the rescue experiments discussed in Chapter 1 and 2 it is clear that to obtain a significant rescue of the phenotype it is necessary to restore function in 60-80% of the neurons in the CNS. Moreover the expression levels needs to be tightly regulated, as over-expression can be detrimental. In our view, at present, the low infection efficiency and difficulty in controlling expression level (together with significant toxicity response) are limiting factors for the successful use of gene therapy for the cure of RS. A similar type of argument can be made for stem cell therapy.

The pharmacological approach.

Unfortunately, there are currently no specific treatments that halt or reverse the progression of the disorders associated with RS, and management is mainly symptomatic and individualized, focusing on alleviating each patient's problems. Pharmacological approaches to managing problems associated with RS include melatonin for sleep disturbances and several agents to control breathing abnormalities, seizures and stereotypic movements. As shown in

chapter 3 the mouse model could become a very helpful tool for phenotypic screening of drugs. In our opinion this could be the most effective and short-term approach to the development of a treatment. This is a distinctly different approach than the biologically driven search for an understanding of the mechanisms, but it could be equally effective. The phenotypic approach capitalizes on the frequent finding of multiple activities in known drugs and the a priori unpredictable nature of phenotypic screening results. One potential issue in using the mouse model for phenotypical screens is that we cannot really infer the degree of rescue of complex brain functions, cognition deficits and network wiring in humans from experimentation in mice. In addition MeCP2 might have slightly different mechanism of action in humans and in mice.

Final considerations.

Two of the most revealing experiments in the recent past were done using a mouse model underscoring the importance and usefulness of its derivation. In the first set of experiments it has been shown that over expression of MeCP2 can be as detrimental as its absence {Collins, 2004 #144;Luikenhuis, 2004 #159}. The phenotype of mice over expressing MeCP2 is not so well characterized, it has some similarities with phenotype of the knock out but it also has many differences. Anyway we learned that levels of MeCP2 protein are crucial for neuronal physiology and must be tightly regulated. The clinical relevance of this observation has been confirmed by the identification of male patients with severe mental retardation that carried duplication or triplications of the Xq28 chromosomal region {Van Esch, 2005 #102}. In the second set of

experiments it has been shown that Rett syndrome is, at least in the mouse model, reversible even at advanced stages of the disease {Guy, 2007 #139}. It remains though to be better studied to which extent this reversibility is complete. Certainly in this study the overt physical symptoms and life span were rescued but higher cognitive functions were not tested. In this contest the limitations of using a mouse model to study a human mental retardation disorder might become obvious. Another intriguing observation is that mutations in the MeCP2 gene are present also in patients diagnosed with autism or other forms of mental retardation, suggesting that the spectrum of phenotypes caused by mutations in this gene goes beyond Rett syndrome. Conversely many aspects of Rett syndrome are reminiscent of other neurological disorders, for example the stereotypic movements, the muscle hypotonia and awkward gait or posture resemble of Parkinson's disease. The microcephaly and the general physical underdevelopment resemble metabolic disorders. The difficulties that patients have to communicate with care givers for example reduced eye contact, unresponsiveness and anxiety are characteristic of autistic individuals, for these reasons Rett syndrome is included by some clinicians among the autism spectrum disorders. These similarities have led many to speculate the existence among different neurological disorders of common biological pathways leading to a common set of primary or secondary manifestations. Some patients diagnosed as severe Rett syndrome variant, characterized by untreatable seizures and early onset, have been found with a mutation in the CDKL5 gene, and not in the MECP2 gene {Scala, 2005 #107}. CDKL5 is a kinase which can *in vitro* phosphorilate MECP2 and many other unknown proteins {Mari, 2005 #106}. The existence of shared pathways would

make us hope that if we find the MeCP2 effector pathway and a way to interfere with it we might learn something relevant for other CNS dysfunctions as well. Unfortunately all the experiments designed to systematically identify genes bound by MeCP2 or at least genes whose expression is misregulated in its absence have not been as informative has hoped. There are two possible explanations for this 1) MeCp2 is a global transcriptional repressor that controls the expression a multitude of genes depending on developmental stage and neuronal subtype. All these transcriptional changes were too many and/or too subtle to be detected 2) MeCP2 is a local transcritption silencer that regulates few key genes in one or more neuronal subtypes. The misregulation of these targets might easily be lost in experimental noise when looking at whole brain samples. To clarify this matter it would be useful to sort different neuronal subtypes using genetic markers and repeat both RNA microarray and chromatin immunoprecipitation experiments, although obtaining a large number of viable cells is not always possible and might be a limiting step in the execution of these experiments. Another informative experiment would be the targeted deletion of Mecp2 in specific neuronal subtypes using appropriate Cre recombinase lines. This experiment would reveal whether specific neuronal subtypes are responsible for different aspects of the disease.

How much is Rett syndrome a cell autonomous disorder and how much is it a neuronal cell network problem? From the experiments in chapter 2 it is clear that even 70% of cell expressing MeCP2 are not enough to achieve complete rescue suggesting that the defect is cell autonomous moreover it shows that the presence of even a minority of mutant neurons can impair the functionality the whole network. *(isn't that in reality the same concept??)*

Given these preconditions it is difficult to imagine gene or cell therapy as potential strategies to rescue the symptoms of MeCP2 deficiency in patients. Conversely if the primary or secondary effects of MeCP2 deficiency converge in one or two common signaling pathway we could think of intervening pharmacologically. Certainly the data on BDNF and IGF1 discussed in chapter 3 would fit this explanation. The data exposed in chapter 3 show that the beneficial effects of (1-3)IGF-1 injections could be mediated by the activation of the PI3K pathway but they do not investigate whether this pathway is in anyway deficient in MeCP2 null mice. It is also possible that BDNF1 and IGF1 have a generic neuroprotective effect or that activation of the PI3K pathway juts incidentally counterbalance the loss of MeCP2. Nevertheless it is interesting to note that, to date, the 4 molecules (BDNF {Chang, 2006 #195}, Ampakine {Ogier, 2007 #226}, (1-3)IGF1 and the corticosteroid releasing hormone CRH) reported to affect Rett syndrome disease progression all signal through the PI3K/Akt pathway. Ampakines are a derivative of benzoic acid used as neuroleptics and antipsychotics that promote plasticity by facilitating transmission at glutamatergic synapses, their action seems to be mediated in part by increasing levels of BDNF. CRH is a polypeptide hormone and neurotransmitter involved in stress response whose signal transduction also relies on PI3K/Akt activation. The ability of BDNF and IGF1 to activate the PI3K route has been discussed above. Taken together these observations, although circumstantial, would suggest that there is at least one, major signaling pathway whose modulation directly affects the Rett syndrome disease progression namely the PI3K/Akt pathway. The PI3K/Akt signaling mechanism is very well characterized in cancer biology but its importance

and function in the brain is juts starting to be unraveled. MeCP2 is a DNA binding molecule that recognizes epigenetic marks (CpG methylation) and controls gene expression. Its action is essential for proper neuronal function, possibly by controlling synaptic development/maturation. In which way though it is not known. The PI3k/Akt pathway has also been shown to be essential for longterm potentiation and synaptic development. Does MeCP2 action controls or relies upon the PI3k/Akt pathway activation? Further experiment will be needed to answer these questions and to identify other potential mechanism of MeCP2 regulation.

Albeit the studies on BDNF {Chang, 2006 #185} and on (1-3)IGF-1 over expression come to similar results and possibly are mediated by the same signaling pathway substantial differences exists. For example BDNF over expression lead to a marginal improvement in life expectancy while over expression of (1-3)IGF-1 was more effective. However over expression of BDNF completely rescued the electrophysiological phenotype of MeCP2 deficient cortical slices whereas over expression of (1-3)IGF-1 only partially improved it. Also the locomotor improvement in BDNF over expressing mice was greater than in (1-3)IGF-1 mice {Chang, 2006 #185}. The comparison between the two experiments is anyway difficult because of the different experimental set up. BDNF was over expressed using a transgene and the extent and localization of over expression haven't been carefully characterized {Chang, 2006 #185}. (1-3)IGF-1 was instead injected systemically and there was no characterization of the amount of peptide that reached the brain and or other organs. Moreover depending on which insulin receptor is activated by (1-3)IGF-1 some neuronal population might be more

sensitive to the treatment than others. It would be therefore very informative to better characterize the molecular mechanism of action of (1-3)IGF-1. (1-3)IGF-1) for example is known to have greater affinity than IGF1 itself for IGFBP proteins therefore it is possible that (1-3)IGF-1 increases levels of IGF1 by competing for binding with the IGFBPs {Sizonenko, 2001 #219}. To overcome the difficulties in interpreting the results obtained in chapter 3 it would be informative to over express IGF1 or (1-3)IGF-1 genetically using the same targeting strategy used to over express BDNF. In this case IGF1 would be over expressed in neurons only at a reproducible level and in defined regions of the brain. The localized CNS and neuronal specific over expression might result in more efficient rescue or, conversely, in a less efficient rescue. May be systemic injections were positively affecting peripheral organs as well. After all, even though there is convincing evidence that CNS restricted deletion is sufficient to cause Rett-like symptoms, the effects of deletion of MeCP2 only in peripheral organs are not know. Moreover arguing for CNS specific deletions using Nestin and Tau driven Cre recombinase is not entirely correct as both promoters have considerable peripheral activity. In light of the promiscuous binding of MeCP2 to the chromosomes and its rather wide expression pattern it would appear to be essential for the silencing of numerous genes in virtually every tissue. However this is difficult to reconcile with the relatively restricted pathology of RS and a role outside of the nervous system (CNS) cannot be excluded, since the phenotype of the mice was analyzed primarily with regard to neuronal function, and more subtle deficiencies outside the CNS may have been overlooked.

Surely what is emerging from the study of Rett syndrome is that DNA

methylation and chromatin remodeling play critical roles in the regulation of gene expression in response to neuronal activity and high cognitive functions.

References.

1. Muotri, A.R., et al., *Somatic mosaicism in neuronal precursor cells mediated by L1 retrotransposition.* Nature, 2005. **435**(7044): p. 903-10.
2. Kandel, E. *Steps towrds molecular grammar for learning: Exploration into the nature of memory.* in *Medicine,Science, and Society (Isselbacker KJ, ed)*. 1984.
3. Hilgard, E.R. and G.H. Bowers, *Theories of Learning.* Englewood Cliffe. N.J.Prentice-Hall, 1975.
4. Brenner, C. and F. Fuks, *A methylation rendezvous: reader meets writers.* Dev Cell, 2007. **12**(6): p. 843-4.
5. Wolffe, A.P. and M.A. Matzke, *Epigenetics: regulation through repression.* Science, 1999. **286**(5439): p. 481-6.
6. Martienssen, R.A. and V. Colot, *DNA methylation and epigenetic inheritance in plants and filamentous fungi.* Science, 2001. **293**(5532): p. 1070-4.

7. Jaenisch, R. and A. Bird, *Epigenetic regulation of gene expression: how the genome integrates intrinsic and environmental signals.* Nat Genet, 2003. **33 Suppl**: p. 245-54.
8. Lyko, F., B.H. Ramsahoye, and R. Jaenisch, *DNA methylation in Drosophila melanogaster.* Nature, 2000. **408**(6812): p. 538-40.
9. Hotchkiss, R.D., *The quantitative separation of purines, pyrimidines, and nucleosides by paper chromatography.* J. Biol. Chem., 1948. **175**: p. 315-332.
10. Bunemann, H. and W. Muller, *[Base specific affinity chromatography of nucleic acids].* Naturwissenschaften, 1977. **64**(12): p. 632-3.
11. Gautier, F., H. Bunemann, and L. Grotjahn, *Analysis of calf-thymus satellite DNA: evidence for specific methylation of cytosine in C-G sequences.* Eur J Biochem, 1977. **80**(1): p. 175-83.
12. McGhee, J.D. and G.D. Ginder, *Specific DNA methylation sites in the vicinity of the chicken beta-globin genes.* Nature, 1979. **280**(5721): p. 419-20.
13. Ginder, G.D., W.I. Wood, and G. Felsenfeld, *Isolation and characterization of recombinant clones containing the chicken adult beta-globin gene.* J Biol Chem, 1979. **254**(17): p. 8099-102.
14. van der Ploeg, L.H. and R.A. Flavell, *DNA methylation in the human gamma delta beta-globin locus in erythroid and nonerythroid tissues.* Cell, 1980. **19**(4): p. 947-58.

15. van der Ploeg, L.H., J. Groffen, and R.A. Flavell, *A novel type of secondary modification of two CCGG residues in the human gamma delta beta-globin gene locus.* Nucleic Acids Res, 1980. **8**(20): p. 4563-74.

16. Sutter, D. and W. Doerfler, *Methylation of integrated adenovirus type 12 DNA sequences in transformed cells is inversely correlated with viral gene expression.* Proc Natl Acad Sci U S A, 1980. **77**(1): p. 253-6.

17. Christman, J.K., et al., *Correlation between hypomethylation of DNA and expression of globin genes in Friend erythroleukemia cells.* Eur J Biochem, 1977. **81**(1): p. 53-61.

18. Taylor, S.M. and P.A. Jones, *Multiple new phenotypes induced in 10T1/2 and 3T3 cells treated with 5-azacytidine.* Cell, 1979. **17**(4): p. 771-9.

19. Holliday, R. and J.E. Pugh, *DNA modification mechanisms and gene activity during development.* Science, 1975. **187**(4173): p. 226-32.

20. Bird, A.P., *Use of restriction enzymes to study eukaryotic DNA methylation: II. The symmetry of methylated sites supports semi-conservative copying of the methylation pattern.* J Mol Biol, 1978. **118**(1): p. 49-60.

21. Pollack, Y., et al., *Methylation of foreign DNA sequences in eukaryotic cells.* Proc Natl Acad Sci U S A, 1980. **77**(11): p. 6463-7.

22. Bestor, T.H., *The DNA methyltransferases of mammals.* Hum Mol Genet, 2000. **9**(16): p. 2395-402.

23. Robertson, K.D. and A.P. Wolffe, *DNA methylation in health and disease.* Nat Rev Genet, 2000. **1**(1): p. 11-9.

24. Okano, M., et al., *DNA methyltransferases Dnmt3a and Dnmt3b are essential for de novo methylation and mammalian development.* Cell, 1999. **99**(3): p. 247-57.

25. Li, E., *Chromatin modification and epigenetic reprogramming in mammalian development.* Nat Rev Genet, 2002. **3**(9): p. 662-73.

26. Jia, D., et al., *Structure of Dnmt3a bound to Dnmt3L suggests a model for de novo DNA methylation.* Nature, 2007.

27. Ooi, S.K., et al., *DNMT3L connects unmethylated lysine 4 of histone H3 to de novo methylation of DNA.* Nature, 2007. **448**(7154): p. 714-7.

28. Li, E., T.H. Bestor, and R. Jaenisch, *Targeted mutation of the DNA methyltransferase gene results in embryonic lethality.* Cell, 1992. **69**(6): p. 915-26.

29. Bourc'his, D., et al., *Dnmt3L and the establishment of maternal genomic imprints.* Science, 2001. **294**(5551): p. 2536-9.

30. Ehrlich, M., et al., *Amount and distribution of 5-methylcytosine in human DNA from different types of tissues of cells.* Nucleic Acids Res, 1982. **10**(8): p. 2709-21.

31. Monk, M., M. Boubelik, and S. Lehnert, *Temporal and regional changes in DNA methylation in the embryonic, extraembryonic and germ cell lineages during mouse embryo development.* Development, 1987. **99**(3): p. 371-82.

32. Kafri, T., et al., *Developmental pattern of gene-specific DNA methylation in the mouse embryo and germ line.* Genes Dev, 1992. **6**(5): p. 705-14.

33. Lander, E.S., et al., *Initial sequencing and analysis of the human genome.* Nature, 2001. **409**(6822): p. 860-921.

34. Venter, J.C., et al., *The sequence of the human genome.* Science, 2001. **291**(5507): p. 1304-51.

35. Antequera, F. and A. Bird, *Number of CpG islands and genes in human and mouse.* Proc Natl Acad Sci U S A, 1993. **90**(24): p. 11995-9.

36. Bird, A.P., et al., *Non-methylated CpG-rich islands at the human alpha-globin locus: implications for evolution of the alpha-globin pseudogene.* Embo J, 1987. **6**(4): p. 999-1004.

37. McKeon, C., et al., *Unusual methylation pattern of the alpha 2 (I) collagen gene.* Cell, 1982. **29**(1): p. 203-10.

38. Jaenisch, R., et al., *DNA methylation, retroviruses, and embryogenesis.* J Cell Biochem, 1982. **20**(4): p. 331-6.

39. Issa, J.P., *CpG-island methylation in aging and cancer.* Curr Top Microbiol Immunol, 2000. **249**: p. 101-18.

40. Jones, P.A., et al., *Methylation and expression of the Myo D1 determination gene.* Philos Trans R Soc Lond B Biol Sci, 1990. **326**(1235): p. 277-84.

41. Harris, M., *Induction of thymidine kinase in enzyme-deficient Chinese hamster cells.* Cell, 1982. **29**(2): p. 483-92.

42. Antequera, F., D. Macleod, and A.P. Bird, *Specific protection of methylated CpGs in mammalian nuclei.* Cell, 1989. **58**(3): p. 509-17.

43. Meehan, R.R., et al., *Identification of a mammalian protein that binds specifically to DNA containing methylated CpGs.* Cell, 1989. **58**(3): p. 499-507.

44. Meehan, R.R., J.D. Lewis, and A.P. Bird, *Characterization of MeCP2, a vertebrate DNA binding protein with affinity for methylated DNA.* Nucleic Acids Res, 1992. **20**(19): p. 5085-92.

45. Lewis, J.D., et al., *Purification, sequence, and cellular localization of a novel chromosomal protein that binds to methylated DNA.* Cell, 1992. **69**(6): p. 905-14.

46. Meehan, R., et al., *Transcriptional repression by methylation of CpG.* J Cell Sci Suppl, 1992. **16**: p. 9-14.

47. Nan, X., R.R. Meehan, and A. Bird, *Dissection of the methyl-CpG binding domain from the chromosomal protein MeCP2.* Nucleic Acids Res, 1993. **21**(21): p. 4886-92.

48. Hendrich, B. and A. Bird, *Identification and characterization of a family of mammalian methyl-CpG binding proteins.* Mol Cell Biol, 1998. **18**(11): p. 6538-47.

49. Ng, H.H., et al., *MBD2 is a transcriptional repressor belonging to the MeCP1 histone deacetylase complex.* Nat Genet, 1999. **23**(1): p. 58-61.

50. Prokhortchouk, A., et al., *The p120 catenin partner Kaiso is a DNA methylation-dependent transcriptional repressor.* Genes Dev, 2001. **15**(13): p. 1613-8.

51. Klose, R.J. and A.P. Bird, *MeCP2 behaves as an elongated monomer that does not stably associate with the Sin3a chromatin remodeling complex.* J Biol Chem, 2004. **279**(45): p. 46490-6.

52. Riggs, A.D., *X inactivation, differentiation, and DNA methylation.* Cytogenet Cell Genet, 1975. **14**(1): p. 9-25.

53. Teter, B., et al., *Methylation of the glial fibrillary acidic protein gene shows novel biphasic changes during brain development.* Glia, 1996. **17**(3): p. 195-205.

54. Takizawa, T., et al., *DNA methylation is a critical cell-intrinsic determinant of astrocyte differentiation in the fetal brain.* Dev Cell, 2001. **1**(6): p. 749-58.

55. Fan, G., et al., *DNA methylation controls the timing of astrogliogenesis through regulation of JAK-STAT signaling.* Development, 2005. **132**(15): p. 3345-56.

56. Levenson, J.M., et al., *Regulation of histone acetylation during memory formation in the hippocampus.* J Biol Chem, 2004. **279**(39): p. 40545-59.

57. Ballas, N., et al., *Regulation of neuronal traits by a novel transcriptional complex.* Neuron, 2001. **31**(3): p. 353-65.

58. Roopra, A., et al., *Localized domains of G9a-mediated histone methylation are required for silencing of neuronal genes.* Mol Cell, 2004. **14**(6): p. 727-38.

59. Ballas, N., et al., *REST and its corepressors mediate plasticity of neuronal gene chromatin throughout neurogenesis.* Cell, 2005. **121**(4): p. 645-57.

60. Ballas, N. and G. Mandel, *The many faces of REST oversee epigenetic programming of neuronal genes.* Curr Opin Neurobiol, 2005. **15**(5): p. 500-6.

61. Takahara, T., et al., *Dysfunction of the Orleans reeler gene arising from exon skipping due to transposition of a full-length copy of an active L1 sequence into the skipped exon.* Hum Mol Genet, 1996. **5**(7): p. 989-93.

62. Yoder, J.A., C.P. Walsh, and T.H. Bestor, *Cytosine methylation and the ecology of intragenomic parasites.* Trends Genet, 1997. **13**(8): p. 335-40.

63. Goll, M.G. and T.H. Bestor, *Eukaryotic cytosine methyltransferases.* Annu Rev Biochem, 2005. **74**: p. 481-514.

64. Challita, P.M. and D.B. Kohn, *Lack of expression from a retroviral vector after transduction of murine hematopoietic stem cells is associated with methylation in vivo.* Proc Natl Acad Sci U S A, 1994. **91**(7): p. 2567-71.

65. Hoeben, R.C., et al., *Inactivation of the Moloney murine leukemia virus long terminal repeat in murine fibroblast cell lines is associated with methylation and dependent on its chromosomal position.* J Virol, 1991. **65**(2): p. 904-12.

66. Moore, T. and D. Haig, *Genomic imprinting in mammalian development: a parental tug-of-war.* Trends Genet, 1991. **7**(2): p. 45-9.

67. Leighton, P.A., et al., *Disruption of imprinting caused by deletion of the H19 gene region in mice.* Nature, 1995. **375**(6526): p. 34-9.

68. Tremblay, K.D., et al., *A paternal-specific methylation imprint marks the alleles of the mouse H19 gene.* Nat Genet, 1995. **9**(4): p. 407-13.

69. Lewis, A. and A. Murrell, *Genomic imprinting: CTCF protects the boundaries.* Curr Biol, 2004. **14**(7): p. R284-6.

70. Jaenisch, R., *DNA methylation and imprinting: why bother?* Trends Genet, 1997. **13**(8): p. 323-9.

71. Stoger, R., et al., *Maternal-specific methylation of the imprinted mouse Igf2r locus identifies the expressed locus as carrying the imprinting signal.* Cell, 1993. **73**(1): p. 61-71.

72. Sleutels, F., R. Zwart, and D.P. Barlow, *The non-coding Air RNA is required for silencing autosomal imprinted genes.* Nature, 2002. **415**(6873): p. 810-3.

73. Nicholls, R.D. and J.L. Knepper, *Genome organization, function, and imprinting in Prader-Willi and Angelman syndromes.* Annu Rev Genomics Hum Genet, 2001. **2**: p. 153-75.

74. Panning, B. and R. Jaenisch, *RNA and the epigenetic regulation of X chromosome inactivation.* Cell, 1998. **93**(3): p. 305-8.

75. Lock, L.F., N. Takagi, and G.R. Martin, *Methylation of the Hprt gene on the inactive X occurs after chromosome inactivation.* Cell, 1987. **48**(1): p. 39-46.

76. Csankovszki, G., A. Nagy, and R. Jaenisch, *Synergism of Xist RNA, DNA methylation, and histone hypoacetylation in maintaining X chromosome inactivation.* J Cell Biol, 2001. **153**(4): p. 773-84.

77. Gonzalgo, M.L. and P.A. Jones, *Mutagenic and epigenetic effects of DNA methylation.* Mutat Res, 1997. **386**(2): p. 107-18.

78. Jones, P.A. and M.L. Gonzalgo, *Altered DNA methylation and genome instability: a new pathway to cancer?* Proc Natl Acad Sci U S A, 1997. **94**(6): p. 2103-5.

79. Feinberg, A.P., *The epigenetics of cancer etiology.* Semin Cancer Biol, 2004. **14**(6): p. 427-32.

80. Gaudet, F., et al., *Induction of tumors in mice by genomic hypomethylation.* Science, 2003. **300**(5618): p. 489-92.

81. Eden, A., et al., *Chromosomal instability and tumors promoted by DNA hypomethylation.* Science, 2003. **300**(5618): p. 455.

82. Lin, H., et al., *Suppression of intestinal neoplasia by deletion of Dnmt3b.* Mol Cell Biol, 2006. **26**(8): p. 2976-83.

83. Yamada, Y., et al., *Opposing effects of DNA hypomethylation on intestinal and liver carcinogenesis.* Proc Natl Acad Sci U S A, 2005. **102**(38): p. 13580-5.

84. Turner, G., et al., *Prevalence of fragile X syndrome.* Am J Med Genet, 1996. **64**(1): p. 196-7.

85. Ashley, C.T., et al., *Human and murine FMR-1: alternative splicing and translational initiation downstream of the CGG-repeat.* Nat Genet, 1993. **4**(3): p. 244-51.

86. Costa, E., et al., *REELIN and Schizophrenia:: A Disease at the Interface of the Genome and the Epigenome.* Mol Interv, 2002. **2**(1): p. 47-57.

87. Chen, Y., et al., *On the epigenetic regulation of the human reelin promoter.* Nucleic Acids Res, 2002. **30**(13): p. 2930-9.

88. Rett, A., *[On a unusual brain atrophy syndrome in hyperammonemia in childhood].* Wien Med Wochenschr, 1966. **116**(37): p. 723-6.

89. Hagberg, B., et al., *A progressive syndrome of autism, dementia, ataxia, and loss of purposeful hand use in girls: Rett's syndrome: report of 35 cases.* Ann Neurol, 1983. **14**(4): p. 471-9.

90. Sirianni, N., et al., *Rett syndrome: confirmation of X-linked dominant inheritance, and localization of the gene to Xq28.* Am J Hum Genet, 1998. **63**(5): p. 1552-8.

91. Amir, R.E., et al., *Rett syndrome is caused by mutations in X-linked MECP2, encoding methyl-CpG-binding protein 2.* Nat Genet, 1999. **23**(2): p. 185-8.

92. Hoffbuhr, K., et al., *MeCP2 mutations in children with and without the phenotype of Rett syndrome.* Neurology, 2001. **56**(11): p. 1486-95.

93. Amir, R.E. and H.Y. Zoghbi, *Rett syndrome: methyl-CpG-binding protein 2 mutations and phenotype-genotype correlations.* Am J Med Genet, 2000. **97**(2): p. 147-52.

94. Miltenberger-Miltenyi, G. and F. Laccone, *Mutations and polymorphisms in the human methyl CpG-binding protein MECP2.* Hum Mutat, 2003. **22**(2): p. 107-15.

95. Weaving, L.S., et al., *Rett syndrome: clinical review and genetic update.* J Med Genet, 2005. **42**(1): p. 1-7.

96. Philippe, C., et al., *Spectrum and distribution of MECP2 mutations in 424 Rett syndrome patients: a molecular update.* Eur J Med Genet, 2006. **49**(1): p. 9-18.

97. Schanen, C., et al., *Phenotypic manifestations of MECP2 mutations in classical and atypical Rett syndrome.* Am J Med Genet A, 2004. **126**(2): p. 129-40.

98. Archer, H.L., et al., *Gross rearrangements of the MECP2 gene are found in both classical and atypical Rett syndrome patients.* J Med Genet, 2006. **43**(5): p. 451-6.

99. Girard, M., et al., *Parental origin of de novo MECP2 mutations in Rett syndrome.* Eur J Hum Genet, 2001. **9**(3): p. 231-6.

100. Trappe, R., et al., *MECP2 mutations in sporadic cases of Rett syndrome are almost exclusively of paternal origin.* Am J Hum Genet, 2001. **68**(5): p. 1093-101.

101. Borg, I., et al., *Disruption of Netrin G1 by a balanced chromosome translocation in a girl with Rett syndrome.* Eur J Hum Genet, 2005. **13**(8): p. 921-7.

102. Mari, F., et al., *CDKL5 belongs to the same molecular pathway of MeCP2 and it is responsible for the early-onset seizure variant of Rett syndrome.* Hum Mol Genet, 2005. **14**(14): p. 1935-46.

103. Scala, E., et al., *CDKL5/STK9 is mutated in Rett syndrome variant with infantile spasms.* J Med Genet, 2005. **42**(2): p. 103-7.

104. Couvert, P., et al., *MECP2 is highly mutated in X-linked mental retardation.* Hum Mol Genet, 2001. **10**(9): p. 941-6.

105. Carney, R.M., et al., *Identification of MeCP2 mutations in a series of females with autistic disorder.* Pediatr Neurol, 2003. **28**(3): p. 205-11.

106. Burford, B., A.M. Kerr, and H.A. Macleod, *Nurse recognition of early deviation in development in home videos of infants with Rett disorder.* J Intellect Disabil Res, 2003. **47**(Pt 8): p. 588-96.

107. Einspieler, C., A.M. Kerr, and H.F. Prechtl, *Is the early development of girls with Rett disorder really normal?* Pediatr Res, 2005. **57**(5 Pt 1): p. 696-700.

108. Zeev, B.B., et al., *Rett syndrome: clinical manifestations in males with MECP2 mutations.* J Child Neurol, 2002. **17**(1): p. 20-4.

109. Bauman, M.L., T.L. Kemper, and D.M. Arin, *Pervasive neuroanatomic abnormalities of the brain in three cases of Rett's syndrome.* Neurology, 1995. **45**(8): p. 1581-6.

110. Subramaniam, B., S. Naidu, and A.L. Reiss, *Neuroanatomy in Rett syndrome: cerebral cortex and posterior fossa.* Neurology, 1997. **48**(2): p. 399-407.

111. Belichenko, P.V., B. Hagberg, and A. Dahlstrom, *Morphological study of neocortical areas in Rett syndrome.* Acta Neuropathol (Berl), 1997. **93**(1): p. 50-61.

112. Johnston, M.V., et al., *Neurobiology of Rett syndrome: a genetic disorder of synapse development.* Brain Dev, 2001. **23 Suppl 1**: p. S206-13.

113. Belichenko, P.V. and A. Dahlstrom, *Studies on the 3-dimensional architecture of dendritic spines and varicosities in human cortex by*

confocal laser scanning microscopy and Lucifer yellow microinjections. J Neurosci Methods, 1995. **57**(1): p. 55-61.

114. Armstrong, D.D., K. Dunn, and B. Antalffy, *Decreased dendritic branching in frontal, motor and limbic cortex in Rett syndrome compared with trisomy 21.* J Neuropathol Exp Neurol, 1998. **57**(11): p. 1013-7.
115. Moretti, P., et al., *Learning and memory and synaptic plasticity are impaired in a mouse model of Rett syndrome.* J Neurosci, 2006. **26**(1): p. 319-27.
116. Asaka, Y., et al., *Hippocampal synaptic plasticity is impaired in the Mecp2-null mouse model of Rett syndrome.* Neurobiol Dis, 2006. **21**(1): p. 217-27.
117. Fukuda, T., et al., *Delayed maturation of neuronal architecture and synaptogenesis in cerebral cortex of Mecp2-deficient mice.* J Neuropathol Exp Neurol, 2005. **64**(6): p. 537-44.
118. Guy, J., et al., *A mouse Mecp2-null mutation causes neurological symptoms that mimic Rett syndrome.* Nat Genet, 2001. **27**(3): p. 322-6.
119. Guideri, F., et al., *Reduced heart rate variability in patients affected with Rett syndrome. A possible explanation for sudden death.* Neuropediatrics, 1999. **30**(3): p. 146-8.
120. Kerr, A.M., et al., *Rett syndrome: analysis of deaths in the British survey.* Eur Child Adolesc Psychiatry, 1997. **6 Suppl 1**: p. 71-4.

121. Julu, P.O., et al., *Characterisation of breathing and associated central autonomic dysfunction in the Rett disorder.* Arch Dis Child, 2001. **85**(1): p. 29-37.

122. Viemari, J.C., et al., *Mecp2 deficiency disrupts norepinephrine and respiratory systems in mice.* J Neurosci, 2005. **25**(50): p. 11521-30.

123. Kriaucionis, S. and A. Bird, *The major form of MeCP2 has a novel N-terminus generated by alternative splicing.* Nucleic Acids Res, 2004. **32**(5): p. 1818-23.

124. Vacca, M., et al., *MECP2 gene mutation analysis in the British and Italian Rett Syndrome patients: hot spot map of the most recurrent mutations and bioinformatic analysis of a new MECP2 conserved region.* Brain Dev, 2001. **23 Suppl 1**: p. S246-50.

125. Kokura, K., et al., *The Ski protein family is required for MeCP2-mediated transcriptional repression.* J Biol Chem, 2001. **276**(36): p. 34115-21.

126. Nan, X., et al., *Transcriptional repression by the methyl-CpG-binding protein MeCP2 involves a histone deacetylase complex.* Nature, 1998. **393**(6683): p. 386-9.

127. Nan, X., S. Cross, and A. Bird, *Gene silencing by methyl-CpG-binding proteins.* Novartis Found Symp, 1998. **214**: p. 6-16; discussion 16-21, 46-50.

128. Fuks, F., et al., *The methyl-CpG-binding protein MeCP2 links DNA methylation to histone methylation.* J Biol Chem, 2003. **278**(6): p. 4035-40.

129. Harikrishnan, K.N., et al., *Brahma links the SWI/SNF chromatin-remodeling complex with MeCP2-dependent transcriptional silencing.* Nat Genet, 2005. **37**(3): p. 254-64.

130. Hu, K., et al., *Testing for association between MeCP2 and the brahma-associated SWI/SNF chromatin-remodeling complex.* Nat Genet, 2006. **38**(9): p. 962-4; author reply 964-7.

131. Narlikar, G.J., H.Y. Fan, and R.E. Kingston, *Cooperation between complexes that regulate chromatin structure and transcription.* Cell, 2002. **108**(4): p. 475-87.

132. Horike, S., et al., *Loss of silent-chromatin looping and impaired imprinting of DLX5 in Rett syndrome.* Nat Genet, 2005. **37**(1): p. 31-40.

133. Blue, M.E., S. Naidu, and M.V. Johnston, *Altered development of glutamate and GABA receptors in the basal ganglia of girls with Rett syndrome.* Exp Neurol, 1999. **156**(2): p. 345-52.

134. Schule, B., et al., *DLX5 and DLX6 expression is biallelic and not modulated by MeCP2 deficiency.* Am J Hum Genet, 2007. **81**(3): p. 492-506.

135. Jung, B.P., et al., *Transient forebrain ischemia alters the mRNA expression of methyl DNA-binding factors in the adult rat hippocampus.* Neuroscience, 2002. **115**(2): p. 515-24.

136. Shahbazian, M.D., et al., *Insight into Rett syndrome: MeCP2 levels display tissue- and cell-specific differences and correlate with neuronal maturation.* Hum Mol Genet, 2002. **11**(2): p. 115-24.

137. Berardi, N., T. Pizzorusso, and L. Maffei, *Critical periods during sensory development.* Curr Opin Neurobiol, 2000. **10**(1): p. 138-45.

138. Chugani, H.T., *A critical period of brain development: studies of cerebral glucose utilization with PET.* Prev Med, 1998. **27**(2): p. 184-8.

139. Cohen, D.R., et al., *Expression of MeCP2 in olfactory receptor neurons is developmentally regulated and occurs before synaptogenesis.* Mol Cell Neurosci, 2003. **22**(4): p. 417-29.

140. Mullaney, B.C., M.V. Johnston, and M.E. Blue, *Developmental expression of methyl-CpG binding protein 2 is dynamically regulated in the rodent brain.* Neuroscience, 2004. **123**(4): p. 939-49.

141. Stearns, N.A., et al., *Behavioral and anatomical abnormalities in Mecp2 mutant mice: a model for Rett syndrome.* Neuroscience, 2007. **146**(3): p. 907-21.

142. Colantuoni, C., et al., *Gene expression profiling in postmortem Rett Syndrome brain: differential gene expression and patient classification.* Neurobiol Dis, 2001. **8**(5): p. 847-65.

143. Kaufmann, W.E., S. Naidu, and S. Budden, *Abnormal expression of microtubule-associated protein 2 (MAP-2) in neocortex in Rett syndrome.* Neuropediatrics, 1995. **26**(2): p. 109-13.

144. Tate, P., W. Skarnes, and A. Bird, *The methyl-CpG binding protein MeCP2 is essential for embryonic development in the mouse.* Nat Genet, 1996. **12**(2): p. 205-8.

145. Chen, R.Z., et al., *Deficiency of methyl-CpG binding protein-2 in CNS neurons results in a Rett-like phenotype in mice.* Nat Genet, 2001. **27**(3): p. 327-31.

146. Gemelli, T., et al., *Postnatal loss of methyl-CpG binding protein 2 in the forebrain is sufficient to mediate behavioral aspects of Rett syndrome in mice.* Biol Psychiatry, 2006. **59**(5): p. 468-76.

147. Shahbazian, M., et al., *Mice with truncated MeCP2 recapitulate many Rett syndrome features and display hyperacetylation of histone H3.* Neuron, 2002. **35**(2): p. 243-54.

148. Percy, A.K., *Rett syndrome. Current status and new vistas.* Neurol Clin, 2002. **20**(4): p. 1125-41.

149. Amir, R.E., et al., *Influence of mutation type and X chromosome inactivation on Rett syndrome phenotypes.* Ann Neurol, 2000. **47**(5): p. 670-9.

150. Dani, V.S., et al., *Reduced cortical activity due to a shift in the balance between excitation and inhibition in a mouse model of Rett syndrome.* Proc Natl Acad Sci U S A, 2005. **102**(35): p. 12560-5.

151. Chao, H.T., H.Y. Zoghbi, and C. Rosenmund, *MeCP2 Controls Excitatory Synaptic Strength by Regulating Glutamatergic Synapse Number.* Neuron, 2007. **56**(1): p. 58-65.

152. Usdin, M.T., et al., *Impaired synaptic plasticity in mice carrying the Huntington's disease mutation.* Hum Mol Genet, 1999. **8**(5): p. 839-46.

153. Eyre, J.A., et al., *Neurophysiological observations on corticospinal projections to the upper limb in subjects with Rett syndrome.* J Neurol Neurosurg Psychiatry, 1990. **53**(10): p. 874-9.

154. Tudor, M., et al., *Transcriptional profiling of a mouse model for Rett syndrome reveals subtle transcriptional changes in the brain.* Proc Natl Acad Sci U S A, 2002. **99**(24): p. 15536-41.

155. Martinowich, K., et al., *DNA methylation-related chromatin remodeling in activity-dependent BDNF gene regulation.* Science, 2003. **302**(5646): p. 890-3.

156. Rios, M., et al., *Conditional deletion of brain-derived neurotrophic factor in the postnatal brain leads to obesity and hyperactivity.* Mol Endocrinol, 2001. **15**(10): p. 1748-57.

157. Ghosh, A., J. Carnahan, and M.E. Greenberg, *Requirement for BDNF in activity-dependent survival of cortical neurons.* Science, 1994. **263**(5153): p. 1618-23.

158. Akbarian, S., et al., *Brain-derived neurotrophic factor is essential for opiate-induced plasticity of noradrenergic neurons.* J Neurosci, 2002. **22**(10): p. 4153-62.

159. Berninger, B. and M. Poo, *Exciting neurotrophins.* Nature, 1999. **401**(6756): p. 862-3.

160. Chen, W.G., et al., *Derepression of BDNF transcription involves calcium-dependent phosphorylation of MeCP2.* Science, 2003. **302**(5646): p. 885-9.

161. Chang, Q., et al., *The disease progression of Mecp2 mutant mice is affected by the level of BDNF expression.* Neuron, 2006. **49**(3): p. 341-8.

162. Cepeda, C., et al., *Increased GABAergic function in mouse models of Huntington's disease: reversal by BDNF.* J Neurosci Res, 2004. **78**(6): p. 855-67.

163. Kells, A.P., et al., *AAV-mediated gene delivery of BDNF or GDNF is neuroprotective in a model of Huntington disease.* Mol Ther, 2004. **9**(5): p. 682-8.

164. Guy, J., et al., *Reversal of neurological defects in a mouse model of Rett syndrome.* Science, 2007. **315**(5815): p. 1143-7.

165. Collins, A.L., et al., *Mild overexpression of MeCP2 causes a progressive neurological disorder in mice.* Hum Mol Genet, 2004. **13**(21): p. 2679-89.

166. Van Esch, H., et al., *Duplication of the MECP2 region is a frequent cause of severe mental retardation and progressive neurological symptoms in males.* Am J Hum Genet, 2005. **77**(3): p. 442-53.

167. Reichwald, K., et al., *Comparative sequence analysis of the MECP2-locus in human and mouse reveals new transcribed regions.* Mamm Genome, 2000. **11**(3): p. 182-90.

168. Klein, M.E., et al., *Homeostatic regulation of MeCP2 expression by a CREB-induced microRNA.* Nat Neurosci, 2007.

169. Young, J.I., et al., *Regulation of RNA splicing by the methylation-dependent transcriptional repressor methyl-CpG binding protein 2.* Proc Natl Acad Sci U S A, 2005. **102**(49): p. 17551-8.

Emanuela Giacometti

EDUCATION:	MASSACHUSETTS INSTITUTE OF TECHNOLOGY Whitehead Institute for Biomedical Research. Conducting doctoral research on genetic etiology of mental retardation.	Cambridge, MA, US (10/2003-11/2007)
	UNIVERSITY OF BASEL Doctoral degree in Neuroscience (GPA: 6)	Basel, CH (10/2002-11/2007)
	NOVARTIS RESEARCH FUNDATION Friedrich Miescher Institute	Basel, CH (10/2002-2003)
	UNIVERSITY OF EDINBURGH Institute of Cell and Molecular Biology Undergraduate studies.	Edinburgh,UK (2000-2002))
	UNIVERSITA' DEGLI STUDI DI UDINE Graduted in Plant biotechnology (110/110)	Udine, IT (1996- 2001)
PUBLICATIONS:	Luikenhuis S, Giacometti E, Beard CF, Jaenisch R *Proc Natl Acad Sci USA*. 2004. Giacometti E., Beard CF, Jaenich R. *Proc Natl Acad Sci USA*. 2006. Giacometti E., Tropea D., Wilson N, Harolg S, Jeanisch R, Su R M. *Nature Medicine*. Submitted	(2004) (2006) (2007)
PATENTS:	M0656.70145US00 : Therapeutic strategy for Rett syndrome and Autism spectrum disorders	(2007)
COURSES AND ACTIVITIES:	MIT BIOLOGY DEPARTMENT	
	The Brain and Cognitive Sciences II	(2002)
	Cellular Neurobiology	(2005)
	SLOAN SCHOOL OF MANAGEMENT, MIT	
	Finance Theory I. (Financial Theory, Markets, Investments, and Corporate Policy)	(5/2006)
	Financial and Managerial Accounting. (Principles of Accrual Accounting, Elements of an Annual Report and Financial Ratios, Marketable Securities)	(7/2006)
	Advanced Corporate Finance. (Valuation, Capital structure, M&A)	
	New Enterprises. (Opportunity Assessment, Value Proposition, Raising Funds. Students develop detailed business plans for a start-up.)	(9/2004)
AWARDS:	Rett Syndrome Research Foundation Grant ($200K)	(8/2006)
	Boehringer Ingelheim Foundation for Basic Research in Medicine. Graduate Fellowship (EU 50K)	(8/2003)
	Novartis Research Foundation. Graduate Fellowship (EU 50K)	(10/2002)
	European Community, Student Mobility Grant	(6/2000)
OTHER ACTIVITIES:	Executive Committee Member, MIT Nautical Association (MITNA) MITNA volunteer sailing instructor.	(11/2004-2007)
	Vice President of Sponsorships of the MIT Science and Engineering Business Club (SEBC) As a SEBC officer I personally initiated and organized a seminar at MIT hosting Dr.Craig Venter (former CEO of Celera Genomics). I was co-organizer of the 3rd MIT/SEBC Annual Technology, Entrepreneurship Forum and Venturefest.	(8/2003-11/2004)
	Volunteer, MIT Entrepreneurship Center, helped organize Biotechnology Fair: "Celebration of Biotechnology in Kendall Square".	(8/2003)
	President of the Friedrich Miescher Institute Graduate Student Council. Organization of the "FMI Student Science Colloquium".	(2/2002)
	Volunteer Organizer, 17th European Drosophila Research Conference, Edinburgh, UK	(9/2001)